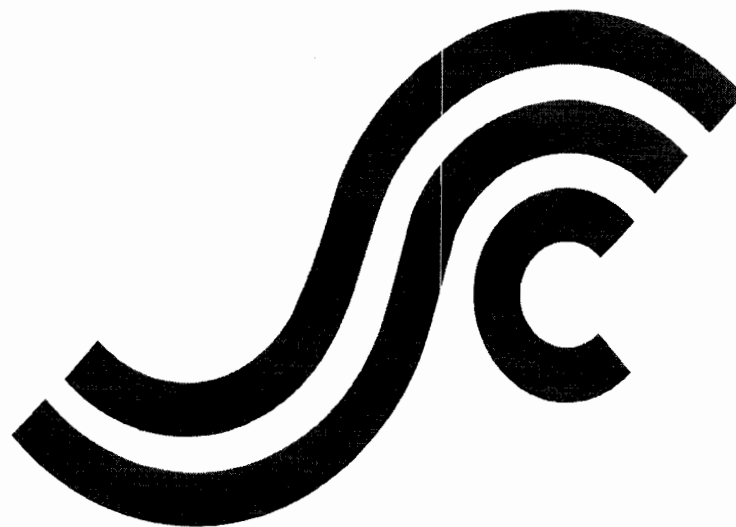


SSC-434

**PREDICTING MOTION AND
STRUCTURAL LOADS IN STRANDED
SHIPS
Phase 1**



This document has been approved
For public release and sale; its
Distribution is unlimited

**SHIP STRUCTURE COMMITTEE
2004**

SHIP STRUCTURE COMMITTEE

RADM Thomas H. Gilmour
U. S. Coast Guard Assistant Commandant,
Marine Safety and Environmental Protection
Chairman, Ship Structure Committee

Mr. W. Thomas Packard
Director,
Survivability and Structural Integrity Group
Naval Sea Systems Command

Mr. Joseph Byrne
Director, Office of Ship Construction
Maritime Administration

Mr. Thomas Connors
Director of Engineering
Military Sealift Command

CONTRACTING OFFICER TECHNICAL REP.
Lieutenant Eric M. Cooper / Ms. Dinah Mulligan
U.S. Coast Guard R & D Center

Dr. Donald Liu
Senior Vice President
American Bureau of Shipping

Mr. Gerard A. McDonald
Director General, Marine Safety,
Safety & Security
Transport Canada

Dr. Neil Pegg
Group Leader - Structural Mechanics
Defence Research & Development Canada - Atlantic

EXECUTIVE DIRECTOR
Lieutenant Eric M. Cooper
U. S. Coast Guard

SHIP STRUCTURE SUB-COMMITTEE

AMERICAN BUREAU OF SHIPPING
Mr. Glenn Ashe
Mr. Yung Shin
Mr. Phil Rynn
Mr. William Hanzalek

MARITIME ADMINISTRATION
Mr. Chao Lin
Mr. Carlos Setterstrom
Mr. Richard Sonnenschein

NAVAL SEA SYSTEMS COMMAND
Mr. Jeffery E. Beach
Mr. Edward E. Kadala
Mr. Allen H. Engle
Mr. Charles L. Null

UNITED STATES COAST GUARD
Mr. Rubin Sheinberg
Mr. Robert Sedat
Commander Ray Petow

DEFENCE RESEARCH & DEVELOPMENT ATLANTIC
Dr David Stredulinsky
Mr. John Porter

MILITARY SEALIFT COMMAND
Mr. Joseph Bohr
Mr. Rick A. Anderson
Mr. Michael W. Touma

TRANSPORT CANADA
Mr. Jacek Dubiel

CANADIAN COAST GUARD
Mr. Daniel Gauvin

Member Agencies:

*American Bureau of Shipping
Defence Research Development Canada
Maritime Administration
Military Sealift Command
Naval Sea Systems Command
Society of Naval Architects & Marine Engineers
Transport Canada
United States Coast Guard*



**Ship
Structure
Committee**

Address Correspondence to:

Executive Director
Ship Structure Committee
U.S. Coast Guard (G-MSE/SSC)
2100 Second Street, SW
Washington, D.C. 20593-0001
Web site: <http://www.shipstructure.org>

**SSC – 434
SR – 1419**

May 2004

PREDICTING MOTION AND STRUCTURAL LOADS IN STRANDED SHIPS

Significant effort has been made and is ongoing to predict structural damage as an immediate result of ship grounding, but little has been done to predict ship motion, structural loads and continued damage after grounding in waves.

This report describes Phase 1 in a three-phase project to develop, validate and apply a model to predict motions, loads and ultimate structural failure in a stranded ship. In Phase 1 a baseline model is developed to predict the dynamic effect of waves on stranded ship motion and loads. A theoretical analysis of the motions and loads in six-degrees of freedom of a grounded ship in waves is performed with an appropriate soil reaction model to estimate dynamic ground reaction forces. The steady-state grounded motion of the stranded ship in waves around the quasi-equilibrium position is treated as a steady-state linear dynamic problem. Comparisons are made to static grounding results and to current ABS/IACS design rules.

Ship groundings are a low probability/high consequence event. A review of ship groundings is included in this report to identify the general characteristics and scope of historic grounding events.

T. H. Gilmour
T. H. GILMOUR

Rear Admiral, U.S. Coast Guard
Chairman, Ship Structure Committee

Technical Report Documentation Page

1. Report No.	2. Government Accession No.	3. Recipient's Catalog No.	
4. Title and Subtitle Predicting Motion, Structural Loads and Damage in Stranded Ships Phase 1		5. Report Date November 2003	
		6. Performing Organization Code	
7. Author(s) Brown, A.J., Simbulan, M., McQuillan, J., Gutierrez, M.		8. Performing Organization Report No. SR-1419	
9. Performing Organization Name and Address Department of Aerospace and Ocean Engineering. Virginia Polytechnic Institute and State University Blacksburg, VA 24061-0203		10. Work Unit No. (TRAIS)	
		11. Contract or Grant No.	
12. Sponsoring Agency Name and Address Ship Structure Committee, US Coast Guard, US Navy NAVSEA OOC		13. Type of Report and Period Covered 9/00-11/03	
		14. Sponsoring Agency Code	
15. Supplementary Notes			
16. Abstract This report describes Phase 1 in a three phase project to develop, validate and apply a model to predict motions, loads and ultimate structural failure in a stranded ship. In Phase 1 a baseline model is developed to predict the dynamic effect of waves on stranded ship motion and loads. A theoretical analysis of the motions and loads in six-degrees of freedom of a grounded ship in waves is performed with an appropriate soil reaction model to estimate dynamic ground reaction forces. The steady-state grounded motion of the stranded ship in waves around the quasi-equilibrium position is treated as a steady-state linear dynamic problem. Comparisons are made to static grounding results and to current ABS/IACS design rules.			
17. Key Words ship grounding, ship damage		18. Distribution Statement Distribution is available to the public through: National Technical Information Service U.S. Department of Commerce Springfield, VA 22151 Ph. (703) 487-4650	
19. Security Classification (of this report) Unclassified	20. Security Classification (of this page) Unclassified	21. No. of Pages	22. Price

CONVERSION FACTORS
(Approximate conversions to metric measures)

To convert from	to	Function	Value
LENGTH			
inches	meters	divide	39.3701
inches	millimeters	multiply by	25.4000
feet	meters	divide by	3.2808
VOLUME			
cubic feet	cubic meters	divide by	35.3149
cubic inches	cubic meters	divide by	61,024
SECTION MODULUS			
inches ² feet ²	centimeters ² meters ²	multiply by	1.9665
inches ² feet ²	centimeters ³	multiply by	196.6448
inches ⁴	centimeters ³	multiply by	16.3871
MOMENT OF INERTIA			
inches ² feet ²	centimeters ² meters	divide by	1.6684
inches ² feet ²	centimeters ⁴	multiply by	5993.73
inches ⁴	centimeters ⁴	multiply by	41.623
FORCE OR MASS			
long tons	tonne	multiply by	1.0160
long tons	kilograms	multiply by	1016.047
pounds	tonnes	divide by	2204.62
pounds	kilograms	divide by	2.2046
pounds	Newtons	multiply by	4.4482
PRESSURE OR STRESS			
pounds/inch ²	Newtons/meter ² (Pascals)	multiply by	6894.757
kilo pounds/inch ²	mega Newtons/meter ² (mega Pascals)	multiply by	6.8947
BENDING OR TORQUE			
foot tons	meter tons	divide by	3.2291
foot pounds	kilogram meters	divide by	7.23285
foot pounds	Newton meters	multiply by	1.35582
ENERGY			
foot pounds	Joules	multiply by	1.355826
STRESS INTENSITY			
kilo pound/inch ² inch ^{3/2} (ksi√in)	mega Newton MNm ^{3/2}	multiply by	1.0998
J-INTEGRAL			
kilo pound/inch	Joules/mm ²	multiply by	0.1753
kilo pound/inch	kilo Joules/m ²	multiply by	175.3

TABLE OF CONTENTS

CHAIRMAN OF SSC LETTER.....	III
TECHNICAL REPORT DOCUMENTATION PAGE	V
CONVERSION FACTORS.....	VI
TABLE OF CONTENTS	VII
LIST OF FIGURES.....	IX
LIST OF TABLES.....	XI
CHAPTER 1 INTRODUCTION	1
1.1 Motivation and Background	1
<i>1.1.1 Salvage Operations</i>	<i>7</i>
1.2 Objective	9
1.3 Prior Research	10
1.4 Outline	11
CHAPTER 2 MODELING GROUND REACTION.....	12
2.1 Background and Development of Soil Models	12
2.2 Lumped Parameter Models	15
2.3 Six Degree of Freedom Soil Model	16
CHAPTER 3 GROUNDED SHIP MOTIONS.....	29
3.1 Overview of the Chapter	29
3.2 Frames of Reference	29
3.3 Equations of Motion	31
<i>3.3.1 Assumptions</i>	<i>31</i>
<i>3.3.2 General Equations for Ship Motions in Regular Waves</i>	<i>32</i>
3.4 Forces and Motions	33
<i>3.4.1 Hydrodynamic Forces.....</i>	<i>35</i>
<i>3.4.2 Strip Theory.....</i>	<i>36</i>
3.5 Solving the Equations of Motion	39
<i>3.5.1 Ship Motions</i>	<i>39</i>
3.6 Structural Loads	40
3.7 Grounded Ship Excitation	40

CHAPTER 4	STATIC EQUILIBRIUM CONDITION.....	42
CHAPTER 5	STRANDED SHIP MOTIONS & LOADS PROGRAM	54
CHAPTER 6	RESULTS AND CONCLUSIONS.....	60
6.1	Box Barge Case Study	60
6.1.1	<i>Motion Response in Regular Waves</i>	60
6.1.1.1	Depth of Embedment Varied	62
6.1.1.2	Wave Direction Varied	72
6.1.1.3	Soil-Type Varied	76
6.1.1.4	Ground Reaction Varied	76
6.1.1.5	Roll Response Varying Grounding Dimensions	86
6.1.2	<i>Bending Moment Response</i>	88
6.1.2.1	Static, Grounding-Induced Bending Moment	88
6.1.2.2	Bending Moment Response in Regular Waves	89
6.1.2.3	Bending Moment Response in Irregular Waves	96
6.1.2.4	Summary of Bending Moments	98
6.2	Series 60 Tanker	99
6.2.1	<i>Static, Grounding-Induced Bending Moment</i>	100
6.2.2	<i>Bending Moment in Regular Waves.....</i>	102
6.2.3	<i>Bending Moment in Irregular Seaway.....</i>	103
6.3	Conclusions	104
6.4	Future Work	105
REFERENCES.....		106

LIST OF FIGURES

FIGURE 1 – VALDIVIA GROUNDED ON SAND (STETTLER, J. 1997)	2
FIGURE 2 - CARGO SHIP GROUNDED ON CORAL (ABC 2002).....	2
FIGURE 3 - FOUR PHASES OF SHIP GROUNDINGS.....	5
FIGURE 4 - HULL SHAPES.....	19
FIGURE 5 - STRANDED AND EMBEDDED SHIP MODELED AS RECTANGULAR EMBEDDED FOUNDATION	19
FIGURE 6 – SIX DEGREES-OF-FREEDOM FOR A FOUNDATION	20
FIGURE 7 - SIX DEGREES-OF-FREEDOM FOR A SHIP.....	21
FIGURE 8 - RECTANGULAR EMBEDDED FOUNDATION ($L>B$)	21
FIGURE 9 - STRANDED AND FULLY EMBEDDED SHIP.....	22
FIGURE 10 - STRIP FOUNDATION.....	24
FIGURE 11 - FRAMES OF REFERENCE.....	30
FIGURE 12 - SIX DEGREES OF FREEDOM OF A SHIP.....	31
FIGURE 13 - UNIFORM GROUND REACTION DISTRIBUTION ON A STRANDED SHIP	44
FIGURE 14 - LINEAR GROUND REACTION DISTRIBUTION.....	45
FIGURE 15 - CHANGE IN TRIM.....	46
FIGURE 16 - FORCES ON A STRANDED SHIP	49
FIGURE 17 - HIGH BENDING MOMENT STRANDINGS	52
FIGURE 18 - PROGRAM FLOWCHART	55
FIGURE 19 - LOCATION OF SOIL REACTION FORCE ($L_E>B_E$).....	56
FIGURE 20 - TRANSFER OF SOIL REACTION FORCE AND MOMENT TO AMIDSHIPS.....	57
FIGURE 21 - BARGE CASE STUDY	61
FIGURE 22 - BARGE CASE FLOW CHART (RAO)	62
FIGURE 23 - SURGE RAO FOR BARGE GROUNDED IN CLAY.....	64
FIGURE 24 - HEAVE RAO FOR BARGE GROUNDED IN CLAY.....	65
FIGURE 25 - PITCH RAO FOR BARGE GROUNDED IN CLAY.....	65
FIGURE 26 - SWAY RAO FOR BARGE GROUNDED IN CLAY.....	66
FIGURE 27 - ROLL RAO FOR BARGE GROUNDED IN CLAY.....	66
FIGURE 28 - YAW RAO FOR BARGE GROUNDED IN CLAY.....	67
FIGURE 29 - HEAVE RAO FOR BARGE GROUNDED IN CLAY.....	67
FIGURE 30 - PITCH RAO FOR BARGE GROUNDED IN CLAY	68
FIGURE 31 - SURGE RAO FOR BARGE GROUNDED IN CLAY, DEPTH OF EMBEDMENT VARIED.....	68
FIGURE 32 - HEAVE RAO FOR BARGE GROUNDED IN CLAY, DEPTH OF EMBEDMENT VARIED.....	69
FIGURE 33 - PITCH RAO FOR BARGE GROUNDED IN CLAY, DEPTH OF EMBEDMENT VARIED	69
FIGURE 34 - SWAY RAO FOR BARGE GROUNDED IN CLAY, DEPTH OF EMBEDMENT VARIED.....	70
FIGURE 35 - HEAVE RAO FOR BARGE GROUNDED IN CLAY, DEPTH OF EMBEDMENT VARIED.....	70
FIGURE 36 - ROLL RAO FOR BARGE GROUNDED IN CLAY, DEPTH OF EMBEDMENT VARIED.....	71
FIGURE 37 - PITCH RAO FOR BARGE GROUNDED IN CLAY, DEPTH OF EMBEDMENT VARIED	71
FIGURE 38 - YAW RAO FOR BARGE GROUNDED IN CLAY, DEPTH OF EMBEDMENT VARIED.....	72
FIGURE 39 - SURGE RAO FOR BARGE GROUNDED IN CLAY, WAVE DIRECTION VARIED	73
FIGURE 40 - SWAY RAO FOR BARGE GROUNDED IN CLAY, WAVE DIRECTION VARIED.....	73
FIGURE 41 - HEAVE RAO FOR BARGE GROUNDED IN CLAY, WAVE DIRECTION VARIED.....	74
FIGURE 42 - ROLL RAO FOR BARGE GROUNDED IN CLAY, WAVE DIRECTION VARIED.....	74
FIGURE 43 - PITCH RAO FOR BARGE GROUNDED IN CLAY, WAVE DIRECTION VARIED.....	75
FIGURE 44 - YAW RAO FOR BARGE GROUNDED IN CLAY, WAVE DIRECTION VARIED.....	75
FIGURE 45 - SURGE RAO FOR GROUNDED BARGE, SOIL-TYPE VARIED.....	77
FIGURE 46 - HEAVE RAO FOR GROUNDED BARGE, SOIL-TYPE VARIED.....	77
FIGURE 47 - PITCH RAO FOR GROUNDED BARGE, SOIL-TYPE VARIED.....	78
FIGURE 48 - SWAY RAO FOR GROUNDED BARGE, SOIL-TYPE VARIED.....	78
FIGURE 49 - SWAY RAO FOR GROUNDED BARGE, CLAY SOIL TYPE.....	79
FIGURE 50 - HEAVE RAO FOR GROUNDED BARGE, SOIL-TYPE VARIED.....	79
FIGURE 51 - ROLL RAO FOR GROUNDED BARGE, SOIL-TYPE VARIED.....	80
FIGURE 52 - PITCH RAO FOR GROUNDED BARGE, SOIL-TYPE VARIED.....	80
FIGURE 53 - YAW RAO FOR GROUNDED BARGE, SOIL-TYPE VARIED.....	81

FIGURE 54 - SWAY RAO FOR BARGE GROUNDED IN CLAY, GROUND REACTION VARIED	82
FIGURE 55 - SWAY RAO FOR BARGE GROUNDED IN CLAY, GROUND REACTION VARIED	82
FIGURE 56 - HEAVE RAO FOR BARGE GROUNDED IN CLAY, GROUND REACTION VARIED.....	83
FIGURE 57 - ROLL RAO FOR BARGE GROUNDED IN CLAY, GROUND REACTION VARIED	83
FIGURE 58 - ROLL RAO FOR BARGE GROUNDED IN CLAY, GROUND REACTION VARIED	84
FIGURE 59 - PITCH RAO FOR BARGE GROUNDED IN CLAY, GROUND REACTION VARIED	84
FIGURE 60 - PITCH RAO FOR BARGE GROUNDED IN CLAY, GROUND REACTION VARIED	85
FIGURE 61 - YAW RAO FOR BARGE GROUNDED IN CLAY, GROUND REACTION VARIED.....	85
FIGURE 62 - ROLL RAO FOR BARGE GROUNDED IN CLAY, LENGTH OF EMBEDMENT VARIED	86
FIGURE 63 - ROLL RAO FOR BARGE GROUNDED IN CLAY, BEAM OF EMBEDDED SECTION	87
FIGURE 64 - ROLL RAO FOR BARGE GROUNDED IN CLAY, LENGTH OF EMBEDMENT AND BEAM OF EMBEDDED SECTION VARIED SIMULTANEOUSLY.....	87
FIGURE 65 - BENDING MOMENT AS VERTICAL DISPLACEMENT (Z) OR GROUND REACTION IS VARIED.....	88
FIGURE 66 - MAXIMUM LONGITUDINAL BENDING MOMENT AS GROUND REACTION IS VARIED	89
FIGURE 67 - BARGE CASE FLOW CHART (BENDING MOMENT).....	89
FIGURE 68 - DIAGRAM OF VERTICAL AND HORIZONTAL BENDING MOMENTS.....	90
FIGURE 69 - LONGITUDINAL BENDING MOMENT , VERTICAL PLANE, REGULAR WAVES	91
FIGURE 70 - LONGITUDINAL BENDING MOMENT , HORIZONTAL PLANE, REGULAR WAVES	91
FIGURE 71 - LONGITUDINAL BENDING MOMENT , VERTICAL PLANE, REGULAR WAVES	92
FIGURE 72 - LONGITUDINAL BENDING MOMENT , HORIZONTAL PLANE, LENGTH OF EMBEDMENT VARIED.....	93
FIGURE 73 - MAXIMUM LONGITUDINAL BENDING MOMENT , HORIZONTAL PLANE, WAVE DIRECTION VARIED.....	94
FIGURE 74 - MAXIMUM LONGITUDINAL BENDING MOMENT , VERTICAL PLANE, SOIL TYPE VARIED	95
FIGURE 75 - MAXIMUM LONGITUDINAL BENDING MOMENT , VERTICAL PLANE, DEPTH OF EMBEDMENT VARIED.....	95
FIGURE 76 - MAXIMUM LONGITUDINAL BENDING MOMENT , VERTICAL PLANE, WAVE HEIGHT VARIED.....	96
FIGURE 77 - LONGITUDINAL BENDING MOMENT , VERTICAL PLANE, IRREGULAR SEAWAY.....	97
FIGURE 78 - MAXIMUM LONGITUDINAL BENDING MOMENT , VERTICAL PLANE, IRREGULAR SEAWAY.....	98
FIGURE 79 - STATIC, GROUNDING INDUCED BENDING MOMENT FOR SERIES 60 TANKER.....	101
FIGURE 80 - SSMLP BENDING MOMENT FOR TANKER GROUNDED IN CLAY , REGULAR WAVES, DEPTH OF EMBEDMENT VARIED, WAVE HEIGHT = 1 METER.....	102
FIGURE 81 - SSMLP BENDING MOMENT FOR TANKER GROUNDED IN CLAY , IRREGULAR SEAWAY, DEPTH OF EMBEDMENT VARIED.....	103
FIGURE 82 - SSMLP BENDING MOMENT FOR TANKER GROUNDED IN CLAY , IRREGULAR SEAWAY, SIGNIFICANT WAVE HEIGHT VARIED.....	104

LIST OF TABLES

TABLE 1 - SHIP GROUNDING CASES	3
TABLE 2 - SOIL PROPERTIES (D` APPOLONIA CONSULTING ENGINEERS 1979).....	15
TABLE 3 - GROUND REACTION CHANGE DUE TO VERTICAL DISPLACEMENT.....	62
TABLE 4 - CALCULATED BENDING MOMENTS.....	99
TABLE 5 - SERIES 60 TANKER GROUNDING SCENARIO.....	100

CHAPTER 1 INTRODUCTION

1.1 *Motivation and Background*

Significant effort has been made and is ongoing to predict structural damage as an immediate result of ship grounding (Sirkar et al 1997, Brown et al 2000, Rawson et al 1998), but little has been done to predict ship motion, structural loads and continued damage after grounding in waves. During salvage operations immediate decisions are required to maximize the potential for successful salvage and minimize environmental pollution. These decisions require accurate information about the stranded ship, the ship's current extent of damage, prevailing sea and surf zone conditions and predicted weather. This information is typically applied in an ad hoc manner based on simplified static analysis, experience and good engineering/seamanship judgment. Potential alternatives considered necessary to mitigate disaster may have significant adverse pollution, safety and cost impacts. These include: premature efforts to refloat or ballast; the rigging of anchors (beach gear), cables and support vessels necessary to stabilize the stranded ship; the lightering or burning of fuel; and the use of explosives. A salvor must have the necessary tools to accurately predict the impact of alternative plans of action or no action.

This report describes Phase 1 in a three phase project to develop, validate and apply a model to predict motions, loads and ultimate structural failure in a stranded ship. In Phase 1 a baseline model is developed to predict the dynamic effect of waves on stranded ship motion and loads. A theoretical analysis of the motions and loads in six-degrees of freedom of a grounded ship in waves is performed with an appropriate soil reaction model to estimate dynamic ground reaction forces. The steady-state grounded motion of the stranded ship in waves around the quasi-equilibrium position is treated as a steady-state linear dynamic problem. Comparisons are made to static grounding results and to current ABS/IACS design rules.

Ship groundings are a low probability / high consequence event. A review of ship groundings was conducted to identify the general characteristics and scope of historic grounding events (Cahill 1991, Bartholomew 1990, Bartholomew et al 1992, NAVSEA OOC 2002, ATSB 2002). A summary of this review is provided in Table 1, which lists a variety of grounding events documented mostly by the U.S. Navy Supervisor of Salvage.

Based on this data, the following general conclusions and observations are made:

1. Groundings occur on a range of bottom types. The general types of bottom may be classified as:

- Sand (Figure 1)
- Clay and mud
- Soft rock and coral (Figure 2)
- Hard rock



Figure 1 – Valdivia grounded on sand (Stettler, J. 1997)



Figure 2 - Cargo ship grounded on coral (ABC 2002)

Table 1 - Ship Grounding Cases

Ship	Orientation	Type of Bottom	Waves	Time	Hull Shape (Idealized)	Year	Location
New Carissa	Broached	Sandy, in surf zone	*15-26ft, breaking, longshore current 8-10kts, wind 25-45kts gusts 70kts, *15-20ft, wind calm	*4 days, *3 days	Rectangle	4-Feb-99	Coos Bay, OR
Valdivia (LST 93) LST 1179 class	Broached, 7ft trim, 2.5deg list to stbd	Sand, small rocks	breaking, in surf zone	55 days	wedge	17-May-97	North Chile Coast
USS La Moure County LST 1194 (LST 1179 Class)		Rock	5-7ft, flood tide, SS2, wind 18-22kts	1.5 hours	wedge	12-Sep-00	Cifuncho Bay, Chile
M/V Kuroshima	Broached	Rocks then sand			rectangle	26-Nov-97	Unalaska Island, Alaska
M/V Concorde Spirit	Entire ship embedded	Mud			rectangle	23-Oct-98	Hampton, VA
T/B Bayou Zachary	Broached	Mud			rectangle		Harvey Canal Intercoastal
USNS Bob Hope				1 day	wedge	19-Sep-01	Chesapeake Bay
Liberty Spirit		Sand			rectangle	29-Mar-99	Columbia River
M/V Sergo Zakariadze	Broached	Rocks	7-10ft (12ft high)		rectangle	18-Nov-99	San Juan, Puerto Rico
Bunga Terati Satu		Coral			rectangle	2-Nov-00	Sudbury Reef, Australia
Monssen DD 798	Broached-fully embedded, 5 deg list	Sand, 7ft deep		45 days	wedge	5-Mar-62	Beach Haven, NJ
Dona Ouriana	180ft of 483 ft aground	Coral			rectangle	27-Apr-62	Pocklington Reef
Frank Knox DDR 742		Coral	Typhoon Gilda, Harriet strong lateral current	37 days	wedge	18-Jul-65	Pratas Reef, South China Sea
Terrell County LST 1157	Broached	Sand			wedge		Tuy Hoa, Vietnam
Summit County LST 1146		Sand			wedge		Chu Lai, Vietnam
T-AK 276		Coral	4 typhoons		wedge	23-Sep-73	Triton Island, South China Sea
Mahnomen County LST 912	Broached	Rocky shore	Breaking, 18ft, wind 25kts		wedge	31-Dec-66	Chu Lai, Vietnam
USNS General Daniel I. Sultan		Coral			wedge		Rukon Shoal, Okinawa
Submarine Tiru SS 416		Coral			cylinder	19-Nov-67	Frederick Reef, Australia
Guardfish SSN 612		Coral		3 days	cylinder	24-Dec-67	Pearl Harbor, Hawaii

Ship	Orientation	Type of Bottom	Waves	Time	Hull Shape (Idealized)	Year	Location
Regulus AP 57		Hard rock and Sand	Typhoon		rectangle	Aug-73	Hong Kong Harbor
Tucumcari PGH 2	25 deg down by bow, 3 deg list to port	Coral, 3ft of water				fall 1972	Caballo Blanco Reef, Puerto Rico
Solar Trader		Coral			rectangle	Dec-71	West Fayu Islands, atoll in Pac
Garfish H-3 (SS30)	Broached	Sand			cylinder	14-Dec-16	Samoa Beach Eureka, CA
Milwaukee C 2	Broached	Sand			wedge	13-Jan-17	Samoa Beach Eureka, CA
DeLong DD129				16 days	wedge	1-Dec-21	Halfmoon Bay, CA
S-19 (SS124)		Sand		64 days	cylinder	13-Jan-25	Nauset Beach near Orleans, MA
S-48 (SS159)		Rocks then Sand			cylinder	29-Jan-25	Jaffrey Point, NH
Omaha (CL4)	1/2 length embedded, 2453 tons on reef (of 8993)	Coral	small tide range	10 days	wedge	19-Jul-37	Castle Is, Bahamas
SS Lancaster		Rocks			wedge	31-Dec-42	El Hank Light
SS Sea Flyer		Sand			wedge	21-Jul-41	Eniwetok Atoll
Seize ARS26	Broached	Sand			wedge		Clipperton Is, Pacific atoll
Missouri-Battleship	whole length embedded	Sand	calm, protected	14 days	wedge	17-Jan-50	near Old Point Comfort
Thai Frigate HMTS Prasae	Broached-7 ft in sand	Sand	6ft		wedge	Jan-51	North Korea
North Korean LST M-370	Broached	Rock			wedge	Mem day'51	Taechong-do, Korea
Cornhusker Mariner-535ft		Rock		over 3 months	rectangle	7-Jul-53	Pusan, Korea
San Mateo Victory		Rock					Cheju-do Pusan
SS Quartette	Broached	Sand			rectangle		Pearl & Hermes Reef, near Midway
Korean LST Suyong (LST677)	Broached			16 days	wedge	13-Mar-83	Tok Son Ri, Korea
Gumi ARS26		Rocks	high seas, high winds	12 days	wedge	13-Mar-83	Tok Son Ri, Korea

Ship	Orientation	Type of Bottom	Waves	Time	Hull Shape (Idealized)	Year	Location
LindenBank	Broached	Coral			rectangle	late'75	Fanning Is, 1,000miles south HI
Anangel Liberty		Coral			rectangle	Apr-80	French Frigate Shoals, HI
USNS Chauvenet T-AG529	hard aground at bow	Coral			wedge	mid 1982	Dausan Reef in Sulu Sea
Torrey Canyon	8 deg stbd list	Rocks	bad weather, almost gale force winds		rectangle	Mar-67	Seven Stones in Scilly Isles
Amoco Cadiz		Rocks	Breaking		rectangle	Mar-77	Portsall on Brittany coast
Exxon Valdez		Coral			rectangle	24-Mar-89	Bligh Reef, Prince William sound, Ak

2. The grounding event may be divided into four distinct phases, as illustrated in Figure 3:

- a. Phase One - Ship underway
- b. Phase Two - Grounding impact event ($t = 0$ to $t = 10$ sec)
- c. Phase Three - Orientation and translation ($t = 10$ sec to $t = 24^+$ hours)
- d. Phase Four - The steady-state grounded position with steady-state periodic motion in response to waves; after one extreme tidal or extreme weather cycle (statistically stationary process)

Grounded ship may go back to phase 3 and then re-enter phase 4

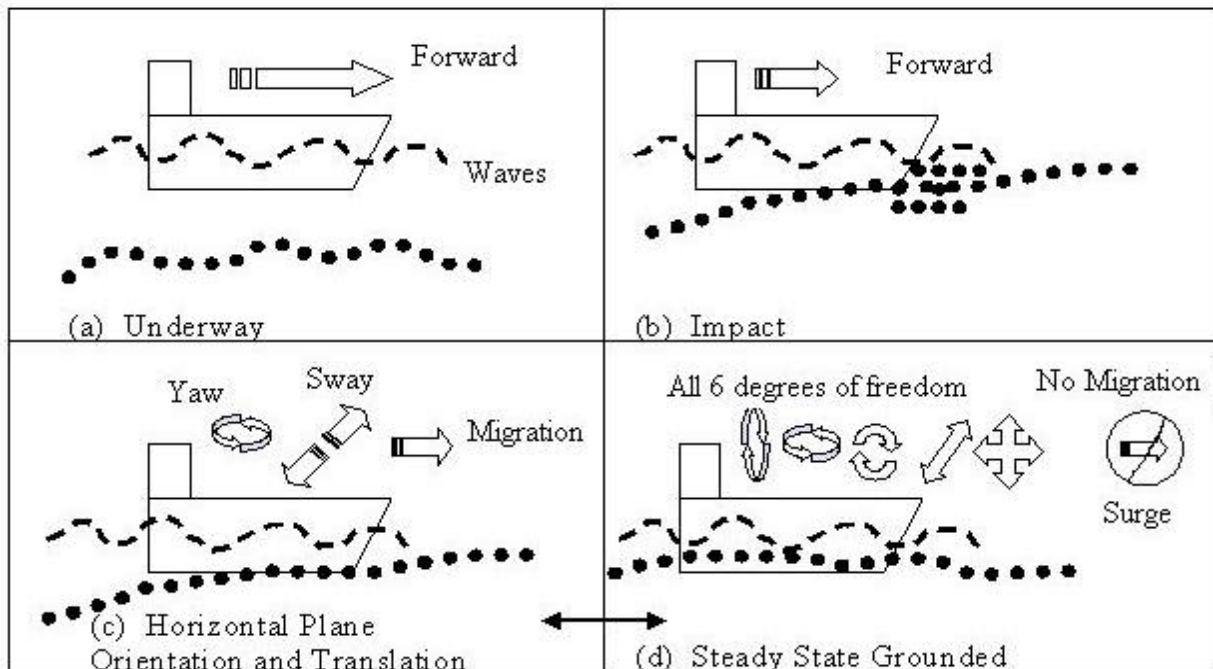


Figure 3 - Four Phases of Ship Groundings

3. The grounded ship orientation cannot be generalized. A ship that grounds may broach if conditions are right, but this is not a certainty. Since ship operators and salvors try to prevent broaching, it cannot be assumed that a ship will broach after grounding. To prevent movement of the ship into a more precarious position until the ship is ready to free, the ship is often stabilized. This is done using anchors (beach gear) or by flooding down.
4. Ships may run aground (Phase Two) bow first or drift aground in any orientation with some portion of the ship length either embedded in the bottom or resting on the bottom, exchanging buoyancy for an equal ground reaction.
5. Groundings may last several hours to several months. The need to understand the motions and loads of the stranded ship is important because both affect rescue and salvage operations. “Stranding salvage is time-critical. Environmental conditions may improve or worsen with time, but the condition of a stranded ship steadily deteriorates.” (Bartholomew et al 1992) The continued wave loading and ground reaction on a stranded ship will eventually cause structural damage even on a hull that was initially undamaged from the Phase Two grounding event.

Most grounding research has focused on the grounding event, Phase Two. Few researchers have investigated the third and fourth phases of grounding. This project analyzes Phase Four of ship grounding. The steady-state grounded motions of the stranded ship in waves around the quasi-equilibrium position are treated as a steady dynamic problem. The equilibrium condition without waves is calculated after one extreme tidal or extreme weather cycle (which includes direction of the waves, wind speed and direction). Calculations are made at a discrete number of tidal stages. If another large tide or extreme weather cycle occurs and changes the equilibrium position of the stranded ship, then the ship may go back to Phase Three. After the ship is re-oriented and stops translation, it enters Phase Four again. Our hypothesis is that a grounded ship in waves will sustain significantly higher loads and bending moments than those predicted by static analysis.

At sea, buoyant force equals total ship weight. When a ship runs aground, a ground reaction is created. At equilibrium the ground reaction is defined as the difference between the ship weight and the remaining buoyancy. It acts approximately through the centroid of the grounded area (Bartholomew et al 1992). The ground reaction can increase if the ship takes on more weight from flooding either by seas or hull damage. If the ship is partially aground then the ship

is free to heel and change its trim about the grounded area until both forces and moments are in equilibrium.

When a ship grounds in mud, the mud is forced down by the weight of the ship, which causes pore water to displace and the mud to condense. The condensed mud severely restricts water flow to the hull. This makes the pressure below the stranded ship constant. If hydrostatic pressure then increases around the ship because of a high tide or waves, a low-pressure region is created below the ship that holds the ship down due to suction. Ships with rectangular shaped hulls experience greater suction effects than wedge-shaped ships (Bartholomew et al 1992).

1.1.1 Salvage Operations

There is no typical salvage operation. By the time salvage vessels arrive to assist a stranded ship, immediate decisions are required to mitigate the situation and to ensure a successful salvage operation. These decisions are often made in the face of adverse weather conditions and must be based on the best and most accurate information available.

While stranded, the ship is often subject to loads not normally encountered by a ship at sea. In addition, the grounding event often results in significant damage to the hull, which may marginalize the residual strength of the hull. Therefore, understanding current and potential loads on the ship is important for determining the potential for future hull deterioration and devising a safe salvage plan. As such, it is important for salvors to know and understand the motions of and loads on a ship after it has grounded.

To prevent movement of the ship into a more precarious position, the ship is often stabilized. This is done using anchors (beach gear) or by flooding down. Currently, the basic techniques used in the salvage industry to free a stranded ship are:

- reducing the ground reaction of the ship,
- pushing or pulling the ship into deeper water,
- increasing the depth of water at the site of the stranded ship, or
- some combination of these techniques.

Removing loads like cargo, fuel, mud and floodwater reduces the ground reaction of a stranded ship, while also reducing the risk of a product release. If the ship is partially grounded then adjusting its trim by moving weights or adjusting ballast may free it. Pushing or pulling the

stranded ship requires enough force to overcome the forces of friction, suction and soil buildup. Friction in sand is a function of the ground reaction force, so reducing the ground reaction by lightening the ship can aid in the operation. Friction in mud is the product of shear strength and contact area so loosening the mud around the hull will aid in the operation. The suction force can be decreased by rocking the ship or by scouring the surrounding soil, which will allow water to flow to the hull. Dredging and scouring can be used to increase the water depth at the stranded ship. Sometimes channels are created for the ship to float into deeper water. Tides may also increase the water depth at the stranded ship site, but only temporarily.

Examples of typical decisions that need to be made by the salvor are:

- Expedite operations to avoid adverse weather or tides,
- Stabilize the stranded ship,
- Remove/destroy some or all of the cargo,
- Request more resources on scene or financial assistance, or
- A combination of these choices.

Currently these decisions are made in an ad hoc manner based on a simplified use of static analysis along with experience and sound engineering/seamanship judgment.

Some courses of action intended to avoid disaster may have significant adverse impact on the safety of personnel, the environment, and salvage costs. Examples of these actions are:

- Efforts to refloat or ballast,
- Rigging of anchors, cables and support vessels that are necessary to stabilize the stranded ship,
- Lightering or burning of fuel, and
- Use of explosives

The salvor must have all the necessary information to accurately predict the impact of alternative plans of action or no action. Ships are not designed for the motions and loads they experience in the grounded condition such as partially constrained hydrodynamic motions and soil reactions. After grounding damage, the ship structure may have only limited residual strength. The longer the ship stays grounded, the worse the situation gets.

1.2 Objective

The overall objective of this project is to develop, validate and apply a model to predict motions, loads and ultimate structural failure in a stranded ship as a function of the stranded ship scenario, sea and weather conditions.

Tasks associated with this objective are:

- Task 1 - Develop a 2 DOF first-order grounded ship model to predict ship motions (pitch and heave), local loads (at grounding point) and global loads (bending moment). The emphasis of this task is on the ground or soil reaction, developed in 6 DOF to support Task 2.
- Task 2 - Develop a baseline 6 DOF first-order grounded ship model to predict ship motions, local loads (at grounding point) and global loads (bending moment). Investigate critical parameters, conduct sensitivity analysis. Determine if loads developed in waves are of sufficient magnitude to warrant further consideration and analysis.
- Task 3 – Develop a model test validation matrix and conduct model tests, measuring motions and bending moments. Assess the sufficiency of the baseline model and identify necessary improvements.
- Task 4 – Based on the assessment in Task 3, correct problems in the model and add complexity as necessary. Determine a “sufficient” model, i.e. minimum complexity and run time, to obtain good engineering results.
- Task 5 – Work with Herbert Engineering Corporation and the USN Supervisor of Salvage towards possible implementation in POSSE/HECSALV software.
- Task 6 – Make initial application of the model to predict local structural damage and reduction in ultimate strength.
- Task 7 – Oversee the completion of applicable student theses. Write SNAME paper(s).
- Task 8 – Write a Ship Structure Committee (SSC) Report.

	Phase 1		Phase 2		Phase 3	
	Y1 (01-02)	Y2 (02-03)	Y1 (03-04)	Y2 (04-05)	Y1 (05-06)	Y2 (06-07)
Task 1 - 2D Model	X	X	X	X	X	
Task 2 - 6D Model		X	X	X	X	X
Task 3 - Model Test			X	X	X	X
Task 4 – Refine 6D Model				X	X	X
Task 5 - HECSALV					X	X
Task 6 - Structural Application					X	X
Task 7 - Thesis/Paper	X	X		X	X	X
Task 8 - Report		X			X	X

The primary objective of Phase 1 in this project is to develop a baseline methodology and model to predict motions and loads on a stranded ship in waves. The scope of Phase 1 includes Task 1, Task 2, applicable theses, papers and this report.

1.3 Prior Research

There have been only limited studies on the motions of and loads on a stranded ship in Phase Three and Four (Figure 3). Most grounding research focuses on the damages sustained by the structure of the ship during the grounding event - Phase Two (Brown et al 2000, Paik 2003). This research does not extend to the motion of and loads on a ship after it has grounded. Studies on Phase 3 motions by McCormick (1999), and later McCormick and Hudson (2002) were very helpful at the start of this study. In McCormick's study, the planar motions of a grounded, broached ship are linearized and solved. The hydrodynamic reactions are analyzed using linear wave theory, and the seabed is treated elastically using a quasi-elastic discrete model. In follow-on work, McCormick and Hudson developed a two-degree of freedom model to predict the wave-induced migration of a structurally intact ship that was grounded, partially embedded, and broached. In their scenario, the ship migrates up a mildly sloping, sandy sea bottom without rock. They compare results from their theoretical model to results obtained from their experimental study. The experimental study measured the migration of a rectangular ship model in a wave tank with a flat middle section consisting of a sandy bottom.

Paik and Pedersen (1997) calculate the Phase 4 static grounding bending moment. Results from their paper were very useful for comparison with the dynamic results and still water results developed in our dynamic model.

The most relevant work involving a suitable model of soil reactions comes from the field of civil engineering. In foundation studies, the soil-structure interaction is very important for structures subjected to earthquakes, machine vibrations, and offshore structures subjected to wave loading. These disciplines have studied soil dynamic behavior for some time and have developed simple and consistent methods to model the soil reactions.

1.4 Outline

A theoretical model of the motions and loads in six-degrees of freedom of a grounded ship in waves is developed. The equations of motion are analytically derived for a stranded ship in waves with an appropriate soil reaction model to generate the soil reaction forces. Forces and loads on a free floating ship and a grounded ship, and IACS/American Bureau of Ships (ABS) design loads are calculated and compared. Chapter One provides an introduction and motivation for solving the grounded ship problem, and describes the overall stranded ship project. Some background is also provided on stranded ship salvage operations and ground reaction. Chapter Two provides the background and development of a six degree-of-freedom lumped-parameter ground reaction soil model. Chapter Three derives the equations of motion for a grounded ship in waves. Chapter Four presents the methods and equations used to calculate the static grounded condition. Chapter Five describes the Stranded Ship Motions & Loads Program (SSMLP). Chapter Six presents motion and load results in the form of response amplitude operator and bending moment plots, provides a parametric study of the effect of soil parameters, and briefly discusses future work.

CHAPTER 2 MODELING GROUND REACTION

2.1 *Background and Development of Soil Models*

Early work by civil engineers in dynamic analysis concentrated on the effects of machine vibrations on foundations. Mainstream study and analysis of soil dynamics did not occur until it was needed to design buildings and foundations to be less susceptible to earthquakes. More recently, the development of offshore gravity platforms which use large concrete foundations to anchor themselves on the ocean floor has increased the need for understanding soil dynamics.

Researchers began their study of soil dynamics by developing general equations, which eventually led to more sophisticated calculations. Over time they discovered the key aspects of soil behavior and developed simple methods that are still used today. Work in the area of soil-structure interaction began in the 1920's. In the 1930's the first analytical solution for vertical displacement on the surface of a linear elastic, homogenous and isotropic half-space subject to a harmonic normal stress uniformly distributed over a circular area with torsional vibrations was developed by Reissner (1936). In 1971, a solution for a rigid circular foundation on the surface of an elastic half-space, covering an extended range of dimensionless frequencies, was presented in graphical and tabular form for coupled horizontal and rocking motions by Veletsos and Wei (1971). By the late 1970's, the capability existed to compute the dynamic stiffness of foundations of arbitrary shape in horizontally stratified soil deposits with any desired degree of accuracy, as long as linear elastic behavior could be assumed.

Seismic studies in soil-structure interaction began in parallel with the early foundation analysis. Early work continued through the 1950's, 60's and 70's with Kausel (1974) developing a substructure approach using linear analysis, that accounts for the response of a rigid foundation to a train of seismic waves. By the late 1970's the basic phenomena of soil-structure interaction was understood. In 1985 the first rigorous and comprehensive treatment of the topic with applications in both machine foundations and seismic problems was addressed by Wolf (1985). Researchers have tried to use simple models to represent the soil such as the simple lumped parameter model consisting of a mass, a spring and a dashpot. As early as 1954, researchers substituted a rotational spring for the foundation in their seismic studies of soil-structure

interaction. Horizontal and rotational springs were used in 1965 to model the soil. Lumped parameter models were used frequently in the late 60's. Work has continued on the improvement of the lumped parameter model, and it is still used today to model soil in various civil engineering applications.

The basic civil engineering problem that applies to this project is the dynamic response of a structure interacting with a soil. The problem is defined as a structure with finite dimensions embedded to some degree in soil, which extends to infinity, with specified loads acting on the structure. It is common to assume the response of the soil and structure will remain linear as is stated by Wolf (1994), "In the majority of cases, both the structure and the soil response will remain linear, but linear analysis is also helpful in more complicated nonlinear areas of application. The results of a nonlinear analysis of certain dynamic systems with strong nonlinearities are often similar to those of a linear calculation." This study assumes linear behavior.

There are two alternate methods for modeling this problem, the direct finite element method and the substructure method. The direct finite element method models the region of linear soil adjacent to the soil-structure interface explicitly with finite elements up to an artificial boundary. The artificial boundary presents some problems in the analysis because it is arbitrary. A large number of degrees of freedom arise from discretizing the adjacent soil region, which requires large computational time. According to Wolf (1994), "a loss of physical insight also results. It follows that the direct finite element method is not appropriate for standard projects of moderate and small sizes." The ship-soil interaction falls into the moderate to small size project range on the scale of typical civil engineering applications.

The substructure method decomposes the global soil-foundation-superstructure system into subsystems, each of which can be analyzed separately using the most appropriate techniques. The irregular (non-linear) structure is modeled with an interconnection of masses, dashpots and springs or equivalently by finite elements. Once the structure is discretized at the nodes located on the structure-soil interface and in its interior, the dynamic equations of motion are developed. The other substructure, the unbounded soil extending to infinity, has equations that are regular and linear. A boundary-integral equation is used to calculate the interaction force-displacement relationship. Dynamic stiffness is the boundary condition used to model the unbounded soil. The responses of the individual subsystems are combined by imposing the interaction conditions

along the separating surfaces. Thus, the overall response of the system is obtained. The substructure method is preferred over the direct finite element method in civil engineering applications.

The equations of motion may be solved in the time domain or the frequency domain. Because ocean waves are a random excitation, frequently described by a sea state and corresponding wave energy spectra, a frequency domain solution to the equations of motion is useful and straight-forward to apply. The solution requires some basic assumptions about the random nature of waves and the linearity of the response. These are discussed in Chapter 3.

In the frequency domain, the excitation can be decomposed using Fourier series and the response determined independently for each Fourier term corresponding to a specific frequency. The dynamic response of the soil is visco-elastic. Damping is modeled using dashpots. The dynamic stiffness of the unbounded visco-elastic soil can be modeled using the boundary-element method or sophisticated finite-element procedures, but these procedures are complicated and require large computation times. Hence, finite-element analysis may not be cost-effective. As Wolf (1994) states, “for most projects the simple physical models of the unbounded soil developed [in his book] can be used”. Lumped parameter models are one of the simple physical models described in his book. This project uses a lumped parameter model to develop the soil reactions for the grounded ship condition.

To find the stiffness and damping coefficients for the lumped parameter model, soil properties are needed. Table 2 from D`Appolonia Consulting Engineers (1979) lists average soil parameter values. Hudson (2001) used the following soil parameter values: sand mass-density = 1,600 kg/m³, Young’s Modulus $E = 60$ MPa and Poisson’s Ratio $\nu = 0.26$. Whitman and Richart (1967) recommend the following values for Poisson’s ratio:

- Sand (dry, moist, partially saturated) $\nu = 0.35-0.4$
- Clay (saturated) $\nu = 0.5$
- A good value for most partially saturated soils is $\nu = 0.4$.

Unless otherwise noted, the soil model developed in this project uses the values from D`Appolonia Consulting Engineers (1979), Table 2. These values are chosen because the work by D`Appolonia Consulting Engineers provides the most comprehensive soil information, and all of the data was generated in the same manner, by the same source.

Table 2 - Soil properties (D`Appolonia Consulting Engineers 1979)

	Sand	Clay (Mud)	Soft Rock (Coral)	Hard Rock
Shear wave velocity, V_s (ft/sec)	1,250	625	2,500	5,000
Poisson's Ratio, ν	0.45	0.499	0.35	0.25
Density, ρ ($10^3 \text{lb}_f\text{-sec}^2/\text{ft}^4$)	4.35×10^{-3}	4.04×10^{-3}	4.66×10^{-3}	4.97×10^{-3}
Shear Modulus, G , ($10^3 \text{lb}_f/\text{ft}^2$)	6.79×10^3	1.58×10^3	29.1×10^3	124.2×10^3

2.2 Lumped Parameter Models

The complex behavior of the soil-structure interaction is modeled using a simple lumped parameter model, which consists of a mass, m (lbm), a spring, k (lb/ft) and a dashpot, c (lb-sec/ft), where the system parameters m , k and c are chosen to match measured response or finite element analysis for each degree of freedom with coupling terms.

For loads applied statically to the structure, the soil is represented by a simple spring. The lumped parameter model is exact for the static case and for the asymptotic value at infinite frequency. The coefficients are frequency dependent.

Wolf (1994) states the model must reflect the following key aspects of the foundation-soil system for all translational and rotational degrees of freedom:

- The shape of the foundation-soil (structure-soil) interface
- The nature of the soil profile
- The amount of embedment
 - Surface - no embedment
 - Embedded - with soil contact along the total height of the wall or only on part of it

D`Appolonia Consulting Engineers (1979) state “both the lumped parameter method and the finite element model can be used for assessing the effect of embedment on the response of a structure. Each method has limitations due to assumptions, but may be used effectively for soil-structure interaction analyses. Lumped parameter methods require more assumptions, but can be

used with an acceptable level of accuracy by using appropriate models. To improve the effectiveness of the lumped parameter method, parametric analyses are needed to reduce uncertainties in determining soil stiffness and damping coefficients under varying conditions of embedment.” The standard lumped parameter method models the static stiffness of the soil half-space using a simple spring with coefficient k . This provides an exact result for static loading. The coefficients of the dashpot, c , and mass, M , are two free parameters that are selected to match as closely as possible the response of the total dynamic system, which may be determined by boundary element or finite element methods. The curve-fitting technique is applied to the total system’s dynamic response and not that of the soil alone as in the substructure method. The mass parameter M is added to that of the structure in the foundation nodes. As Wolf (1994) explains, “this added mass does not mean that an identifiable mass of the soil really exists that moves with the same amplitude and in phase with the structure over the whole range of frequency. It is an additional inertia which provides a better fit between the dynamic response of the lumped parameter model and that of the actual soil.”

The lumped parameter model chosen for use in this project comes from the report, *Stochastic Response of Foundations*, published by Pais and Kausel (1985). In their report they analyze previous data from other researchers that used complex and expensive procedures, such as finite element and boundary element methods, to model soil dynamics and soil-structure interaction. They plot the data presented by various other researchers and curve fit an equation to match the data as accurately as possible. This allows for the use of the simple equations, which match the data well, in applications that do not require large complicated soil models.

The soil model equations presented in Section 2.3 calculate the k and c terms in the transfer function where the mass, M , includes only the mass of the ship. The soil model does not include added mass because the soil added mass values are much less than the ship mass. Once these values are calculated, the soil force and moment terms are added to the hydrodynamic equations of motion for the grounded ship.

2.3 Six Degree of Freedom Soil Model

The Pais and Kausel (1985) soil model applies to rigid foundations embedded in a half-space and subjected to horizontally propagating shear waves, but is valid and useful for other dynamic

problems such as the soil-ship interaction. When seismic waves hit the foundation, which is more rigid than the surrounding soil, the equilibrium and compatibility equations are satisfied by adding the effect of the waves scattered by the foundation and the waves generated by its vibration to the free field motion. Using the superposition theorem, the total dynamic interaction between the soil and the foundation can be separated into two parts, the kinematic and inertial interaction.

The exact solution for the kinematic interaction problem is very complex. Some analytical solutions exist, but only for specific geometries. Analytical solutions were derived for cylindrical or disc shaped foundations. These are the only known geometries to have been solved analytically. Then as the analysis and understanding improved, researchers studied strip foundations, square foundations and then rectangular foundations using finite elements. This project assumes the specific geometry of a rectangular shape to model the ship hull form. Finite element methods solve the kinematic interaction accurately, but they are expensive. In most cases, an approximate solution is adequate. A more detailed and complex solution is only required if it improves the design of the structure; and reliable and accurate data on the properties of the soil and dynamic loads must be available. The modeling of the soil-ship interaction does not warrant large complex soil models.

Pais and Kausel (1985) combine the stiffness and damping coefficients into a single term that they call dynamic stiffness, Equation (2.1):

$$K^d = K^s (k + ia_0 c) \quad (2.1)$$

where:

- K^s is the static stiffness
- a_0 is the dimensionless frequency ($a_0 = \omega B/V_s$, where ω = frequency of the motion, rad/sec, B = width of the foundation, ft, V_s = shear wave velocity in the soil, ft/sec)
- k (stiffness) and c (damping) are functions of a_0 , ν (Poisson's ratio) and degree of embedment E/B (where E = depth of embedment)

In the derivation of the stiffness equations, it is assumed that:

- The elastic medium, which supports the ship, is a homogeneous, isotropic, and semi-infinite body.

- The ship is rigid.
- The ship maintains full contact with the soil.
- There is no slip between the ship and soil.
- The soil remains linear elastic.
- The ship grounding length and embedment are symmetric.
- The soil rate dependency is introduced via a damping coefficient by a dashpot in the lumped parameter model.
- The effective added soil mass is much smaller than the mass of the ship and is neglected in this analysis.
- For the purpose of calculating ground reaction, the hull shapes of the ships are modeled as:
 - Rectangular box shape for cargo type ships
 - Wedge shape for warships
 - Cylindrical shape for submarines
- The geometry of cargo ships is further simplified by not considering a bulbous bow or the small bilge radius as shown in Figure 4. The warship geometry does not account for sonar domes.
- To apply the soil model (which describes the forces and moments on a fully rectangular embedded foundation surrounded by soil on all four sides) to the condition of a stranded ship requires the assumption that the difference between the two situations is minimal. A partially embedded grounded ship, Figure 5, has only three sides that are surrounded by soil versus four sides for a foundation or fully embedded grounded ship. This project assumes that the effect of this discrepancy is small. The soil model assumes that the portion of the grounded ship that is embedded is fully surrounded by soil on all four sides.

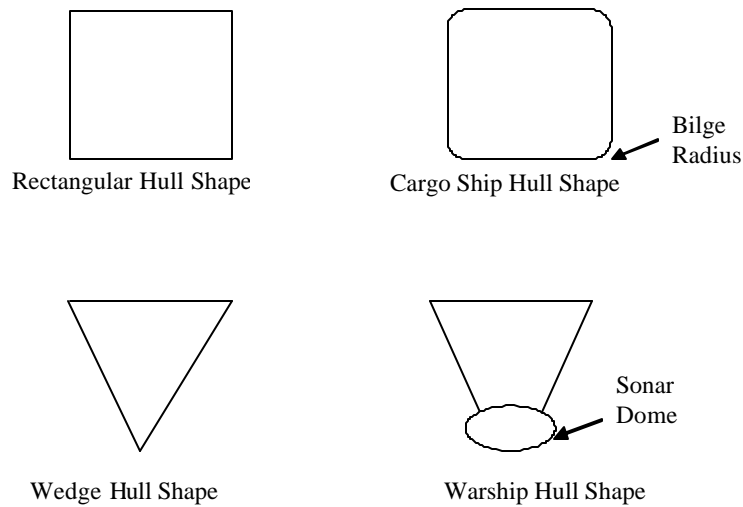


Figure 4 - Hull Shapes

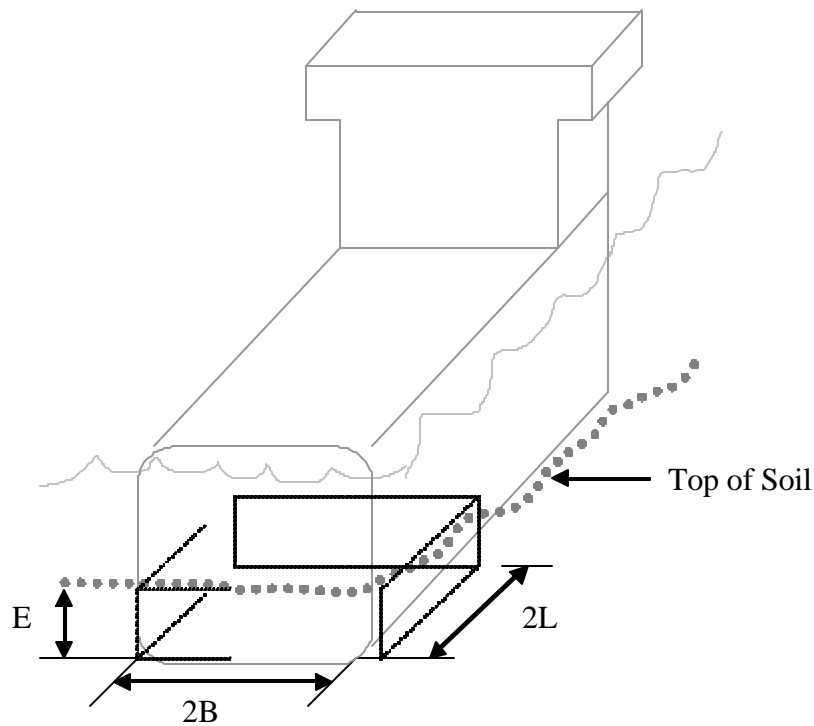


Figure 5 - Stranded and Embedded Ship Modeled as Rectangular Embedded Foundation

The foundation motion is described in six degrees of freedom - three displacements and three rotations. When the foundation vibrates, it generates waves that carry away energy through the soil. This provides damping in the motion of the foundation and is referred to as either radiation or geometric damping. Damping is modeled using a dashpot in the lumped parameter model. To model this energy loss, the soil model used in numerical methods must include a large region beyond the foundation or use finite or boundary elements. The data used for curve-fitting is

found in this manner. This project uses the simple lumped-parameter equations to avoid modeling the soil using finite elements or boundary value methods.

The ship hull is approximated as a rectangular embedded foundation. This is a valid approximation because:

- The shape of a large cargo ship hull is approximately a rectangular shape.
- The ship is rigid, meaning its stiffness is several orders of magnitude larger than the soil stiffness.
- The grounded ship is assumed to have uniform distribution of weight.

Figure 6 shows the six degrees of freedom for a foundation. This project applies this soil model to a grounded ship. Figure 7 shows the six degrees of freedom for a grounded ship. Figure 8 shows the foundation parameters and Figure 9 shows the parameters for the grounded ship. Figure 8 assumes the grounded ship is fully embedded. The soil model allows for a partially embedded ship.

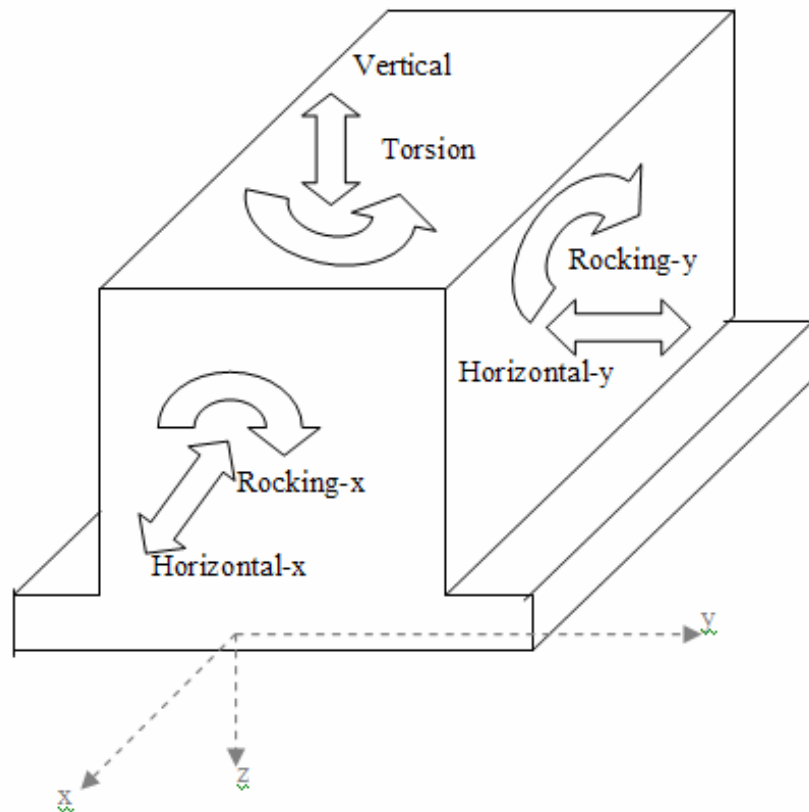


Figure 6 – Six Degrees-of-freedom for a foundation

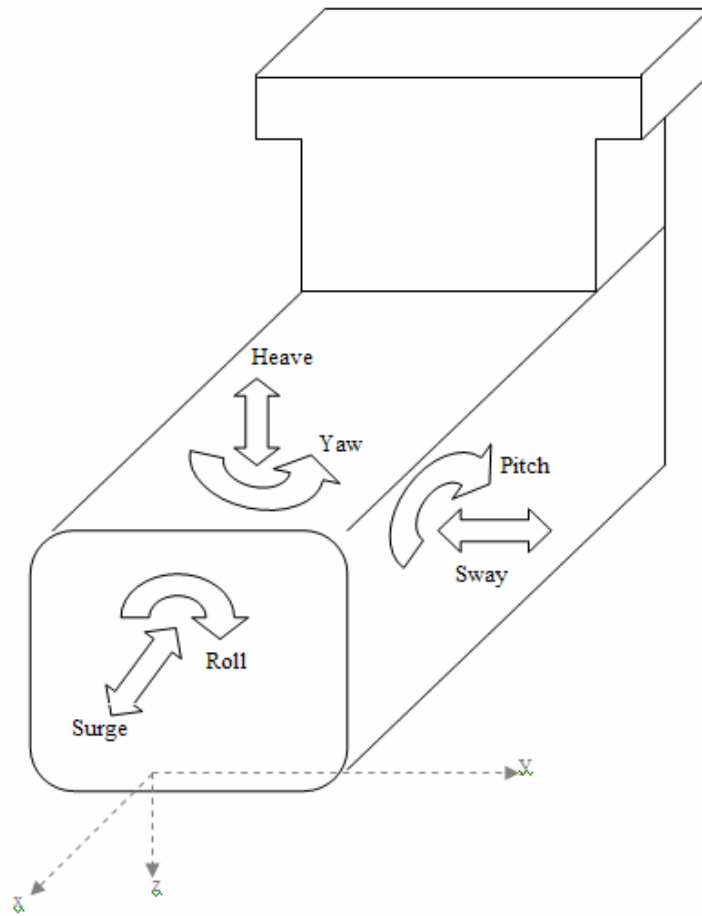


Figure 7 - Six Degrees-of-Freedom for a Ship

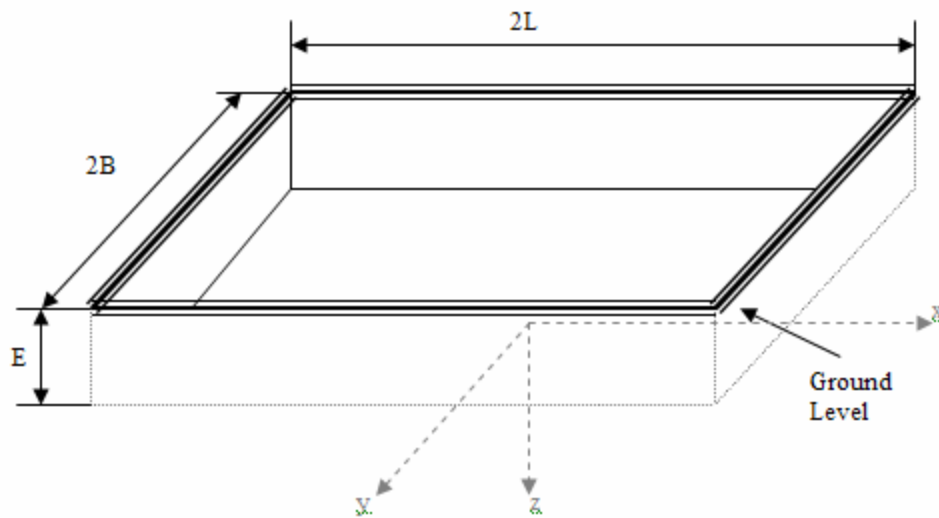


Figure 8 - Rectangular Embedded Foundation ($L > B$)

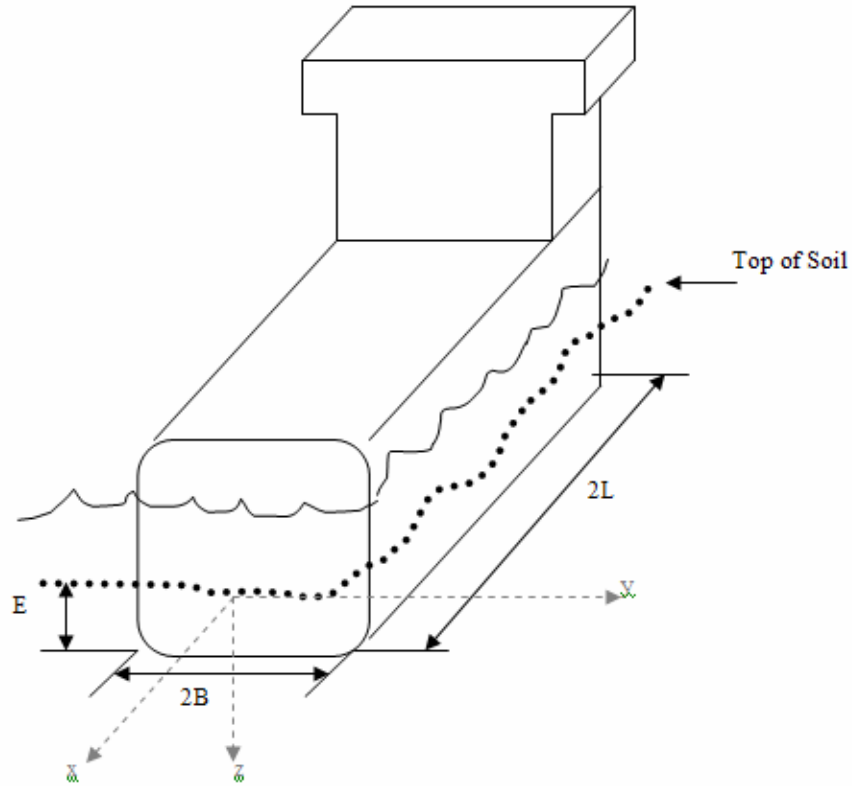


Figure 9 - Stranded and Fully Embedded Ship

Rectangular foundations are assumed to be symmetric. Asymmetry increases the difficulty of the problem, and there are no analytical solutions available, even for the surface foundation. The ratio of the length to width, L/B , which defines the geometry of

the foundation, must be considered. It is assumed that the foundation length is greater than the foundation width, $L > B$, which is a reasonable assumption because the ship length is greater than the ship width. The dependence on Poisson's ratio, ν , is assumed to be the same for embedded and surface foundations. The influence of Poisson's ratio on the variation of the stiffness with frequency is not taken into account. The amount of material damping is assumed to be independent of the value of Poisson's ratio.

To build the model of the embedded rectangular foundation, the static stiffnesses of a surface rectangular foundation are required. Equations (2.2) to (2.7) calculate static stiffness, K^o for each degree of freedom. The superscripts o , s , and d refer to the stiffness for a static surface, static embedded and dynamic embedded foundation, respectively. The static coupling stiffnesses are neglected in the equations because their values are very small for a surface foundation.

These equations approximate data found by boundary integral methods for a square foundation. The equations compare well with the results for a square foundation calculated by Abascal (1984), Dominguez (1978), and Wong and Luco (1978). To represent the variation of the static stiffnesses with the shape of the foundation (length-width ratio, L/B) with $\nu = 1/3$, the equations approximate the data found by Wong and Luco, and Dominguez for various L 's and B 's.

$$\text{Vertical (Heave)} \quad K_V^O = \frac{[3.1(L/B)^{0.75} + 1.6]GB}{(1-n)} \quad (2.2)$$

$$\text{Horizontal- x (Surge)} \quad K_{Hx}^O = \frac{[6.8(L/B)^{0.65} + 2.4]GB}{(2-n)} \quad (2.3)$$

$$\text{Horizontal- y (Sway)} \quad K_{Hy}^O = \frac{K_{Hx}^O (2-n) + 0.8(L/B-1)GB}{(2-n)} \quad (2.4)$$

$$\text{Rocking- x (Roll)} \quad K_{Rx}^O = \frac{[3.2(L/B) + 0.8]GB^3}{(1-n)} \quad (2.5)$$

$$\text{Rocking- y (Pitch)} \quad K_{Ry}^O = \frac{[3.73(L/B)^{2.4} + 0.27]GB^3}{(1-n)} \quad (2.6)$$

$$\text{Torsion (Yaw)} \quad K_t^O = [4.25(L/B)^{2.45} + 4.06]GB^3 \quad (2.7)$$

where G is the soil shear modulus.

The exponent of (L/B) in Equations (2.2) to (2.7) is less than one for the vertical and horizontal modes, equal to one for rocking around the longitudinal axis, and greater than one for the torsion mode and rocking around a transverse axis. These values approach the stiffness of a strip foundation as the length/width ratio increases.

With the static stiffness for a surface rectangular foundation defined, the equations for an embedded rectangular foundation are developed. The equations assume the stiffness depend linearly on the depth of embedment, E . The determination of the stiffnesses of rectangular embedded foundations is a very complex problem and therefore there is very little data available. Dominguez (1978) obtained results for square and rectangular ($L/B = 2$) embedded foundations and Abascal (1984) analyzed a square foundation. In both studies the maximum amount of embedment analyzed was equal to the width of the foundation, $E/B = 2$.

Pais and Kausel (1985) developed the following equations for static stiffness as a function of embedment:

$$\text{Vertical (Heave)} \quad K_V^S = K_V^O \left[1.0 + \left(0.25 + \frac{0.25}{L/B} \right) (E/B)^{0.8} \right] \quad (2.8)$$

$$\text{Horizontal-x (Surge)} \quad K_{Hx}^S = K_{Hx}^O \left[1.0 + \left(0.33 + \frac{1.34}{1 + L/B} \right) (E/B)^{0.8} \right] \quad (2.9)$$

$$\text{Horizontal-y (Sway)} \quad K_{Hy}^S = K_{Hy}^O \left[1.0 + \left(0.33 + \frac{1.34}{1 + L/B} \right) (E/B)^{0.8} \right] \quad (2.10)$$

$$\text{Rocking-x (Roll)} \quad K_{Rx}^S = K_{Rx}^O \left[1.0 + E/B + \left(\frac{1.6}{0.35 + (L/B)} \right) (E/B)^2 \right] \quad (2.11)$$

$$\text{Rocking-y (Pitch)} \quad K_{Ry}^S = K_{Ry}^O \left[1.0 + E/B + \left(\frac{1.6}{0.35 + (L/B)^4} \right) (E/B)^2 \right] \quad (2.12)$$

$$\text{Torsion (Yaw)} \quad K_t^S = K_t^O \left[1.0 + \left(1.3 + \frac{1.32}{L/B} \right) (E/B)^{0.9} \right] \quad (2.13)$$

These equations agree well with Abascal's results. The dependence on the depth of embedment is not linear, the exponent (E/B) is less than one, except for rocking where a second-degree parabola gives good agreement. The asymptotic values for a strip foundation are matched for both rocking around the x-axis and for swaying along the y-axis. When the foundation is very long, its stiffness in the short direction should approach the stiffness of a strip foundation, which is 2-D. The effect of embedment was assumed to be split evenly between each side, because a strip foundation has only two sides instead of four as shown in Figure 10.

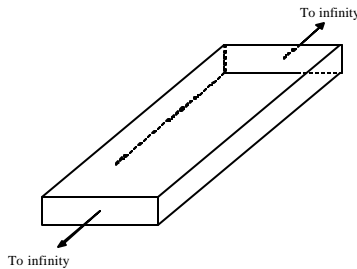


Figure 10 - Strip Foundation

The decay with the ratio (L/B) is such that the error relative to Dominguez's results is more or less constant. As shown by Dominguez, the height of the center of stiffness is approximately

1/3 of the height of embedment. The coupling stiffness is not as important and can be taken simply as:

Coupling of Horizontal-x (Surge) and Rocking-x (Roll):

$$K_{HRx}^S = \frac{1}{3}(E/B) K_{Hx}^S \quad (2.14)$$

Coupling of Horizontal-y (Sway) and Rocking-y (Pitch):

$$K_{HRy}^S = \frac{1}{3}(E/B) K_{Hy}^S \quad (2.15)$$

Pais and Kausel acknowledge that stiffness in the vertical and rocking modes depends on the value of Poisson's ratio, but for simplicity its influence is not taken into account. So for values of ν that are higher than 0.4 the equations should be used with care especially at high frequencies. The equations produce acceptable results in the high frequency range because the imaginary part of the stiffness is much more important than the real part.

Dynamic stiffness is derived from static stiffness with embedment by including damping and considering the frequency of motion. There are two types of damping in the real system: one introduced by the loss of energy through propagation of elastic waves away from the immediate vicinity of the foundation, the other associated with internal energy losses within the soil due to hysteretic and viscous effects. The equivalent damping corresponding to the elastic-wave propagation is called geometric damping or radiation damping. The lumped damping parameter for any particular foundation-soil system includes both the effects of geometric and internal damping.

Dominguez (1978) and Abascal (1984) present data showing the variation of the stiffness in the low frequency range ($a_0 < 1.5$ from Dominguez and $a_0 < 2.0$ from Abascal, where a_0 refers to the dimensionless frequency by the equation, where V_s is the soil shear wave velocity:

$$a_o = \frac{\omega B}{V_s} \quad (2.16)$$

This corresponds to frequencies less than 0.33 rad/sec and 0.44 rad/sec for a 50-foot wide ship grounded in clay (mud); or 2.62 rad/sec and 3.5 rad/sec for a 50-foot wide ship grounded in hard rock. This is well within the frequency range of ocean wave energy. It is assumed that the

variation of the stiffness with frequency is the same for surface and embedded foundations, because of the lack of better data.

Equations (2.17) through (2.26) define dynamic stiffness based on the Dominguez (1978) and Abascal (1984) data. A coefficient \mathbf{a} is used to represent the ratio between the celerity of pressure waves and shear waves.

$$\text{Note: } L \geq B; a_o = \frac{wB}{V_s}; \mathbf{a} = \frac{V_p}{V_s} = \sqrt{\frac{2(1-n)}{1-2n}}; \mathbf{a} \leq 2.45 \quad (2.17)$$

$$\text{Vertical (Heave)} \quad K_{33}^d = \bar{K}_V^d = K_V^S (k + ia_o c) \quad (2.18)$$

$$k = 1.0 - \frac{da_o^2}{b + a_o^2} \quad c = \frac{4[\mathbf{a} L/B + \frac{E}{B}(1 + L/B)]}{K_V^S}$$

$$d = 0.4 + \frac{0.2}{L/B} \quad b = \frac{10.0}{1 + 3(L/B - 1)}$$

$$\text{Horizontal-x (Surge)} \quad K_{11}^d = \bar{K}_{Hx}^d = K_{Hx}^S (k + ia_o c) \quad (2.19)$$

$$k = 1.0 \quad c = \frac{4[L/B + E/B(\mathbf{a} + L/B)]}{K_{Hx}^S}$$

$$\text{Horizontal-y (Sway)} \quad \bar{K}_{Hy}^d = K_{Hy}^S (k + ia_o c) \quad (2.20)$$

$$k = 1.0 \quad c = \frac{4[L/B + E/B(1 + \mathbf{a} L/B)]}{K_{Hy}^S}$$

$$\text{Rocking-x (Roll)} \quad K_{44}^d = \bar{K}_{Rx}^d = K_{Rx}^S (k + ia_o c) \quad (2.21)$$

$$k = 1.0 - \frac{da_o^2}{b + a_o^2} \quad d = 0.55 + 0.1\sqrt{L/B - 1}$$

$$b = 2.4 - \frac{0.4}{(L/B)^3}$$

$$c = \frac{4[\frac{1}{3}(E/B) + \frac{1}{3}(E/B)^3 + \frac{\mathbf{a}}{3}(L/B)(E/B)^3 + (E/B)(L/B) + \frac{\mathbf{a}}{3}(L/B)]}{K_{Rx}^S} \cdot \frac{a_o^2}{f + a_o^2} + D \frac{f}{f + a_o^2}$$

$$f = 2.2 - \frac{0.4}{(L/B)^3} \quad D = \frac{\frac{4}{3}(\mathbf{a} \frac{L}{B} + 1)(E/B)^3}{K_{Rx}^S}$$

Rocking-y (Pitch) $K_{55}^d = \bar{K}_{Ry}^d = K_{Ry}^S (k + ia_o c)$ (2.22)

$$k = 1.0 - \frac{0.55a_o^2}{b + a_o^2} \quad b = 0.6 + \frac{1.4}{(L/B)^3}$$

$$c = \frac{4[\frac{1}{3}(L/B)^3(E/B) + \frac{a}{3}(E/B)^3(L/B) + \frac{1}{3}(E/B)^3 + (E/B)(L/B)^2 + \frac{a}{3}(L/B)^3]}{K_{Ry}^S} \bullet \frac{a_o^2}{f + a_o^2} + D \frac{f}{f + a_o^2}$$

$$f = \frac{1.8}{1.0 + 1.75(L/B - 1)} \quad D = \frac{\frac{4}{3}(L/B + a)(E/B)^3}{K_{Ry}^S}$$

Torsion (Yaw) $K_{66}^d = \bar{K}_t^d = K_t^S (k + ia_o c)$ (2.23)

$$k = 1.0 - \frac{da_o^2}{b + a_o^2} \quad d = 0.33 - 0.03\sqrt{L/B - 1}$$

$$b = \frac{0.8}{1 + 0.33(L/B - 1)}$$

$$c = \frac{4[(L/B)(E/B) + \frac{a}{3}(L/B)^3(E/B) + (L/B)^2(E/B) + \frac{1}{3}(L/B)^3 + \frac{1}{3}(L/B)]}{K_t^S} \bullet \frac{a_o^2}{f + a_o^2}$$

$$f = \frac{1.4}{1 + 3(L/B - 1)^{0.7}}$$

Coupling

Coupling of Horizontal-x (Surge) and Rocking-x (Roll):

$$K_{41}^d = \bar{K}_{HRx}^d = \frac{1}{3}(E/B) \bar{K}_{Hx}^d \quad (2.24)$$

Coupling of Horizontal-y (Sway) and Rocking-y (Pitch):

$$K_{45}^d = \bar{K}_{HRy}^d = \frac{1}{3}(E/B) \bar{K}_{Hy}^d \quad (2.25)$$

Additional coupling is also generated due to moments around the origin in the equations of motion (COG in this project) because the ground reaction force is not located at the origin, Equation (2.26). Otherwise $K_{jk}^d = 0$.

$$\begin{aligned} K_{42}^d &= -z_{ground} K_{22}^d \\ K_{51}^d &= z_{ground} K_{11}^d \\ K_{53}^d &= -x_{ground} K_{33}^d \\ K_{62}^d &= x_{ground} K_{22}^d \end{aligned} \quad (2.26)$$

The asymptotic values of the coefficient c are obtained by computing geometrical inertias and areas. The rocking modes exhibit a non-zero value of c in the static case. This value is chosen in such a way that it is related to the translation of the sidewalls during rotation of the foundation, and it agrees well with Abascal's results.

The soil model also requires assumptions in its development and application. The assumption that the soil is a homogeneous, isotropic, elastic body is not exact. Often a soil stratum is layered and may have a hard stratum of soil or rock at a shallow depth below the grounded ship. The amplitudes of vibration at resonance increase by the presence of the underlying rigid layer. This indicates that radiation of energy from the grounded ship is impeded by the presence of the rigid layer and that part of this elastic-wave energy is reflected back to the grounded ship. Further studies need to be conducted on the damping related to vibrations of grounded ships supported by layered media as well as of grounded ships supported by soils, which vary in stiffness with depth or confining pressure. During the vibration of foundations, there is a mass of soil under the foundation, which vibrates along with the foundation.

Since it is assumed that the ship maintains contact with the soil without slip or separation, all friction and suction effects depend on internal soil properties and response. Separation occurs when a partial gap forms between the side-wall and the adjacent soil of an embedded foundation for large seismic excitation because tension is not sustained in soil. In the grounded ship case, separation may occur after the ship rocks back and forth causing a gap between the embedded ship structure and the surrounding soil. This is a non-linear effect that can be approximated. In Wolf and Weber (1986), they analyze the effects of soil separation. For the case of separation occurring between a circular cavity and the adjacent thin layer, the effect was minimal on the spring coefficient, but the effect halved the damping coefficient for horizontal and vertical motions when compared to the linear case. For the torsion and rocking degrees of freedom, the spring coefficients are halved and the damping coefficients are reduced somewhat less. Separation effects similar to these are also discussed in Gazetas (1983). Separation effects are neglected in this analysis because of their complexity; however they may require consideration in future work.

CHAPTER 3 GROUNDED SHIP MOTIONS

3.1 *Overview of the Chapter*

This chapter provides an overview of the method used to compute the dynamic response of a grounded ship in regular waves. The method derived is based on the linear theory of ship motions (Salvesen et al 1970). The first section of this chapter provides a description of the coordinate systems used to describe wave and ship motions in regular waves. The second section summarizes the derivation of the equations of motion in six degrees of freedom: surge, sway, heave, roll, pitch, and yaw. This derivation is adapted from Lloyd (1998). The primary differences between this model and typical strip theory seakeeping models is the inclusion of ground reaction forces, the assumption that the ship has zero forward speed and the calculation of waterplane characteristics around the center of ground reaction. Following this is a brief summary of strip theory and the derivation of hydrodynamic coefficients (SNAME 1989). A simplified multi-pole method using Lewis forms is used to determine 2-D added mass and damping coefficients. This is advantageous because only load waterline beam, draft and sectional area are required for the equilibrium position of the stranded ship. Surge coefficients are calculated using Journee's (2001) empirical method based on theoretical results from 3-D calculations. Strip theory provides reasonably accurate results with minimal computational effort relative to other methods. It is sufficient for a first approximation of grounded ship motions and loads. Once it is determined that the magnitude of these loads is significant, model testing and a more sophisticated analysis may be performed.

3.2 *Frames of Reference*

The following right-handed coordinate systems are used to describe grounded ship motions. Figure 11 corresponds with this description.

- $(E \ x \ y \ z)$ is fixed to the earth at E with the x -axis in the direction of advance of the incident waves, the $E \ x \ y$ plane is at the calm water level, and the z -axis is positive downwards. This system is used to define the incident waves.

- $(O \ x_1 \ x_2 \ x_3)$ is also fixed to the earth at O , but is rotated through the heading angle, μ , so that $O \ x_1$ coincides with the mean heading of the ship. O and E are in the same location. The $O \ x_1 \ x_2$ plane is at the calm water level, and the x_3 -axis is positive downwards.
- The mean position of the center of gravity of the ship, G_0 , lies vertically above O and is taken as the origin of the axis system $G_0 \ x_1 \ x_2 \ x_3$.
- Another right handed set of axes $G \ x_{b1} \ x_{b2} \ x_{b3}$ is fixed in the ship and is used to define locations within the structure of the ship. The $G \ x_{b1} \ x_{b3}$ plane corresponds with the ship's centerline plane, and is a plane of port and starboard symmetry. The positive x_{b1} axis points to the bow, the positive x_{b2} axis points to starboard, and the positive x_{b3} axis points vertically downwards. The point, G , is located at $(0, 0, 0)$ in this system. When the ship is not in motion, the coordinate systems $G_0 \ x_1 \ x_2 \ x_3$ and $G \ x_{b1} \ x_{b2} \ x_{b3}$ are coincident.

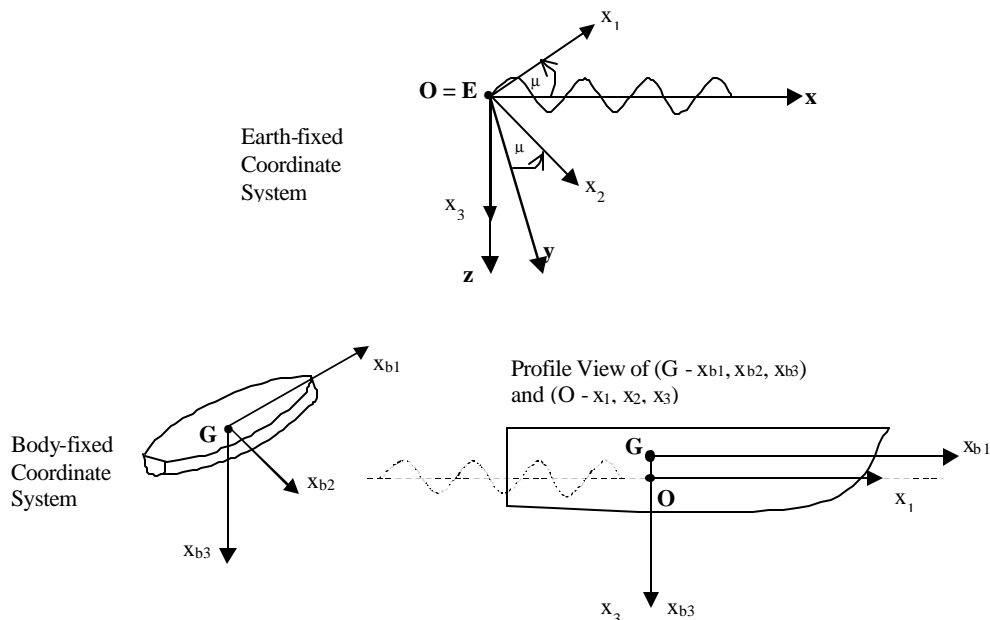


Figure 11 - Frames of Reference

At any instant of time, ship motions are measured as displacements of the ship's center of gravity, G , relative to the origin, G_0 . The six degrees of freedom include three translations: surge (x_1), sway (x_2) and heave (x_3); and three rotations: roll (x_4), pitch (x_5) and yaw (x_6), as shown in Figure 12.

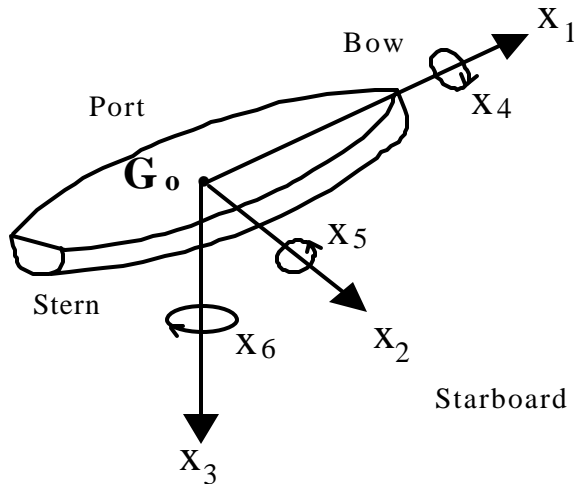


Figure 12 - Six degrees of freedom of a ship

For deep-water waves, the wave depression at any point relative to G_0 x_1 x_2 x_3 is:

$$z = z_o \sin(kx_1 \cos \mathbf{m} - kx_2 \sin \mathbf{m} - \mathbf{w}t) \quad (3.1)$$

where k is the wave number, \mathbf{w} is the circular wave frequency, λ is the wave length, T is the wave period, z_o is the wave amplitude and the time t is measured from an arbitrary datum.

3.3 Equations of Motion

3.3.1 Assumptions

In deriving the equations of motion, the following assumptions are made:

- The ship is aground and has zero forward speed.
- The grounded equilibrium condition for the ship is known.
- Waves are regular (sinusoidal) with deep-water dispersion.
- The heading of the ship has a constant angle, \mathbf{m} measured in a counter-clockwise direction from the wave direction of travel.
- There are no transient effects due to initial conditions; linear dynamic motions and loads are harmonically oscillating with the same frequency as the wave excitation.
- The motions are small relative to the inertial reference frame. This assumption is valid for a stable ship with small incident wave amplitude, but it is not valid in near-resonant conditions. This assumption is necessary to linearize the problem.

- For the net hydrostatic force calculation, it is assumed that the vessel rotates in the roll, pitch and yaw degrees of freedom about a point which is on the centerline above the longitudinal center of the ground reaction at the waterline. This is only valid for small motions. This point is the grounded longitudinal center of flotation.

3.3.2 General Equations for Ship Motions in Regular Waves

Starting with Newton's Second Law, $\mathbf{F} = m\mathbf{a}$, applied in the inertial coordinate system, the equations of motion are derived for six degrees of freedom:

$$\sum_{j=1}^6 \Delta_{ij} \cdot \ddot{x}_j(t) = F_i(t) \quad (i = 1, 2 \dots 6) \quad (3.2)$$

where Δ_{ij} denotes the components of the inertia matrix for the ship:

$$\Delta_{ij} = \begin{bmatrix} m & 0 & 0 & 0 & m\bar{x}_{b3} & 0 \\ 0 & m & 0 & -m\bar{x}_{b3} & 0 & m\bar{x}_{b1} \\ 0 & 0 & m & 0 & -m\bar{x}_{b1} & 0 \\ 0 & -m\bar{x}_{b3} & 0 & I_{44} & 0 & -I_{46} \\ m\bar{x}_{b3} & 0 & -m\bar{x}_{b1} & 0 & I_{55} & 0 \\ 0 & m\bar{x}_{b1} & 0 & -I_{46} & 0 & I_{66} \end{bmatrix} \quad (3.3)$$

With the following assumptions:

- motions are linear and small with no transient effects,
- the ship has port/starboard symmetry, and
- the origin is at the center of gravity,

The inertia matrix reduces to the following for motions around the center of gravity:

$$\Delta_{ij} = \begin{bmatrix} m & 0 & 0 & 0 & 0 & 0 \\ 0 & m & 0 & 0 & 0 & 0 \\ 0 & 0 & m & 0 & 0 & 0 \\ 0 & 0 & 0 & I_{44} & 0 & -I_{46} \\ 0 & 0 & 0 & 0 & I_{55} & 0 \\ 0 & 0 & 0 & -I_{46} & 0 & I_{66} \end{bmatrix} \quad (3.4)$$

I_{46} , the roll-yaw product, is the only product of inertia that remains with the origin at the center of gravity. In typical ships it is small and is often neglected.

The equations of motion reduce to:

$$\begin{aligned}
m(\ddot{x}_1) &= \mathbf{F}_1 \\
m(\ddot{x}_2) &= \mathbf{F}_2 \\
m(\ddot{x}_3) &= \mathbf{F}_3 \\
I_{44}\ddot{x}_4 - I_{46}\ddot{x}_6 &= \mathbf{F}_4 \\
I_{55}\ddot{x}_5 &= \mathbf{F}_5 \\
I_{66}\ddot{x}_6 - I_{64}\ddot{x}_4 &= \mathbf{F}_6
\end{aligned} \tag{3.5}$$

3.4 Forces and Motions

Considering the gravitational, fluid and ground reaction forces acting on the ship :

$$\sum_{j=1}^6 \Delta_{ij} \cdot \ddot{x}_j(t) = F_i(t) = F_{Gi} + F_{Hi} + F_{Groundi} \quad (i = 1, 2 \dots 6) \tag{3.6}$$

where F_{Gi} is the component of the gravity force acting on the vessel in the i -direction, F_{Hi} is the component of the fluid forces acting in the i -direction, and $F_{Ground i}$ is the component of the ground reaction force acting in the i -direction.

In linear theory, the responses of the vessel are linear with wave amplitude and occur at the frequency at which the ship perceives the incident waves. As a result, the time-dependent responses of the vessel, $x_j(t)$, are sinusoidal at the frequency of encounter (\mathbf{w}_e).

$$x_j(t) = \overline{x_j} e^{i\mathbf{w}_e t} \tag{3.7}$$

In this case, there is no forward speed, so the frequency of encounter is the wave frequency (\mathbf{w}):

$$\begin{aligned}
\mathbf{w}_e &= \mathbf{w} - \frac{\mathbf{w}^2}{g} U_0 \cos \mathbf{m} \\
\mathbf{w}_e &= \mathbf{w} \quad (\text{for } U = 0) \\
&\text{and} \\
x_j(t) &= \overline{x_j} e^{i\mathbf{w} t}
\end{aligned} \tag{3.8}$$

Since the mean gravitational forces F_{Gi} plus equilibrium (static) ground reaction forces $F_{GroundSi}$ cancel the mean grounded equilibrium buoyant (hydrostatic) forces, they can be combined with the hydrostatic part of the fluid forces to give the net hydrostatic fluid forces:

$$F_{HSi}^* = F_{Gi} + F_{HSi} + F_{GroundSi} \tag{3.9}$$

where net fluid forces F_{Hi} and ground reaction forces $F_{Groundi}$ are the sum of static and dynamic components:

$$\begin{aligned}
F_{Hi} &= F_{HSi} + F_{HDi} \\
F_{Groundi} &= F_{GroundSi} + F_{GroundDi} \\
\sum_{j=1}^6 \Delta_{ij} \ddot{x}_j(t) &= F_{Gi} + F_{HSi} + F_{HDi} + F_{GroundSi} + F_{GroundDi} = F_{HSi}^* + F_{HDi} + F_{GroundDi}
\end{aligned} \tag{3.10}$$

Details of the integral evaluation for the net hydrostatic forces are found in Newman (1977). For a vessel with port and starboard symmetry, the net hydrostatic forces are:

$$\begin{aligned}
(\text{Surge}) \quad F_{HS1}^* &= 0 \\
(\text{Sway}) \quad F_{HS2}^* &= 0 \\
(\text{Heave}) \quad F_{HS3}^* &= -\mathbf{r}gSx_3 + \mathbf{r}gS_1x_5 \\
(\text{Roll}) \quad F_{HS4}^* &= -\mathbf{r}g\nabla GM_T x_4 \\
(\text{Pitch}) \quad F_{HS5}^* &= \mathbf{r}gS_1x_3 - \mathbf{r}gS_2x_5 \\
(\text{Yaw}) \quad F_{HS6}^* &= 0
\end{aligned} \tag{3.11}$$

where \overline{GM}_T is the grounded transverse metacentric height, and:

$$S = A_w = \text{grounded waterplane area} = \int_L B(x)dx$$

$$S_1 = \text{first moment of grounded waterplane area around O below } G_0 = \int_L xB(x)dx$$

$$S_2 = \text{second moment of waterplane area around O below } G_0 = \int_L x^2 B(x)dx$$

$$B(x) = \text{local Breadth of grounded waterplane at } x$$

The equations for the net hydrostatic force may also be written in a general matrix notation format with hydrostatic stiffness coefficients:

$$F_{HSj}^* = -\sum_{k=1}^6 C_{jk}^H \bar{x}_k e^{ivt} \quad (j = 1,2,..6) \tag{3.12}$$

where $C_{jk}^H = 0$ except:

$$\begin{aligned}
C_{33}^H &= \mathbf{r}gS \\
C_{35}^H &= C_{53}^H = -\mathbf{r}gS_1 \\
C_{44}^H &= \mathbf{r}g\nabla GM_T \\
C_{55}^H &= \mathbf{r}gS_2
\end{aligned} \tag{3.13}$$

The dynamic ground reaction F_{GroundDi} is defined using the ‘‘Dynamic Stiffness’’ Equations (2.17) through (2.26) developed in Chapter 2. Because this form of stiffness includes damping and frequency dependence, it is added to the other force terms in the frequency domain form of the equations of motion, Equation (3.23).

3.4.1 Hydrodynamic Forces

The contributions from hydrodynamic forces (F_{HDj}) are calculated using Bernoulli's equation with zero forward speed:

$$F_{HDi} = \mathbf{r} \iint_S \left(-\frac{\partial \Phi}{\partial t} - \frac{1}{2} \nabla \Phi \bullet \nabla \Phi \right) n_i ds \tag{3.14}$$

The complete derivation of the hydrodynamic forces acting on the ship is described in detail in Salvesen et al (1970), and SNAME (1989). Hydrodynamic forces resulting from ship motion are linearized as a function of the ship displacement velocities and accelerations. The remaining hydrodynamic forces are due to the incident and diffracted waves:

$$F_{HDi} = -\sum_{j=1}^6 [A_{ij} \ddot{x}_j + B_{ij}^H \dot{x}_j] + F_i^I + F_i^D \tag{3.15}$$

where $F_i^I + F_i^D$ are the forces due to incident and diffracted waves respectively, A_{ij} is the hydrodynamic added mass term and B_{ij}^H is the hydrodynamic damping term. The coefficients for added mass (A_{ij}), damping (B_{ij}^H), and the diffracted wave force complex amplitude are found using strip theory. The Froude-Krylov exciting force, $\overline{F_i^I}$, is found by direct integration of the incident wave potential over the ship hull.

3.4.2 Strip Theory

To find $A_{ij}, B_{ij}, \overline{F_i^D}$ the hydrodynamic problem must be solved. Strip theory (Salvesen 1970) is used to calculate local (strip) hydrodynamic coefficients (2-D problem) and to integrate these local coefficients along the length of the ship to calculate ship coefficients in 5 DOF. Surge coefficients are calculated using Journee's (2001) empirical method based on theoretical results from 3-D calculations. Strip theory provides reasonably accurate results with minimal computational effort relative to other methods. It is sufficient for a first approximation of grounded ship motions and loads. Once it is determined that the magnitude of these loads is significant, model testing and a more sophisticated analysis may be performed.

In strip theory, the following standard assumptions are made:

1. The ship is slender (Length \gg Beam or Draft).
2. The hull is rigid so that no flexure of the structure occurs (rigid body motion).
3. No planning hulls.
4. The motions are small.
5. The ship hull sections are wall-sided.
6. The water depth is much greater than the wave length so that deep water wave approximations may be applied.
7. The presence of the hull has no effect on the waves (Froude-Krylov hypothesis).

Local coefficients are calculated by solving the 2-D hydrodynamic mixed boundary value problem. Methods for solving for these coefficients were developed by Ursell (1949), Grim and Kirsch (1966), and others. These methods generally begin by examining the properties of a cylinder of infinite length, floating in water of infinite depth and oscillating in small harmonic motion. The oscillating cylinder generates surface waves, which radiate away from the cylinder. The coefficients are then calculated with the usual potential flow assumptions of negligible viscosity and compressibility, no flow separation and no skin friction. Ursell presents a comprehensive treatment of this problem. SNAME 1989 also provides an in-depth discussion of this material.

Since ship hull sections are generally not circular in shape, conformal mapping is used to extend the results for a cylinder into solutions for more realistic hull shapes. This is accomplished by defining a mapping function, which can map the ship section to a circular

section. Once this mapping is defined, it can be used with Ursell's known solution for a circular cylinder to find the solution for the actual ship section. In this project, a simplified multi-pole method using Lewis forms is used to determine 2-D added mass and damping coefficients. This is advantageous because only the load waterline beam, draft and sectional area are required to define the equilibrium position of the stranded ship. Surge coefficients are calculated using Journee's (2001) empirical method based on theoretical results from 3-D calculations. Since the contribution of large bulbous sections to the total added mass and damping can be significant, the problem cannot be by-passed. To solve this problem, a family of bulbous section representations was created and a procedure derived for the calculation of added mass and damping of these sections (Demanche 1968). This method is used in this project.

Once local coefficients are calculated, they are integrated along the length of the ship to obtain ship coefficients as shown in Equations (3.16) thru (3.21) where A_{jk} and B_{jk}^H equal zero except for:

Sway (x_2):

$$\begin{aligned}
 A_{22} &= \int a'_{22} dx_{b1} \\
 B_{22}^H &= \int b'_{22} dx_{b1} \\
 A_{24} &= \int a'_{24} dx_{b1} - OG \int a'_{22} dx_{b1} \\
 B_{24}^H &= \int b'_{24} dx_{b1} - OG \int b'_{22} dx_{b1} \\
 A_{26} &= \int x_{b1} a'_{22} dx_{b1} \\
 B_{26}^H &= \int x_{b1} b'_{22} dx_{b1}
 \end{aligned} \tag{3.16}$$

Heave (x_3):

$$\begin{aligned}
 A_{33} &= \int a'_{33} dx_{b1} \\
 B_{33}^H &= \int b'_{33} dx_{b1} \\
 A_{35} &= - \int x_{b1} a'_{33} dx_{b1} \\
 B_{35}^H &= - \int x_{b1} b'_{33} dx_{b1}
 \end{aligned} \tag{3.17}$$

Roll (x_4):

$$\begin{aligned}
A_{44} &= \left[a'_{44} dx_{b1} - 2OG \right] a'_{42} dx_{b1} \\
B_{44}^H &= \left[b'_{44} dx_{b1} - 2OG \right] b'_{42} dx_{b1} + OG \left[b'_{22} dx_{b1} \right] \\
A_{42} &= \left[a'_{42} dx_{b1} - OG \right] a'_{22} dx_{b1} \\
B_{42}^H &= \left[b'_{42} dx_{b1} - OG \right] b'_{22} dx_{b1} \\
A_{46} &= \left[x_{b1} a'_{42} dx_{b1} - OG \right] x_{b1} a'_{22} dx_{b1} \\
B_{46}^H &= \left[x_{b1} b'_{42} dx_{b1} - OG \right] x_{b1} b'_{22} dx_{b1}
\end{aligned} \tag{3.18}$$

Pitch (x_5):

$$\begin{aligned}
A_{55} &= \left[x_{b1}^2 a'_{33} dx_{b1} \right] \\
B_{55}^H &= \left[x_{b1}^2 b'_{33} dx_{b1} \right] \\
A_{53} &= - \left[x_{b1} a'_{33} dx_{b1} \right] = A_{35} \\
B_{53}^H &= - \left[x_{b1} b'_{33} dx_{b1} \right]
\end{aligned} \tag{3.19}$$

Yaw (x_6):

$$\begin{aligned}
A_{66} &= \left[x_{b1}^2 a'_{22} dx_{b1} \right] \\
B_{66}^H &= \left[x_{b1}^2 b'_{22} dx_{b1} \right] \\
A_{62} &= \left[x_{b1} a'_{22} dx_{b1} \right] = A_{26} \\
B_{62}^H &= \left[x_{b1} b'_{22} dx_{b1} \right] \\
A_{64} &= \left[x_{b1} a'_{24} dx_{b1} - OG \right] x_{b1} a'_{22} dx_{b1} \\
B_{64}^H &= \left[x_{b1} b'_{24} dx_{b1} - OG \right] x_{b1} b'_{22} dx_{b1}
\end{aligned} \tag{3.20}$$

Surge (x_1):

$$\begin{aligned}
A_{11} &= \left[a'_{11} dx_{b1} \right] \\
B_{11}^H &= \left[b'_{11} dx_{b1} \right]
\end{aligned} \tag{3.21}$$

3.5 Solving the Equations of Motion

3.5.1 Ship Motions

Substituting Equations (3.12) and (3.15) into Equation (3.10) and rearranging terms results in the linear differential equations of motion for a grounded ship in waves:

$$\sum_{k=1}^6 \Delta_{jk} \ddot{x}_k(t) + \sum_{k=1}^6 [A_{jk} \ddot{x}_k + B_{jk}^H \dot{x}_k + C_{jk}^H x_k] - F_{GroundDj} = F_j^I + F_j^D = F_{wj} \quad j = 1, 2, \dots, 6 \quad (3.22)$$

Once the global coefficients and excitation forces are determined, and assuming a sinusoidal regular wave excitation and response, Equations (3.22) are transformed into a system of six linear equations with six unknowns in the frequency domain, Equations (3.23). The six unknowns are the complex motion amplitudes \bar{x}_k (magnitude and phase angle). The dynamic ground reaction $F_{GroundDj}$ is included using the dynamic stiffness Equations (2.17) through (2.26) for K_{jk}^d developed in Chapter 2.

$$\sum_{k=1}^6 [-\omega^2 (\Delta_{jk} + A_{jk}) + i\omega B_{jk}^H + (C_{jk}^H + K_{jk}^d)] \bar{x}_k = \bar{F}_{wj} \quad j = 1, 2, \dots, 6 \quad (3.23)$$

where $x_{Gj} = 1$ for $j = 1$ to 3 , $x_{Gj} = x_G$, the longitudinal center of the ground reaction, for $j = 5$ and 6 .

For a single degree of freedom system, the frequency response function would be:

$$H_r(\omega) = \frac{\bar{x}_j}{\bar{F}_{wj}} = \frac{1}{[-\omega^2 (\Delta_j + A_j) + i\omega B_j^H + (C_j^H + K_j^d)]} \quad (3.24)$$

For our six degree of freedom system, the equations of motion are solved multiple times for a range of wave frequencies assuming a unit amplitude regular wave excitation. The magnitude of each response is the magnitude of the frequency response function for that response at each frequency $|H_r(\omega)|$.

Several methods have been developed to solve a system of linear equations, such as matrix inversion, Cramer's rule, etc. SSMLP uses a technique based on LU factorization to solve the system of linear equations. The linear solver is part of the Compaq Visual Fortran software package.

3.6 Structural Loads

The calm water shear force and bending moment are generated from the static equilibrium load curve. The load curve is determined by superimposing the weight distribution (w), buoyancy distribution (b) and ground reaction.

The calculation of dynamic longitudinal bending moments and shear forces in regular waves is based on strip theory and the linearized equations of motion. The total dynamic load per unit length operating on a ship section is the sum of the unsteady fluid forces, mass inertial forces and ground reaction forces (Salvesen et al 1970).

In the $G x_{b1}x_{b2}x_{b3}$ axis system the vertical dynamic load can be written as:

$$q(x) = \frac{-w(x)}{g}(\ddot{x}_3 - x_{b1}\ddot{x}_5) - \mathbf{m}(x)\ddot{x}_3 - N(x)\dot{x}_3 - \mathbf{r}gY(x) + x_{b1}\mathbf{m}(x)\ddot{x}_5 + x_{b1}N(x)\dot{x}_5 + \mathbf{r}gx_{b1}Y(x)x_5 + \frac{dF_o(x)}{dx}$$

where $w(x)$ = weight per foot for each section (3.25)

$\frac{dF_o(x)}{dx}$ = excitation for per foot

x_3 is the amplitude of the heave motion

x_5 is the amplitude of the pitch motion

The dynamic shear force is the integral of the dynamic load on the sections, and the dynamic bending moment is the integral of the dynamic shear force.

3.7 Grounded Ship Excitation

Ocean waves provide a random excitation. By assuming:

- Normal distribution of wave heights,
- Zero mean
- *Ergodic* process: any one sample is typical of the process.
- *Stationary* process: the statistics of the process samples don't change over time.
- Narrow band

- Fully developed seas
- Linear system

With these assumptions, the ship motion energy spectrum can be calculated as a function of the encountered wave energy spectrum by multiplying the wave energy spectrum by the square of the magnitude of the frequency response function:

$$S_r(\omega) = RAO \cdot S_z(\omega)$$

where $RAO = |H_r(\omega)|^2$

$S_r(\omega)$ is the motion response spectrum.

$S_z(\omega)$ is the wave energy spectrum.

(3.26)

This project uses a two-parameter wave spectrum, which represents seaways in all stages of development (Bretschneider 1967):

$$S_z(\omega) = \frac{5}{16} \frac{\omega_m^4}{\omega^5} (\bar{H}_{1/3})^2 e^{-1.25 \left(\frac{\omega_m}{\omega} \right)^4}$$
(3.27)

where $\bar{H}_{1/3}$ is the significant wave height or average wave height of the highest one-third waves, and ω_m is the modal frequency. For the purpose of this analysis, the seas are considered to be fully developed, where the modal frequency in Equation (3.27) is defined by:

$$\omega_m = 0.4 \sqrt{\frac{g}{\bar{H}_{1/3}}}$$
(3.28)

g is the acceleration due to gravity.

CHAPTER 4 CALCULATION OF STATIC EQUILIBRIUM CONDITION

The Stranded Ship Motions & Loads Program (SSMLP) is used to analyze the motions of and loads on a stranded ship. It requires as input a definition of the equilibrium grounded condition of the ship. This chapter describes the process and equations used to determine this equilibrium condition (Bartholomew et al 1992).

The magnitude and location of the static ground reaction is determined by comparing the attitudes and positions of the ship before and after stranding. Four different grounding scenarios are considered:

- stranding on one pinnacle
- stranding on two pinnacles
- stranding on a shelf
- stranding on a penetrable shelf

In addition to knowing the free-floating pre-grounded condition of the ship, one of the following inputs is required to calculate ground reaction:

1. The observed drafts of the vessel in the stranded condition, or
2. The actual depth of water at each grounding location.

For the two case studies in this project, ground reactions are calculated by finding the difference between the total weight of the ship for the current loaded condition and the buoyancy of the vessel as determined by integration of the hull offsets. (Lost Buoyancy Method).

When the observed drafts of the vessel are specified in the stranded condition, hull buoyancy and center of buoyancy are calculated by integration of hull offsets to the defined waterline. The center of gravity is defined by the specified load case or pre-ground condition. The center of ground reaction is determined by balancing weight, buoyancy, and ground reaction moments. For a ship stranded on one pinnacle, the longitudinal center of ground reaction is required to be within the length of the ground contact. For a ship stranded on two pinnacles, the longitudinal positions of the two grounding points (assumed to be at the center of each pinnacle) are required. Ground reaction at each pinnacle is determined by balancing weight, buoyancy, and ground

reaction moments about the other pinnacle. For a ship stranded on a shelf, the forward and after ends of the shelf are specified. The center of ground reaction must be within the grounded length.

When the actual depth of water at each grounding location for one or two pinnacles is specified, an iterative solution is used. For a single pinnacle, the buoyancy is calculated for a trial waterline that passes through the point defined by the water depth at the pinnacle. Weight and buoyancy moments are summed about the center of ground reaction, taken as the center of the pinnacle. The vessel is trimmed and the process is repeated until equilibrium is reached. For two pinnacles, the trimmed waterline is defined by the water depths at the pinnacle locations. No trim iteration is necessary. Specifying water depth at the ends of a shelf defines a waterline in the same way as specifying forward and after drafts.

For ships stranded on a penetrable shelf, the penetration into the shelf is evaluated at each draft and trim iteration. The penetration volume, horizontal area at the mudline, and length are computed. The ground reaction is evaluated based on the soil bearing capacity, F_q , using Equation (4.1). The iterative process continues until equilibrium is achieved for longitudinal moments, and for weight versus buoyancy plus ground reaction. The longitudinal and transverse centers of ground reaction are assumed to be at the longitudinal and transverse centers of the penetration volume.

$$F_q = 5AS_u[1+0.2(D/B)][1+0.2(B/L)] \quad (4.1)$$

where A = horizontal area at mudline

D = embedment depth

B = equivalent breadth

L = equivalent length

S_u = undrained shear strength, assumed to be $q_u/(N_cK_c)$

q_u = bearing capacity for cohesive soil

N_c, K_c = dimensionless soil and geometry coefficients,
taken as 5.1 and 1.05 respectively

This approach is based on the method presented in the U.S. Navy Salvage Engineer's Handbook (Bartholomew 1992). The ratios D/B and B/L are limited to a maximum value of 1.

The ground reaction, for most cases, is assumed to be uniformly distributed along the grounded length of the ship as is shown in Figure 13. If the center of ground reaction is at or near the center of grounded length, ground reaction may be assumed to be distributed symmetrically about this point. If the ship grounds on a uniformly sloping seafloor, the ground reaction is distributed as a right triangle as is shown in Figure 14. If the center of ground reaction lies towards one end of the grounded length, the ground reaction distribution is weighted towards that end in an asymmetrical shape.

For ships stranded on pinnacles, ground reaction is assumed to be evenly distributed over the pinnacle length. For ships stranded on a shelf, ground reaction is distributed as a trapezoid if the center of ground reaction falls within the center third of the grounded length. If the center of ground reaction lies outside the center third of the grounded length, ground reaction is distributed as a right triangle. The right angle is fixed at the end of the shelf nearest the center of ground reaction. The height and base length are adjusted so the center of area coincides with the center of ground reaction.

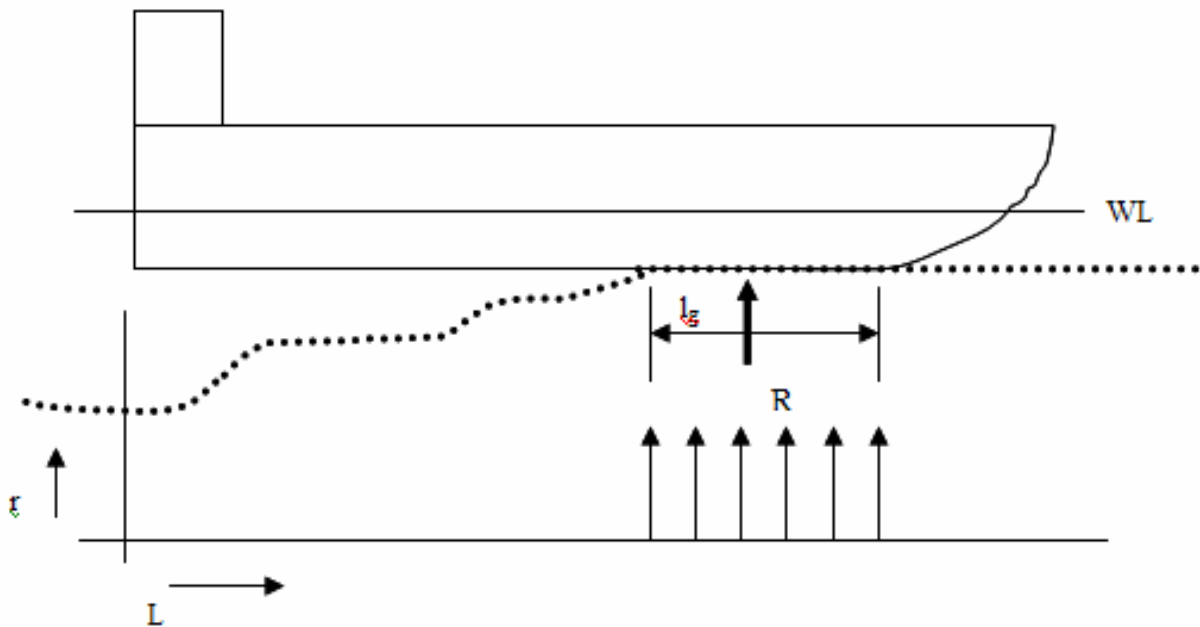
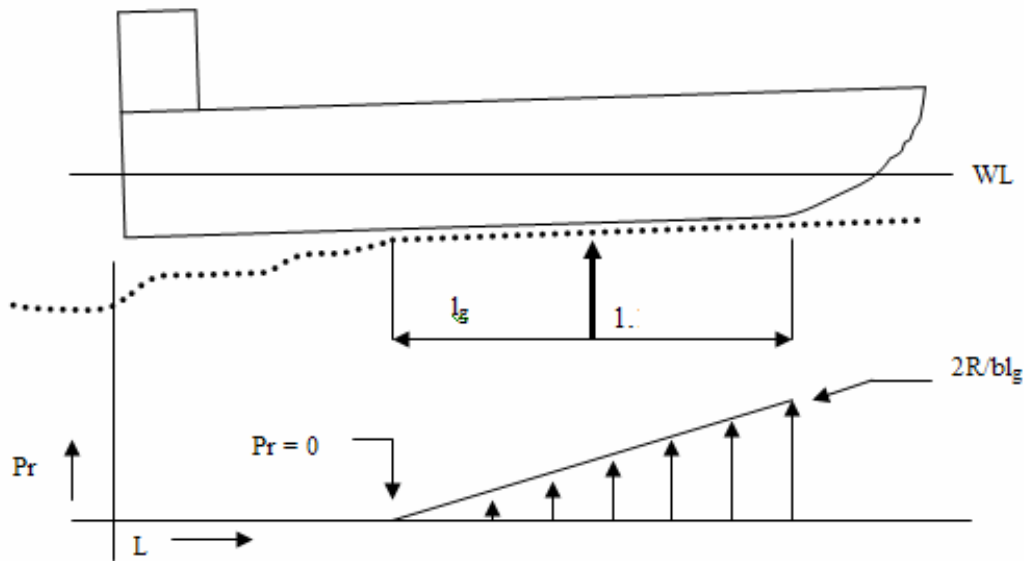


Figure 13 - Uniform Ground Reaction Distribution on a stranded ship



where $P_{max} = 2R/l_g b_{avg}$ $r = Pr b$

with P_{max} = maximum grounding pressure, lton/ft², R = ground reaction, lton,
 l_g = grounded length, feet, b_{avg} = average breadth of contact area over
grounded length, feet, b = breadth of contact area, feet

Figure 14 - Linear Ground Reaction Distribution

The ground reaction force is taken into account as a negative weight, which effects the static orientation of the ship in the grounded position. Ground reaction can be determined by any of the five methods described below. All these methods assume that the ship and supporting ground are perfectly rigid bodies. The case studies in this project are performed using the lost buoyancy method.

1) Lost Buoyancy Distribution Method. The area between the weight curve and the buoyancy curve for the stranded waterline is the total ground reaction. For equilibrium to exist, ground reaction must be distributed in increments over the grounded length so that the combined center of buoyancy and ground reaction is in vertical line with the center of gravity. The area and buoyancy curves are developed from section areas taken from Bonjean curves.

2) Change of Displacement Method. Ground reaction can be estimated by entering the Curves of Form or Hydrostatic Table with the drafts before and after grounding and reading the displacements for the two conditions. Then:

$$R = \Delta_b - \Delta_g \tag{4.2}$$

where: R = ground reaction

Δ_b = displacement immediately before stranding

Δ_g = displacement after stranding

If the stranded ship is trimmed, a correction to displacement for trim must be made.

3) Change of Draft Forward Method. This method considers the ground reaction as equivalent to a weight removal that causes both parallel rise and change of trim. It is calculated using the following equations as shown in Figure 15:

Change of draft forward = change from parallel rise + change forward from trim

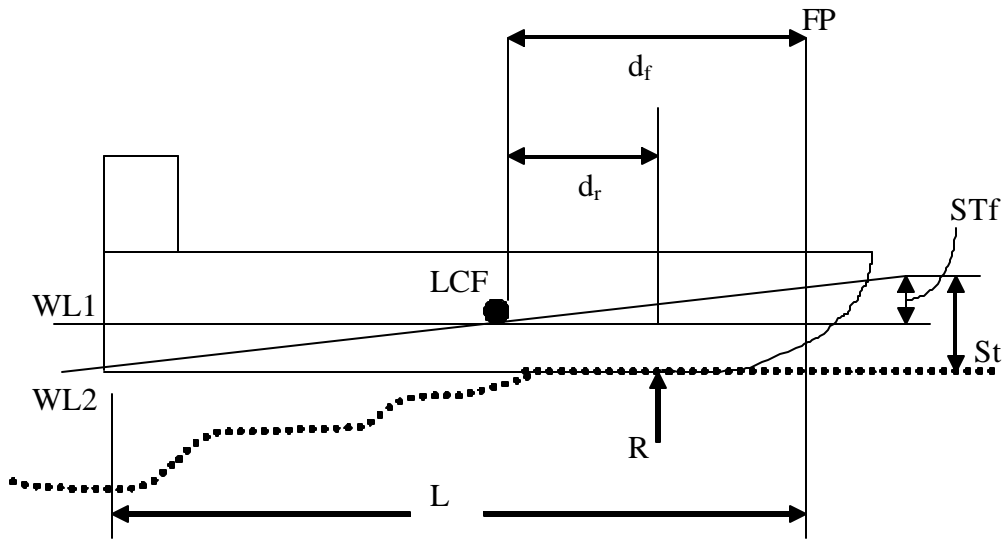


Figure 15 - Change in Trim

$$\begin{aligned}
 \Delta T_{parallel\ rise} &= \frac{R}{TPI} \\
 \Delta t &= \frac{R d_r}{MT1}, \quad \Delta T_{forward, trim} = \frac{d_f}{L} \Delta t \\
 \Delta T_f &= \frac{R}{TPI} + \left[\frac{R d_r}{MT1} \right] \times \left[\frac{d_f}{L} \right] \\
 &= \frac{R}{TPI} + \frac{R(d_r)(d_f)}{MT1(L)} \\
 \frac{R(L)(MT1) + R(d_r)(d_f)(TPI)}{TPI(MT1)(L)} &= \frac{R[(L)(MT1) + (d_r)(d_f)](TPI)}{TPI(MT1)(L)} \\
 R &= \frac{\Delta T_f (TPI)(MT1)(L)}{(L)(MT1) + (d_r)(d_f)(TPI)}
 \end{aligned} \tag{4.3}$$

where:

Δt = total change of trim, in.

ΔT_f = change of draft forward = $T_{fb} - T_{fa}$

d_f = distance from the center of flotation to the forward perpendicular

d_r = distance from the center of flotation to the center of ground reaction

R = ground reaction, tons

$MT1$ = moment to trim one inch

TPI = tons per inch immersion

The basic relationship can also be solved for d_r :

$$d_r = \frac{1}{TPI(d_f)} \times \left\{ \frac{\Delta T_f (MT1)(TPI)L}{R} - L(MT1) \right\} \quad (4.4)$$

4) Tons per Inch Immersion Method. An estimate of the ground reaction can be made by multiplying the change in mean draft on stranding by the tons per inch immersion (TPI):

$$R = (T_{mbs} - T_{mas})TPI \quad (4.5)$$

where:

T_{mbs} = mean draft before stranding

T_{mas} = mean draft after stranding

This method only considers the bodily rise of the ship and is a good estimate if the trim has not been changed greatly by the stranding. The mean draft for trim can be corrected if the stranding causes a significant change of trim.

5) Change of Trim Method. Best used when the total trim exceeds one percent of the ship's length, the center of pressure of the ground reaction is known or can be estimated with reasonable accuracy, and change of trim is the dominant effect of stranding. Ground reaction is treated as a force that causes only a change of trim by the equation below:

$$R = \frac{MT1(\Delta t)}{d_r} \quad (4.6)$$

where:

Δt = total change of trim, inches

Tides change the static condition of the stranded ship. The waterline of a stranded ship rises and falls with the tide. When the tide is highest, the buoyancy of the ship is greatest, and the ground reaction is decreased by the amount of buoyancy regained. When the tide falls, buoyancy decreases and ground reaction increases. For a ship that cannot trim, the change in ground reaction caused by the tide is nearly equal to the change in height of the tide multiplied by TPI. For a ship that can trim with tide changes, the change in ground reaction can be estimated by relating the change in ground reaction to the change in draft at the LCF. For a change of trim, draft is constant at the center of ground reaction. The change of draft at the LCF from trim is found using Equation (4.7):

$$\Delta T_{LCF,trim} = \Delta t \left(\frac{d_r}{L} \right) \quad (4.7)$$

where:

Δt = change of trim, in.

d_r = distance from the center of ground reaction, or assumed pivot point,
to the center of flotation

L = length between perpendiculars

The total change in draft at the LCF is the sum of the changes caused by trim and the rise or fall of the tide. The change in draft because of tide is simply the change in tide height. The two changes are opposed; a falling tide tends to decrease draft, but the rotation of the ship about the pivot point tends to increase draft at the LCF. A rising tide has the opposite effect. The total change in draft at the LCF is found by the following equation:

$$\Delta T_{LCF} = \Delta h - \left(\frac{d_r}{L} \right) \Delta t \quad (4.8)$$

where: Δh = tide change in inches.

The change in ground reaction is estimated by multiplying the change in draft at the LCF by TPI as shown below:

$$\Delta R = \left(\Delta h - \left(\frac{d_r}{L} \right) \Delta t \right) TPI = \Delta h TPI - \left(\frac{d_r}{L} \right) \Delta t TPI \quad (4.9)$$

If the change of trim, Δt , is expressed as $\Delta R d_r / MT1$, then the following equations can be used:

$$\begin{aligned}
 \Delta R &= \Delta h b TPI g - \left(\frac{d_r}{L} \right) TPI g \left(\frac{\Delta R d_r}{MT1} \right) \\
 \Delta h b TPI g &= \Delta R + \frac{d_r^2 b TPI g \Delta R}{L b MT1 g} = \Delta R \left[1 + \frac{d_r^2 b TPI g}{L b MT1 g} \right] \\
 \Delta R &= \frac{\Delta h b TPI g}{\left[1 + \frac{d_r^2 b TPI g}{L b MT1 g} \right]} = \frac{\Delta h b TPI g}{\left[\frac{C d_r^2 h b TPI g + b L g b MT1 g}{L b MT1 g} \right]} \quad (4.10) \\
 \Delta R &= \frac{\Delta h b TPI g b L g b MT1 g}{C d_r^2 h b TPI g + b L g b MT1 g}
 \end{aligned}$$

Using the above equations with Δt expressed as $\Delta R d_r / MT1$, assumes that the ship is trimming about its center of flotation, which it is not. This assumption introduces errors into the ground reaction predictions for different heights of tide.

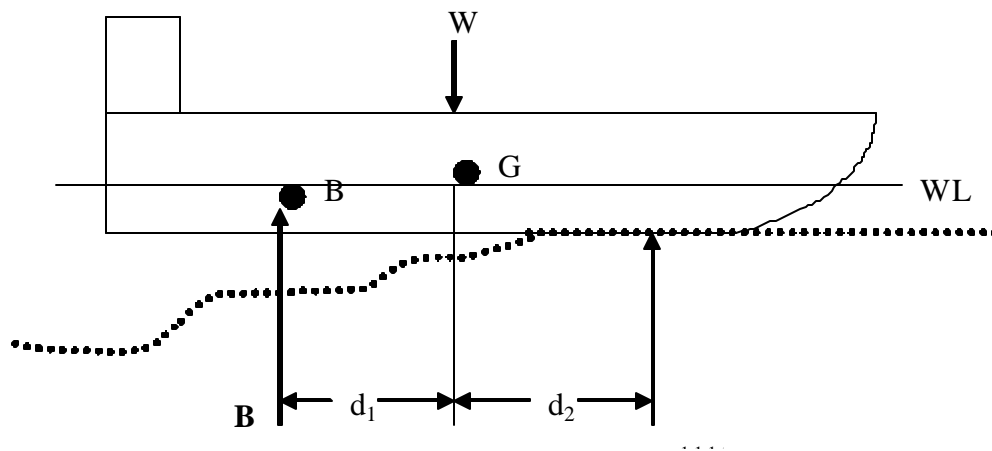


Figure 16 - Forces on a stranded ship

The center of ground reaction, if the ship is aground over only one segment of its length, can be found by summing moments about a convenient point, for example the LCG. This calculation is shown below (referring to Figure 16):

$$B d_1 = R d_2 \Rightarrow d_2 = B d_1 / R \quad (4.11)$$

where:

d_1 = distance from LCB to LCG

d_2 = distance from LCG to the center of ground reaction

The centers of gravity and buoyancy are in a vertical line in a floating ship so the LCG can be determined from the pre-stranding LCB adjusted for flooding. The LCB can be determined from the hydrostatic curves of form or tables if the prestranding drafts are known. If the ship was trimmed before grounding, the LCB from even keel hydrostatic data must be corrected by the following equation:

$$BB_1 = BM_L(t)/L \quad (4.12)$$

where:

BB_1 = movement of LCB because of trim

BM_L = longitudinal metacentric radius

t = trim

L = length between perpendiculars

The grounded LCB can be found from the sectional area curve or taken from hydrostatic data for the grounded drafts and corrected for trim. If hydrostatic data are not available, but LCF and MT1 can be estimated, the center of ground reaction can be estimated by assuming that the ship trims about the LCF, and then use Equation (4.11) where:

d_1 = distance from LCF to the center of ground reaction

d_2 = distance from LCB to LCF

Waves also affect the initial orientation of a stranded ship. Waves move buoyant or partially buoyant objects with their cumulative effects. Near the crest, the buoyancy of a stranded ship is increased and the ground reaction is reduced. Ground reaction distribution and location of the center of pressure are changed; the levering action of the ship disrupts suction and may reduce friction. A stranded ship just inside the breaker line will be battered by short-period water waves. A grounded ship outside the breaker line is exposed to long-period swells and commensurately greater variations in buoyancy over a greater percentage of its length. Wave lengths nearly equal to the ship's length can cause severe hogging or sagging loads.

The grounding of a ship affects its center of gravity. Ground reaction is equivalent to removing an equal weight from the keel, and causes a virtual rise in the center of gravity similar to that caused by the block reaction on a ship in drydock. The following equations calculate the new center of gravity:

$$GG_1 = \frac{R(KG)}{W - R} \quad (4.13)$$

The effective height of the grounded ship center of gravity is calculated directly by the following equation:

$$KG_1 = \frac{KG(W)}{W - R} \quad (4.14)$$

where:

GG_1 = virtual rise of the center of gravity

KG_1 = effective height of the center of gravity when the ship is aground

KG = original height of the center of gravity above the keel

W = weight of the ship

R = ground reaction

The metacentric height, KM , is also affected by grounding. KM for a stranded ship is related to the residual buoyancy of the ship, and can be found from the Curves of Form with post-stranding drafts. With a large range of tide, the movement of the metacenter is significant and large negative metacentric heights may develop, Equation (4.15). A stranded ship with a negative metacentric height is unstable. A stranding off centerline, so that the center of ground reaction is off the centerline, will experience both a loss of displacement and an upsetting moment. If free to incline, the ship will assume a list.

$$GM = KM - KG = KB + BM - KG \quad (4.15)$$

Static loads are based on buoyancy (hull offsets) and weight distribution. The buoyancy distribution is based on hull offsets for all strength calculations. For the stranded ship, the distributed ground reaction is added to buoyancy as an upward force. The weight distribution is constructed by adding the weight distribution for a specific salvage case to the lightship weight. Shear force and bending moment are changed. The relative magnitude and distribution of ground reaction and buoyancy also vary with the tide and passage of swells. The expression for maximum bending moment for a simply supported beam under uniform load ($M = WL/8$) can be modified by empirically derived factors to give a first estimate of maximum static bending moment for stranded ships on pinnacles as shown in Figure 17:

$$M_{\max} = \frac{Rl}{k} \quad (4.16)$$

where:

M_{\max} = maximum bending moment, [length - force]

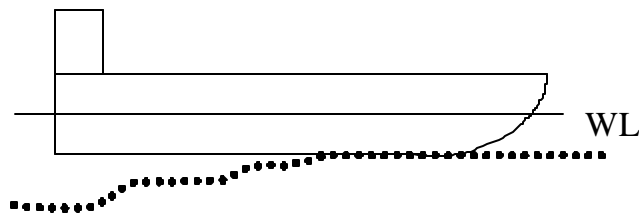
R = ground reaction [force]

l = length of span = length between perpendiculars or distance between pinnacles [length]

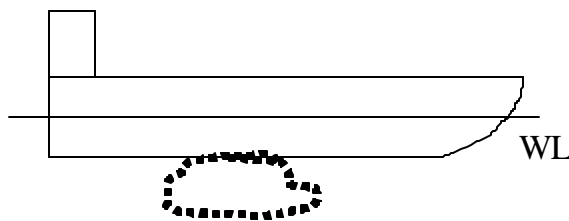
k = factor to account for nonuniformity of force distribution

= 6 for stranded ship supported at both ends

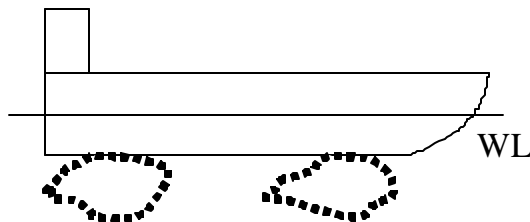
= 7 for stranded ship supported near midships



(a) One end aground, other end in deep water



(b) Aground amidships, no support under bow and stern



(c) Aground at ends, no support amidships

Figure 17 - High Bending Moment Strandings

Hull form characteristics, the forward and aft grounding extreme locations, the water depth at the forward and aft grounding extremes, and the varying tidal heights are used to calculate the bending moments for free floating and stranded cases. The new grounded drafts are used to generate grounded hull form data including local beam, draft and sectional area at station locations. This data also considers grounded trim and are used in the Lewis form strip theory solution.

This project uses the static grounded condition as an input to the dynamic Stranded Ship Motions & Loads Program with the dynamic soil model. The static condition is calculated based on the above methods and equations using HECSALV. HECSALV is a commercial program used in the salvage industry.

CHAPTER 5 STRANDED SHIP MOTIONS & LOADS PROGRAM (SSMLP)

The Stranded Ship Motions & Loads Program (SSMLP) calculates the forces and moments on a grounded ship in six degrees of freedom. It considers the dynamic effects of regular waves plus the dynamic effects of the soil reaction. It is adapted from a two degree of freedom ship motion program by Loukakis (1970). The program requires the following input:

- A description of the immersed grounded hull form by section. This includes local beam, draft and sectional area for a number of stations.
- A complete weight curve including the upward ground reaction.

The program output includes:

- Calm water shear forces and bending moments
- Shear forces and bending moments for the free-floating ship in waves.
- Shear forces and bending moments for the grounded ship in waves.
- Heave and pitch response amplitude operators and phase plots for the grounded ship in waves.

The program uses English units, lb_f, ft, sec. For input-output only:

- angles are in degrees
- frequency is in radians per second
- weight, weight/foot, shearing forces and bending moments are in tons, tons/foot, tons and foot-tons respectively. If the length between perpendiculars is less than 50 feet, the units are pounds, pound/foot, pounds, and foot-pounds respectively.

SSMLP uses Simpson's Rule or the Trapezoidal Rule for integration. These integration methods are performed in subroutines SIMPUN and TRAPIN respectively.

Figure 18 is the flowchart for the program. It starts with MAIN calling INPUT and then MAIN calls the subroutines clockwise around the diagram. MAIN contains the body of the program with all the necessary bookkeeping functions.

INPUT reads in the input data. INPUT collects and stores the following information: vessel description, weight curve description, control constants which enable or disable various program functions, and grounding description. Once INPUT is finished, MAIN calculates hull volume, weight, block coefficient (C_B) and the longitudinal center of buoyancy (LCB), and compares the calculated values with input principal characteristics. These calculations are performed using the function SIMPUN for unequally spaced Simpson's rule integrations. MAIN also calculates the longitudinal center of gravity (LCG) and the radius of gyration from the input weight curve.

BENDSH1 calculates calm water bending moments and shear forces using the weight, ground reaction and buoyancy distributions. It also calculates inertial coefficients for the subsequent calculation of wave shearing forces and bending moments in subroutine BENDSH2. The coefficients $V1I(I)$, $V2I(I)$, $BM1I(I)$ and $BM2I(I)$ represent properties of the weight curve, which together with the motions along the hull, are used for the calculation of the dynamic part of the loads in waves.

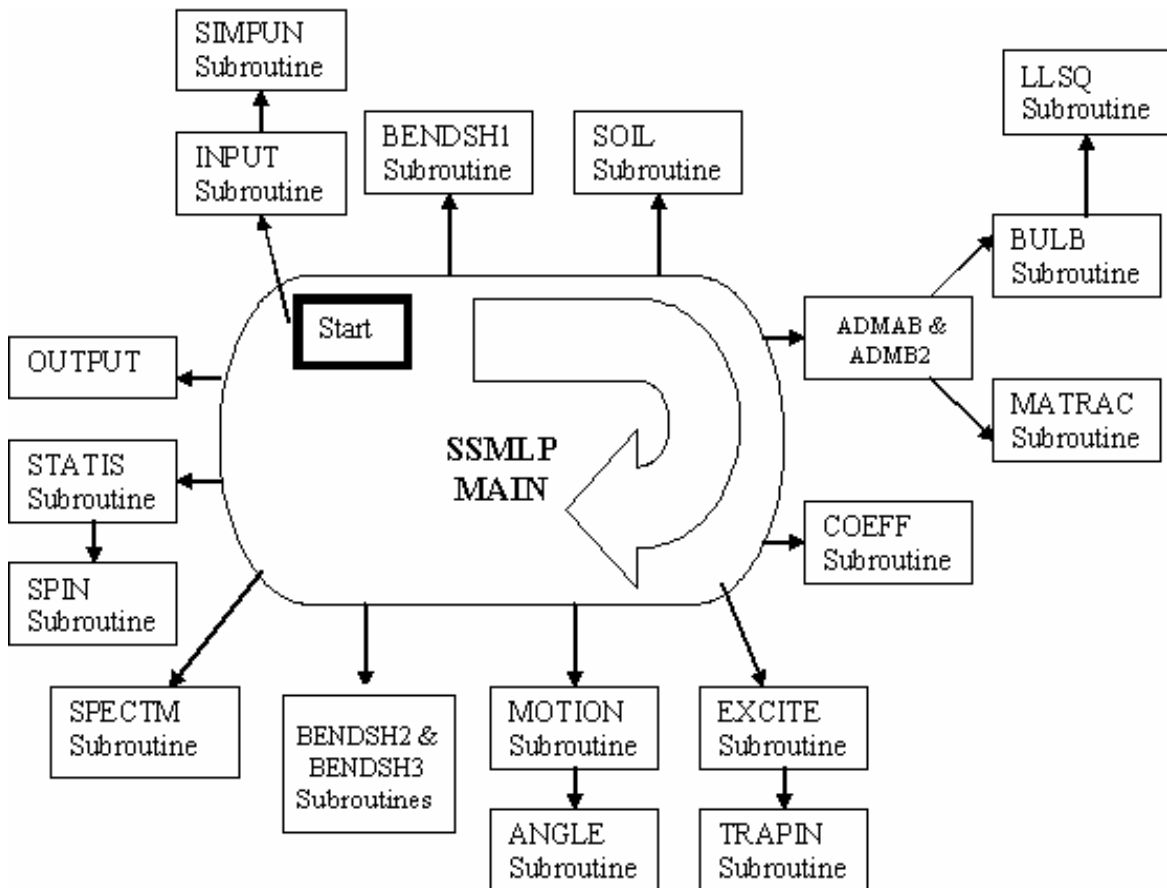


Figure 18 - Program Flowchart

BENDSH1 also calculates the weight of the hull, the LCG and the radius of gyration based on the weight curve. If the results for weight and LCB are not within specified tolerances (0.1% for the weight and 0.01% of LBP for the LCG) from the input values, the calculation is terminated. This is done to avoid large errors for the calm water results and smaller errors for results in waves.

The SOIL subroutine calculates the dynamic stiffness for the soil reaction. These calculations use Equations (2.17-2.26). The soil model requires that the length of the embedded section be greater than the embedded beam section. If this is not the case, the subroutine switches L and B, and calculates the dynamic stiffness value for pitch using the roll equation.

Figure 19 shows the location of the soil reaction force within the grounded length. Since all forces and moments acting on the ship are calculated about the origin of the body-fixed reference frame (center of gravity, COG), the subroutine transfers the soil reaction force to the COG as is shown in Figure 20. Since the vertical dynamic ground reaction force (F_g) shown in the figure is not applied at the COG, it creates a vertical force and moment about the COG by including these moments in the ground reaction dynamic stiffness coupling terms, Equation (2.26).

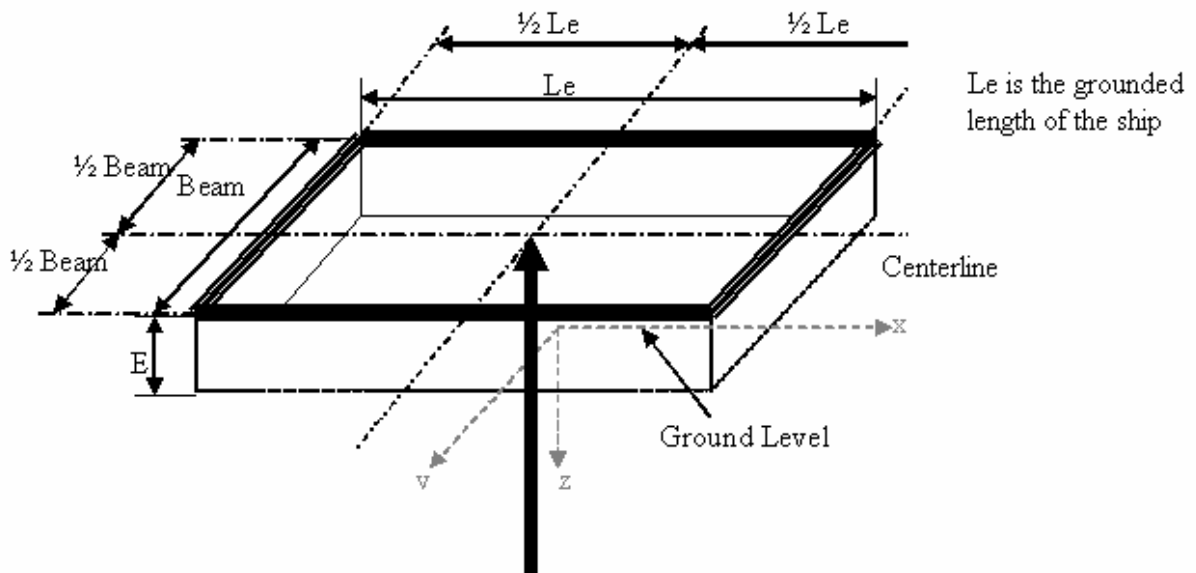


Figure 19 - Location of Soil Reaction Force ($Le > Be$)

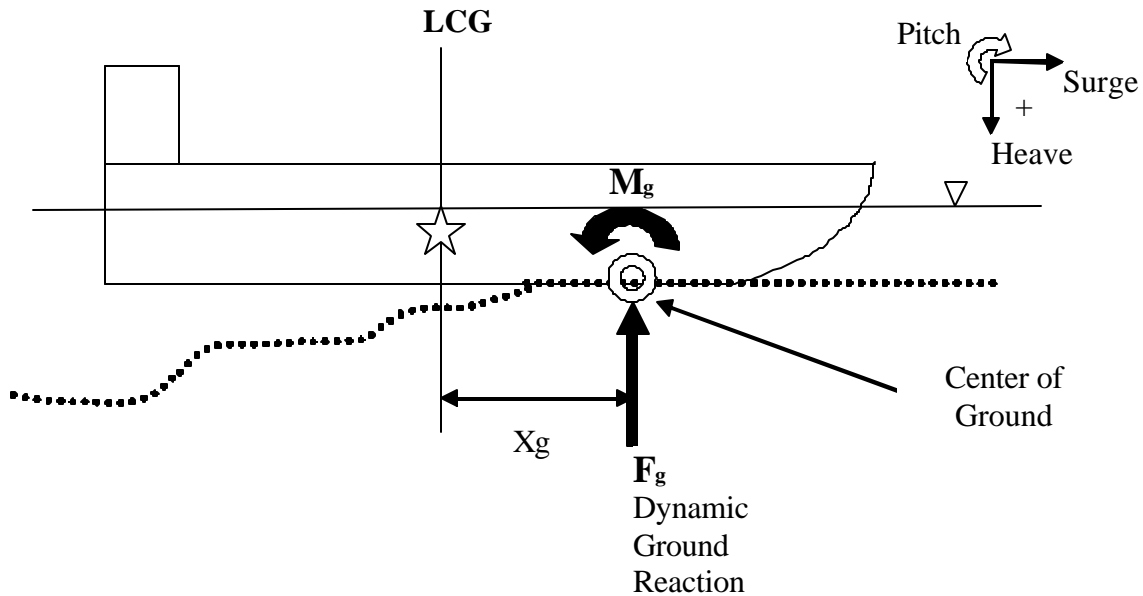


Figure 20 - Transfer of Soil Reaction force and Moment to Amidships

The hydrodynamic problem consists of determining the added mass and damping for a cylinder of infinite length, floating in water of infinite depth and vertically oscillating in small harmonic motion. Viscous contributions are neglected. SSMLP calculates the hydrodynamic coefficients using the Lewis form mapping described in Section 3.7.7. The Lewis form mapping requires only the local sectional properties of beam, draft and area, which are provided in the program input. The exact shape of the section need not be known using Lewis forms. A sectional area curve, design waterline and a keel line are adequate for the conformal description of the hull.

The subroutine ADMAB and ADMB2 uses the input beam, draft, and section area at each station to generate a Lewis form. The added mass and damping coefficients for the two dimensional Lewis form sections at a given encounter frequency are then read from the file DATA.IN which contains a table of sectional coefficients for a range of Lewis forms. Once the sectional coefficients for the Lewis form are located, ADMAB and ADMB2 scale the coefficients to match the actual ship sections.

For large bulbous sections, the added mass and damping coefficients are calculated in subroutine BULB using the MIT bulb mapping functions (Demanche 1968). The subroutine uses LLSQ for the solution of the simultaneous equations generated in BULB.

The subroutine COEFF computes the global coefficients for the equations of motion. The global terms are calculated by summing up the sectional coefficients generated in MAIN, ADMAB, SOIL, and BENDSH1, and integrating along the length of the hull using Equations (3.16) to (3.21).

The subroutine EXCITE calculates the wave-induced and sectional exciting forces and moments. The forces and moments are returned in their real and imaginary parts. It calls subroutine TRAPIN to sum the sectional forces and moments.

Subroutine MOTION solves the equations of motion using Equation (3.23) as described in Section 3.5.1. The motions are returned to the main program as complex numbers in polar form. MOTION calls Function ANGLE, which converts radians to degrees.

Subroutines BENDSH2 and BENDSH3 calculate the dynamic shear forces and bending moments in regular waves using Equation (3.25). If the entire weight distribution along the length of the hull is given, the shear forces and bending moments are computed at each hydrodynamic station for RMS, H1/3 and H1/10. The results are returned in the form of amplitudes and phase angles for each frequency. The calculations are performed keeping the hydrodynamic and the inertial effects separate until the final addition to determine the amplitudes and phase angles. The calculation of the inertial part of the shearing forces and bending moments is done by using the coefficients calculated in BENDSH1. The hydrodynamic forces are integrated along the hull by a Hermitian integration with first derivative terms.

Regular wave motion and load results are generated for unit amplitude waves at a series of discrete wave frequencies. These results are then used to build RAO values for each response and frequency. These values are applied to the wave energy spectra at each discrete frequency to calculate the response spectra using Equations (3.26) through (3.28). RMS and significant response values are calculated from the response spectra.

The default values for spectral frequencies are determined based on the modal frequency. The 25 default ω/ω_p values are 0.6 to 2.5 in multiples of 0.1 then 0.84, 0.94, 1.06, 2.75 and 3.0. The wave spectra values are calculated in SPECTM at specified or default frequencies as a function of input significant wave height and modal frequency.

The program can generate a family of two-parameter sea spectra (which includes the fully developed sea spectra recommended by the 11th ITTC and decaying sea spectra) using Equation (3.27). If the modal frequency is not given, the program assumes a fully developed sea using Equation (3.28).

STATIS calculates the response spectrum, spectral moments, broadness factor, and significant response. The function SPIN is used to perform the spectral integrations.

CHAPTER 6 RESULTS AND CONCLUSIONS

Two case studies using SSMLP are described in this section with results and conclusions. The first case study analyzes grounding motions and bending moments in a simple box barge. The box barge case was used to troubleshoot the model, generate preliminary results, and assess model behavior. The second case study analyzes the grounding of a Series 60 tanker. The Series 60 tanker was chosen because it is the same vessel modeled in the Paik and Pedersen paper (1997) that considers static grounding bending moment, and it provides a more realistic case study for comparison to class society design bending moments.

6.1 *Box Barge Case Study*

This case study analyzes a box barge with the following dimensions: length = 177-ft, beam = 59-ft, draft = 9-ft (free-floating), block coefficient = 1.0. The barge is grounded with the first 10-ft of the bow in contact with the bottom. The center of ground reaction is located 5-ft from the forward perpendicular, shown in Figure 21. The matrix of studies performed with this case is illustrated in Figure 22. Motion and bending moment are calculated for 364 conditions. The stranded barge is evaluated for the free-floating condition and for three different ground reactions. Each ground reaction corresponds with a vertical displacement as listed in Table 3. For example, the 32-LT ground reaction is produced by a 0.5 foot displacement from the free-floating condition at the center of the ground reaction. For the specified grounding condition, the motion and loads are determined while varying depth of embedment, wave frequency, wave direction, and soil-type.

6.1.1 *Motion Response in Regular Waves*

Motion results generated in SSMLP are assembled as Response Amplitude Operator (RAO) plots. These plots were assessed for consistency and reasonableness in the process of troubleshooting the model. Bending moment plots are compared to still water results and IACS/ABS design values. The first set of RAO plots (Figure 23 to Figure 53) are for the grounding scenario shown in Figure 21 with a specified ground reaction of 32-LT. Given this scenario, the following items are varied: wave frequency, depth of embedment, wave direction, and soil-type.

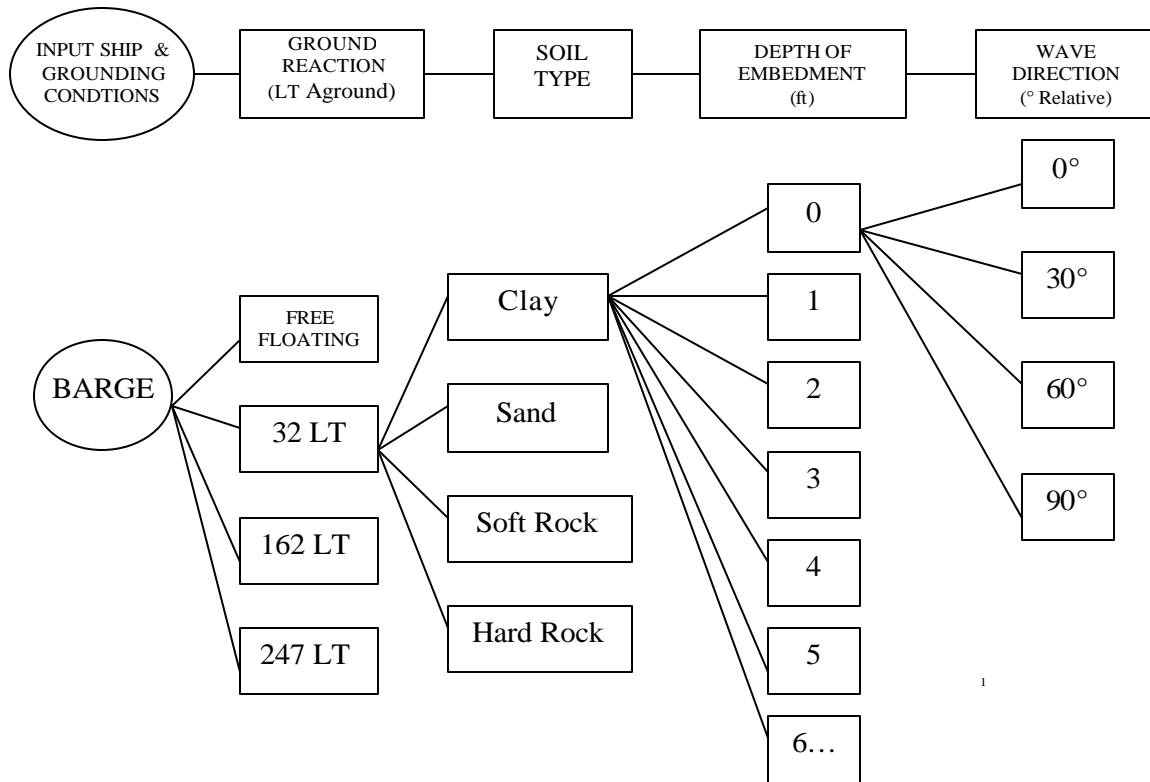


Figure 22 - Barge Case Flow Chart (RAO)

Table 3 - Ground reaction change due to vertical displacement

Tidal change	Draft fwd (ft)	Draft aft (ft)	Ground Rxn (LT)
floating	8.98	8.98	0
-0.5	8.45	9.29	32
-1.5	6.80	10.06	162
-2.5	5.70	10.60	247

6.1.1.1 Depth of Embedment Varied

Figure 23 to Figure 38 show the ship motion RAOs for the barge grounded in clay-type soil. Clay is the softest of the four soil-types listed in Table 2 and allows the most motion to demonstrate the effect of varying depth of embedment.

Figure 23 to Figure 25 show the vertical plane motion RAOs for the grounded barge, which is subject to regular waves from 180°R (astern). In following seas, the barge only responds in the vertical plane (surge, heave, and pitch degrees of freedom).

Figure 26 to Figure 30 show the horizontal and vertical plane motion RAOs for the grounded barge, which is subject to regular waves coming from 090°R (beam). In Figure 23 to Figure 30,

the RAOs for the free-floating condition were plotted for comparison. Since it is difficult to see the effect of the depth of embedment in these figures, Figure 31 to Figure 38 are provided. These figures do not include the RAOs for the free-floating case.

When comparing the responses of the free-floating barge with those of the grounded barge, Figure 23 to Figure 30 show that the grounded vessel motion is restrained significantly, but not entirely by the ground reaction. The vessel motion becomes more restrained as the depth of embedment is increased.

Figure 23 shows that with seas from the stern the barge is relatively motionless in the surge degree of freedom. This is due to the embedment of the barge and the relatively small force which is generated by regular waves from the stern.

Figure 24 and Figure 25 show heave and pitch motion RAOs, respectively. These figures show that the heave and particularly pitch motions are relatively large when compared with the other degrees of freedom. With the barge only supported over 10% of its length, it is very free to pitch, rotating around the grounding point vice the LCF as in the free-floating case.

Figure 26 and Figure 27 show the sway and roll motion RAOs, respectively. These figures show that the barge is relatively motionless when compared to the free-floating case. These degrees of freedom are discussed further with Figure 34 and Figure 36.

In Figure 28, there is no motion in the yaw degree of freedom when the barge is free-floating. This is due to the fact that the underwater hull profile does not vary along the length of the hull. Therefore the exciting force in the sway direction does not vary along the length of the hull, resulting in no yaw. Once the ground reaction and soil model are applied, a yaw motion results. This also occurs in the pitch degree of freedom, Figure 30.

When comparing the free-floating heave response with the heave response of the grounded barge in Figure 29, it appears that the application of the dynamic soil reaction causes the peak in the heave response curve to shift to a higher frequency. This is expected because application of the soil model increases the stiffness of the system. By increasing the stiffness without changing the mass, the frequency of resonance is increased.

With waves coming from 180°R (following seas), Figure 31 indicates that the surge response increases with wave frequency with a maximum response at approximately 3.8 radians/second.

Figure 32 and Figure 33 indicate the response in heave and pitch is greater at lower frequencies. The peak in Figure 32 at approximately 1.7 radians/second also suggests that there is a frequency of resonance in the heave degree of freedom. RAO plots for the sway, roll, and yaw degrees of freedom are not included because the grounded barge does not respond in these degrees of freedom when the waves are from 180°R.

Figure 34 to Figure 38 show the response of the grounded barge when the waves are coming from 090°R (beam seas). With the depth of embedment at zero and 1-foot, the peak in the sway response curves indicates there is a frequency of resonance. As in Figure 32, the heave response curve in Figure 35 has a peak at a wave frequency of 1.7 radians/second. However, this peak is more pronounced when compared to the one in Figure 32. The response is larger in Figure 35 because the waves are coming from 090°R. The waves are acting along the entire length of the hull and producing a greater excitation in the heave degree of freedom. Figure 36 to Figure 38 indicate that the response of the grounded barge in the roll, pitch, and yaw degrees of freedom is greater at lower frequencies. The grounded barge does not respond in the surge degree of freedom when waves are coming from 090°R.

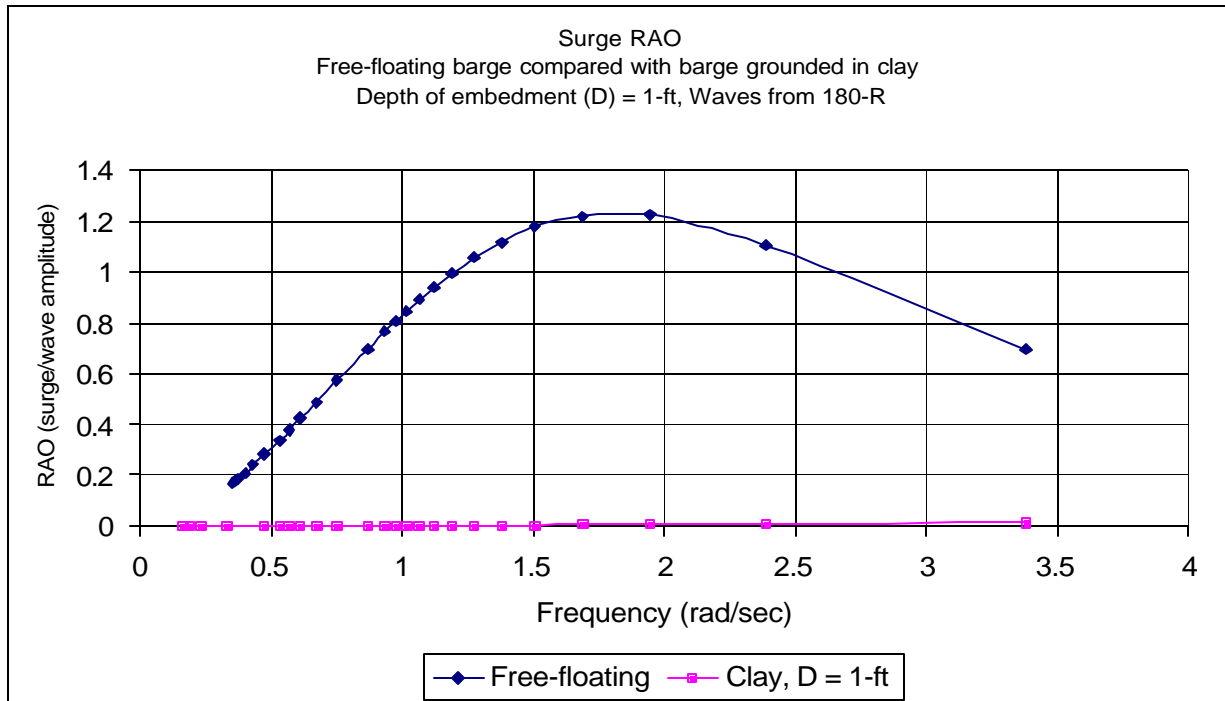


Figure 23 - Surge RAO for barge grounded in clay.

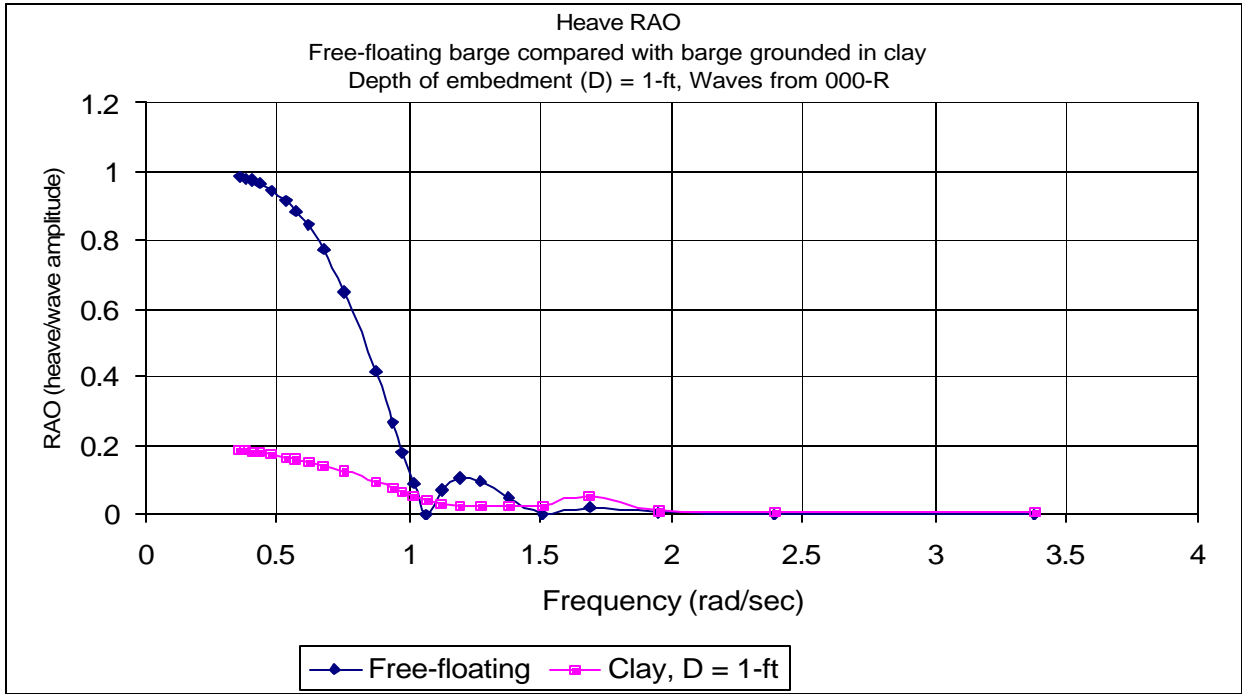


Figure 24 - Heave RAO for barge grounded in clay

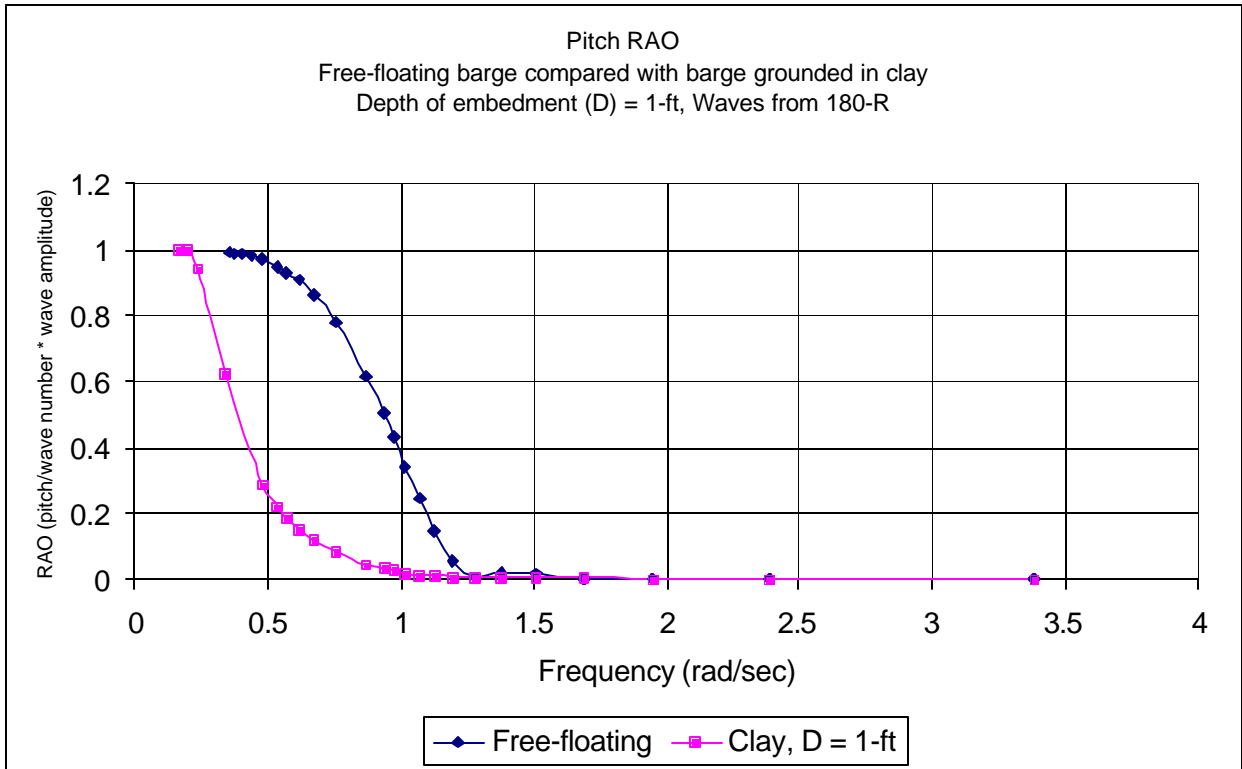


Figure 25 - Pitch RAO for barge grounded in clay

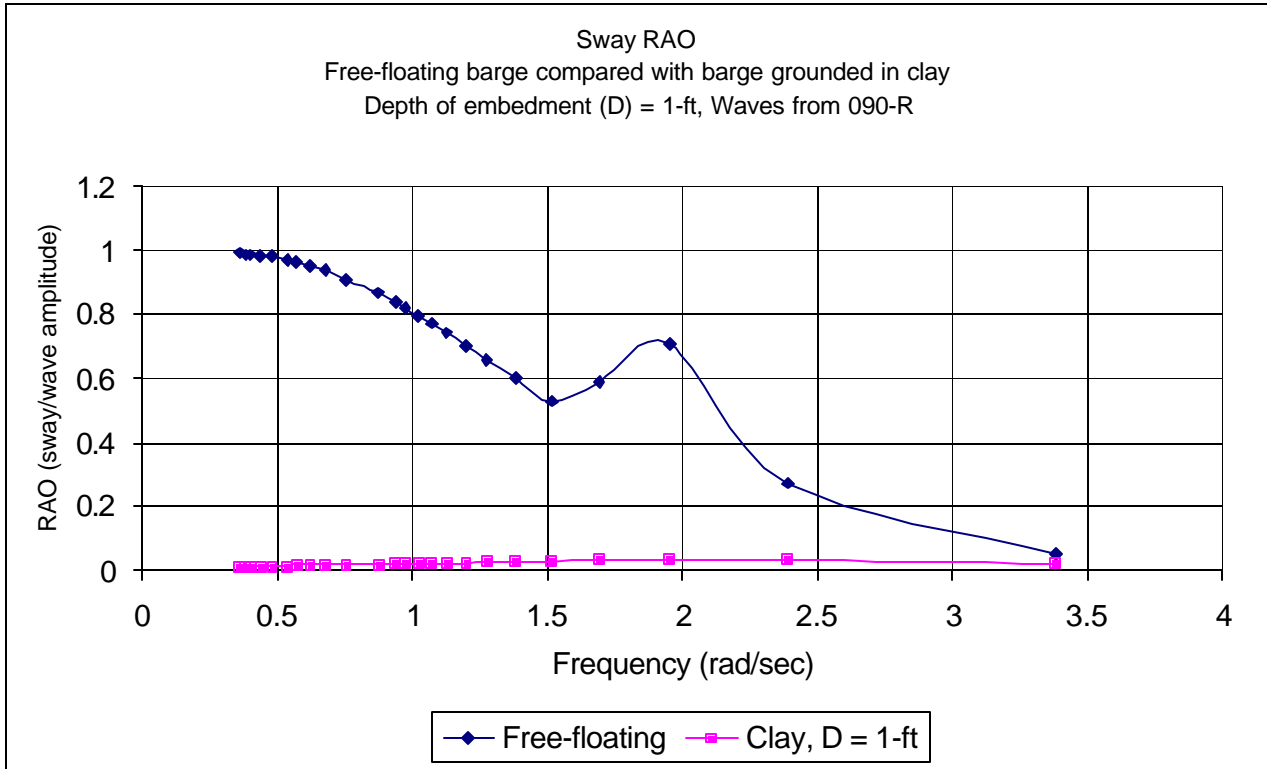


Figure 26 - Sway RAO for barge grounded in clay

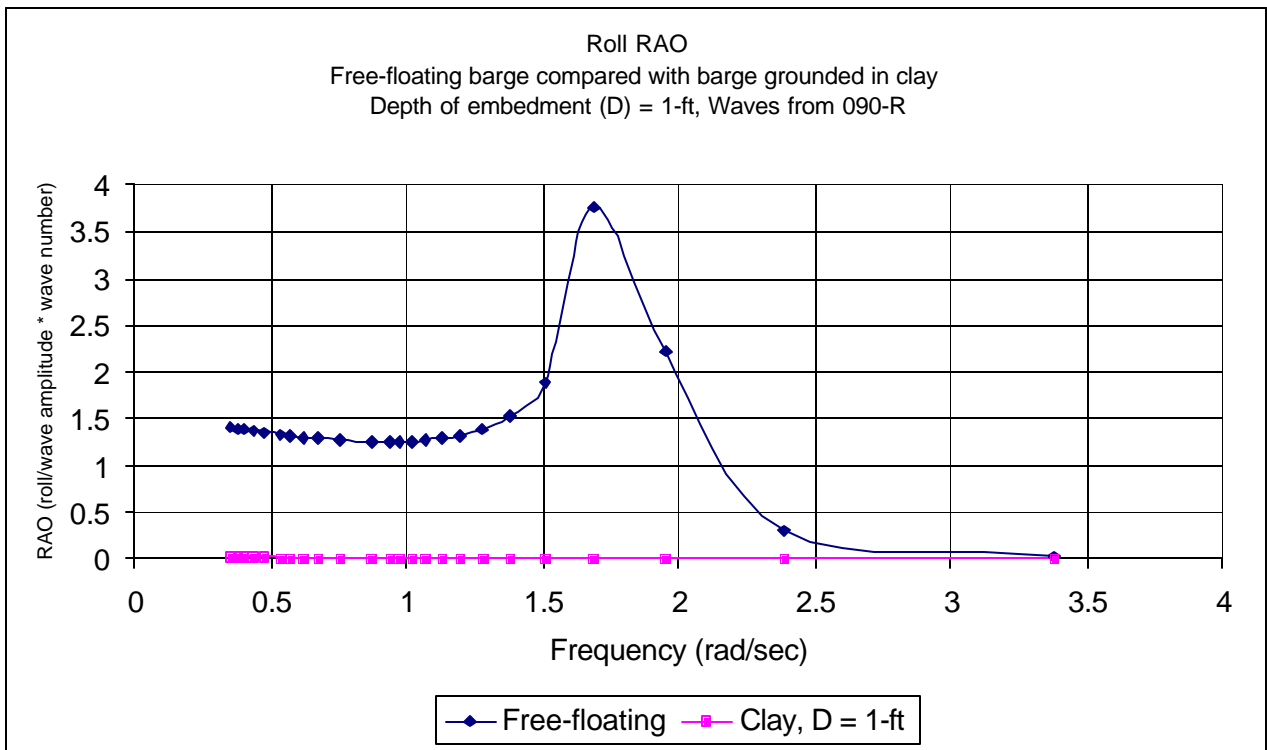


Figure 27 - Roll RAO for barge grounded in clay

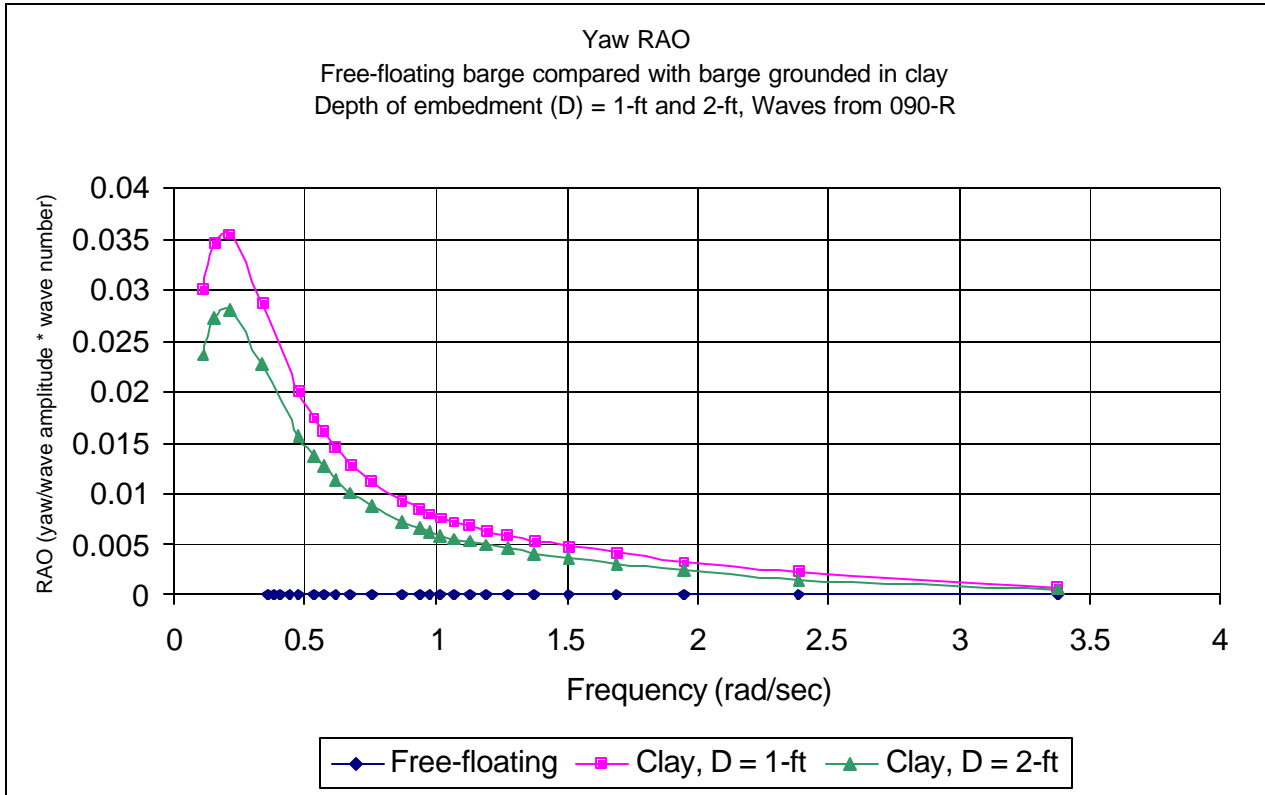


Figure 28 - Yaw RAO for barge grounded in clay

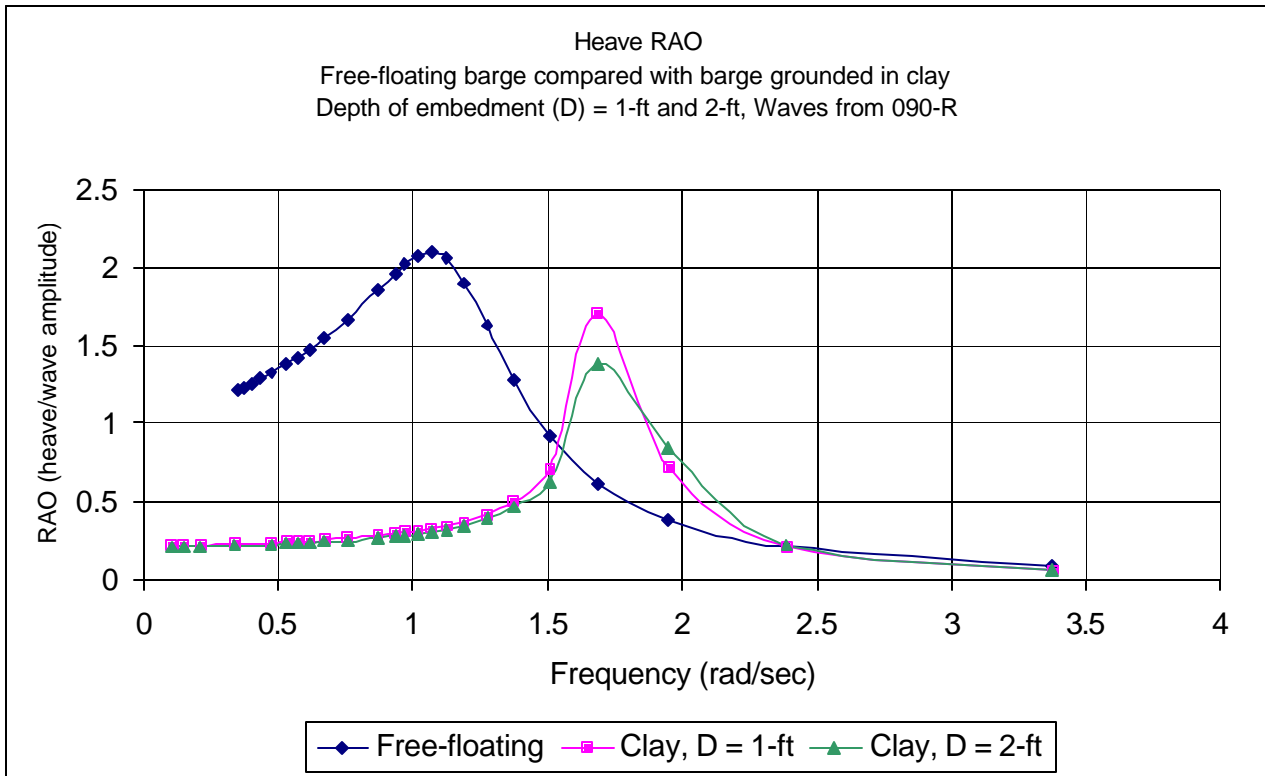


Figure 29 - Heave RAO for barge grounded in clay

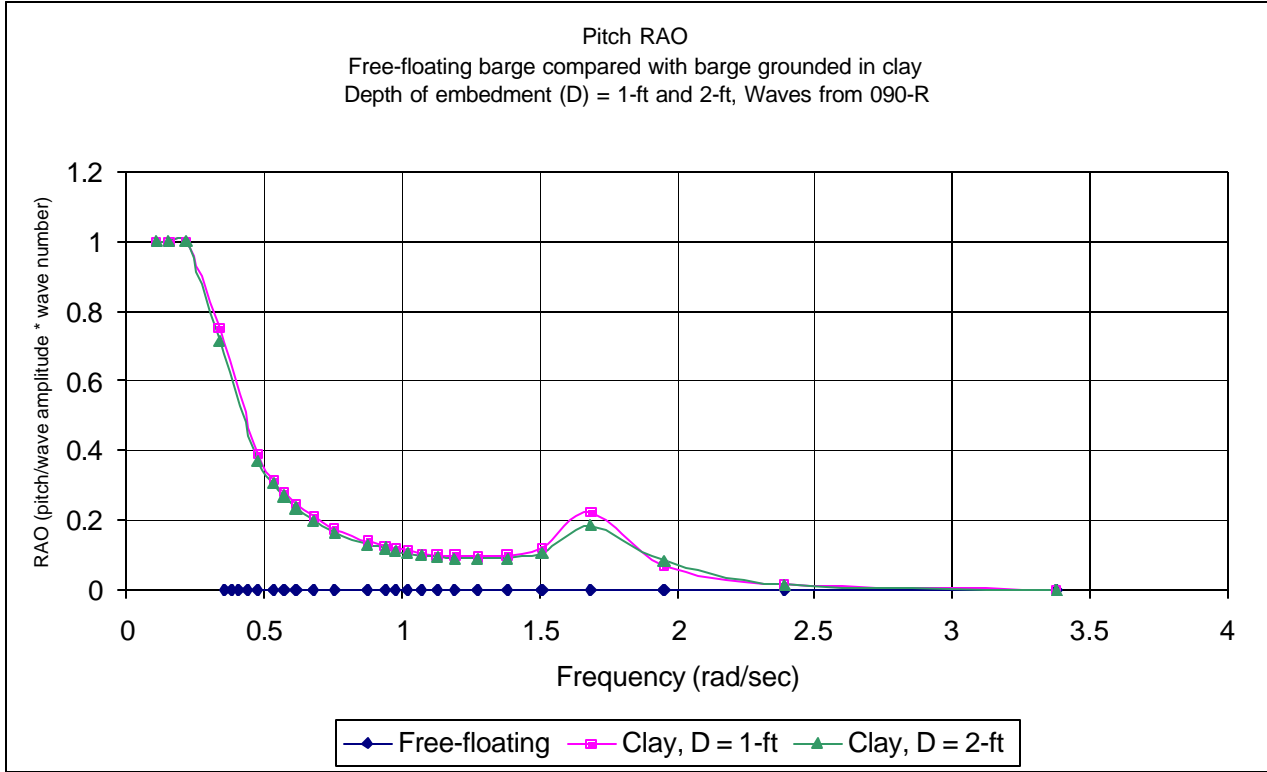


Figure 30 - Pitch RAO for barge grounded in clay

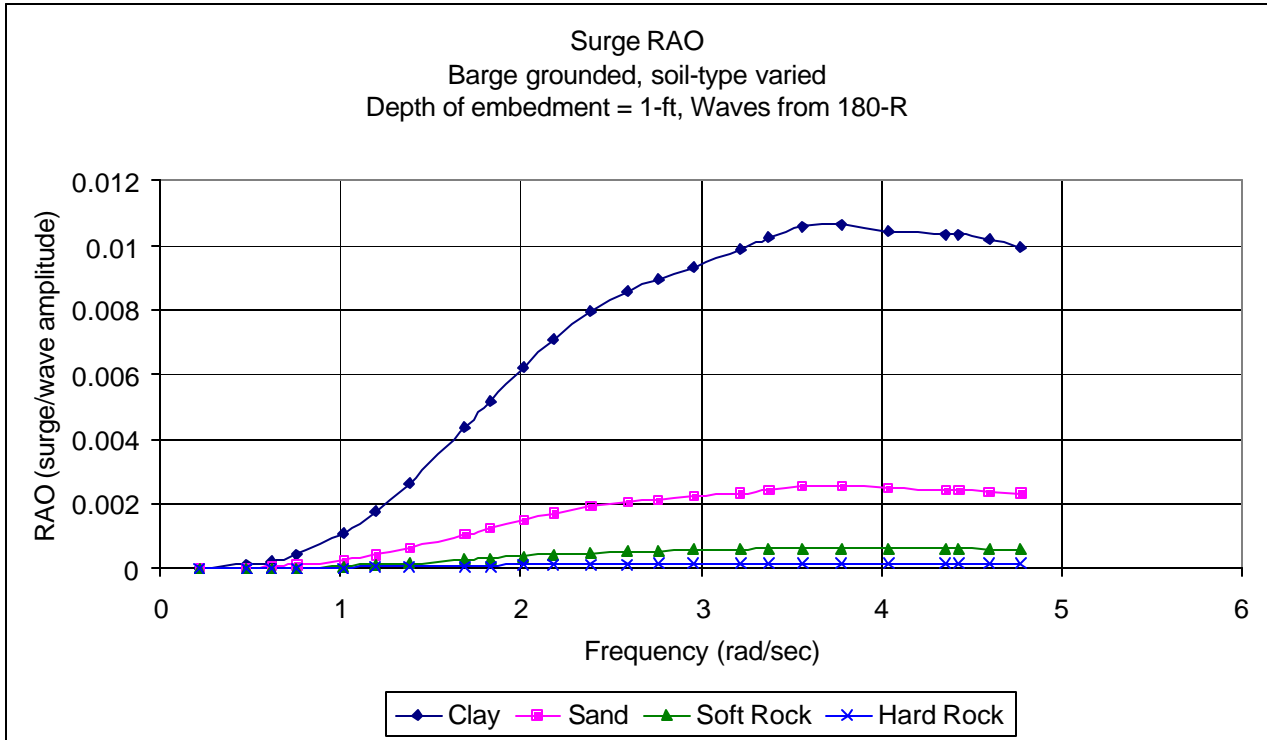


Figure 31 - Surge RAO for barge grounded in clay, depth of embedment varied

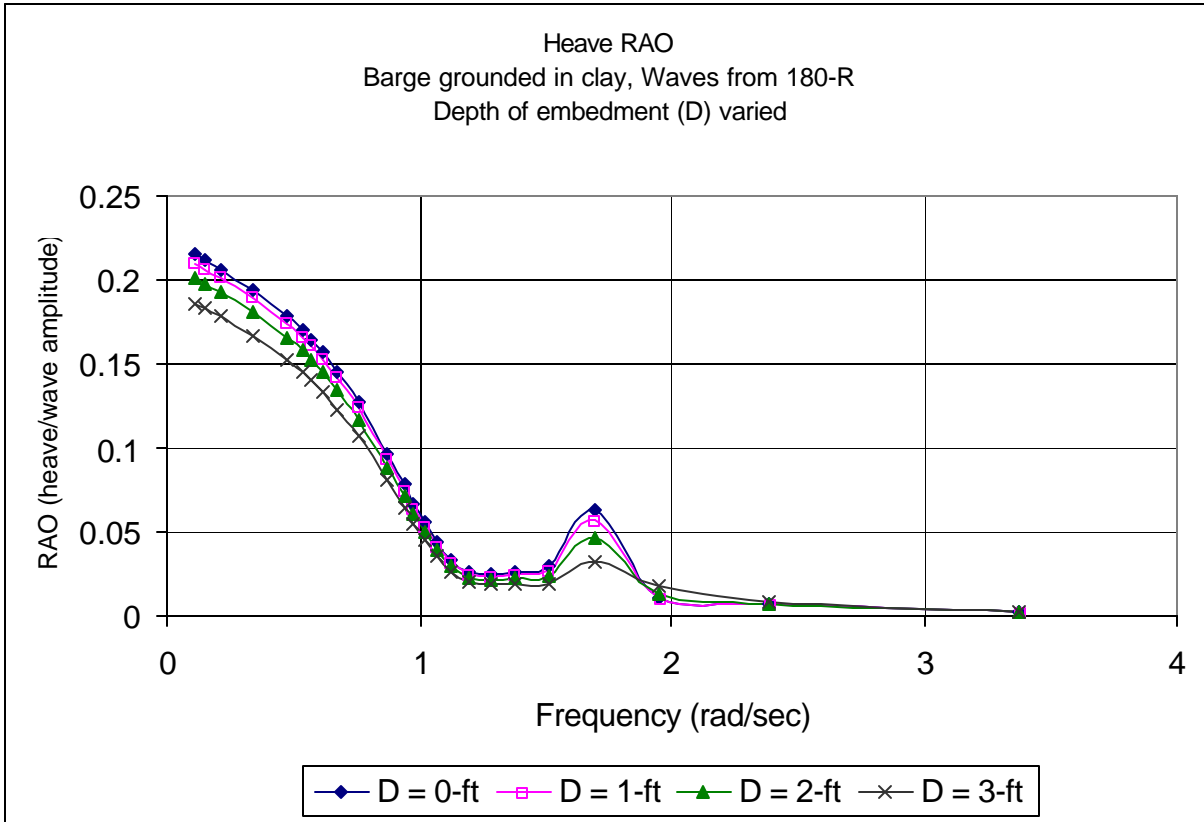


Figure 32 - Heave RAO for barge grounded in clay, depth of embedment varied

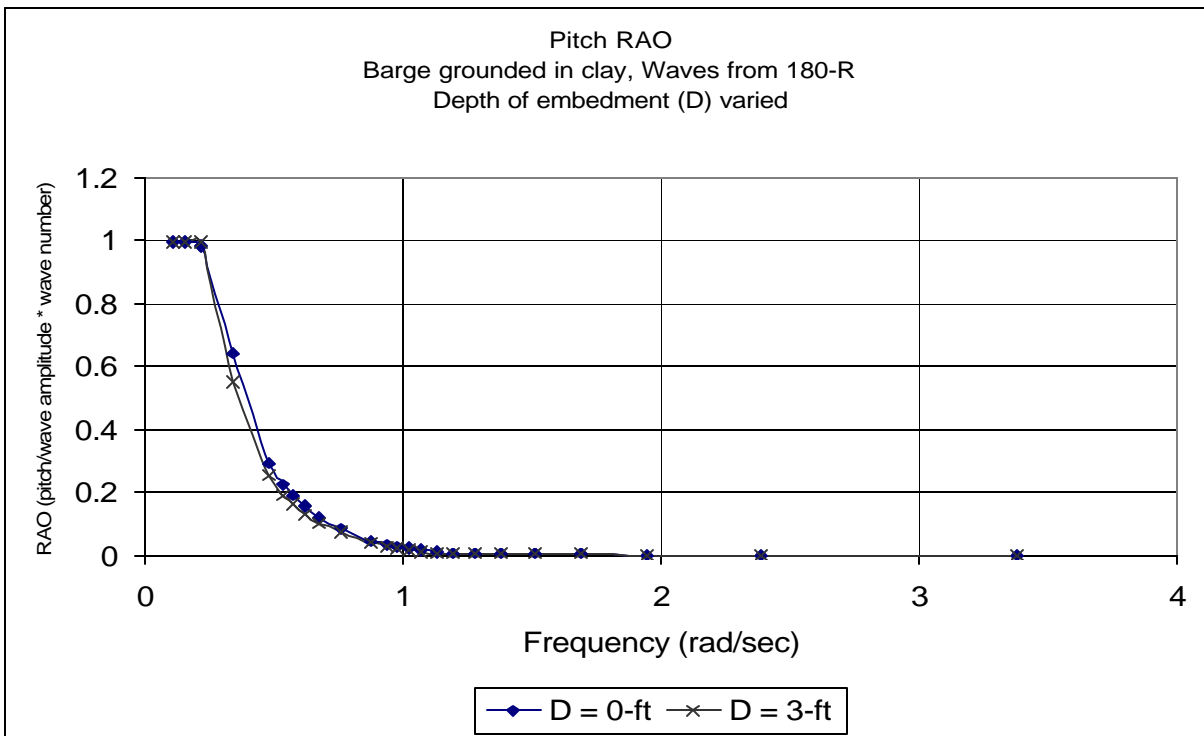


Figure 33 - Pitch RAO for barge grounded in clay, depth of embedment varied

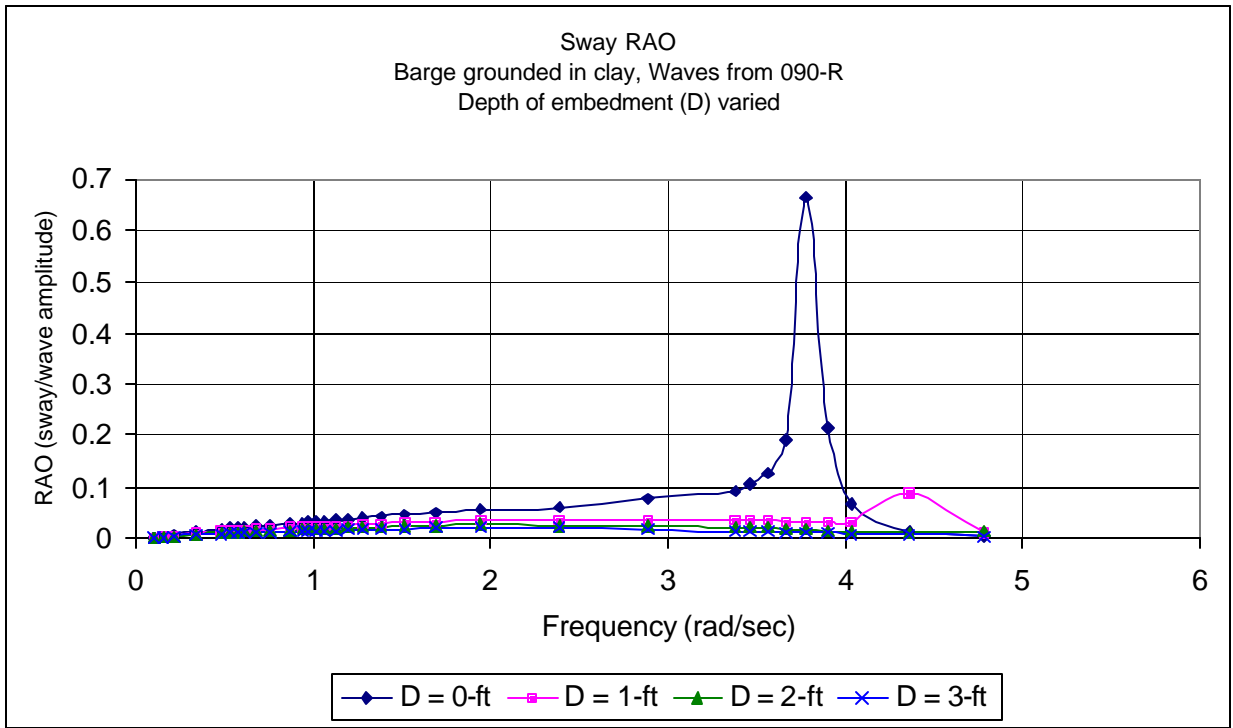


Figure 34 - Sway RAO for barge grounded in clay, depth of embedment varied

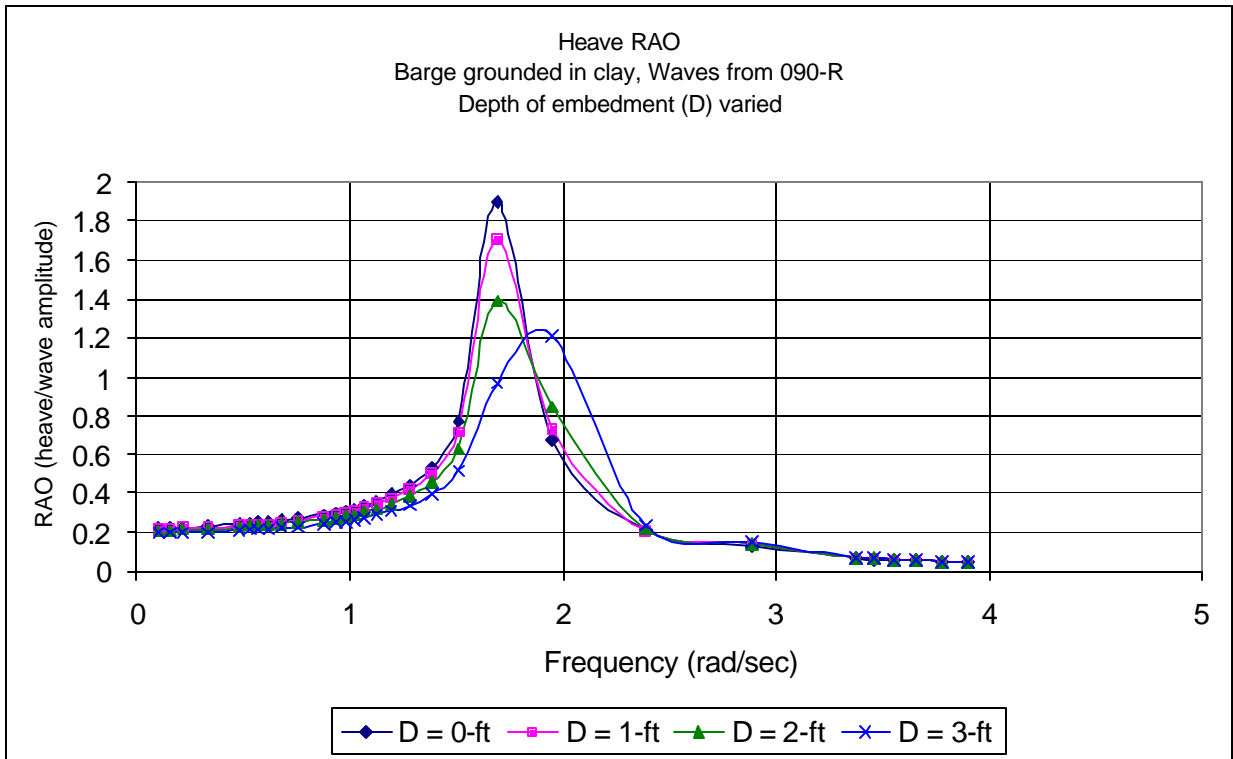


Figure 35 - Heave RAO for barge grounded in clay, depth of embedment varied

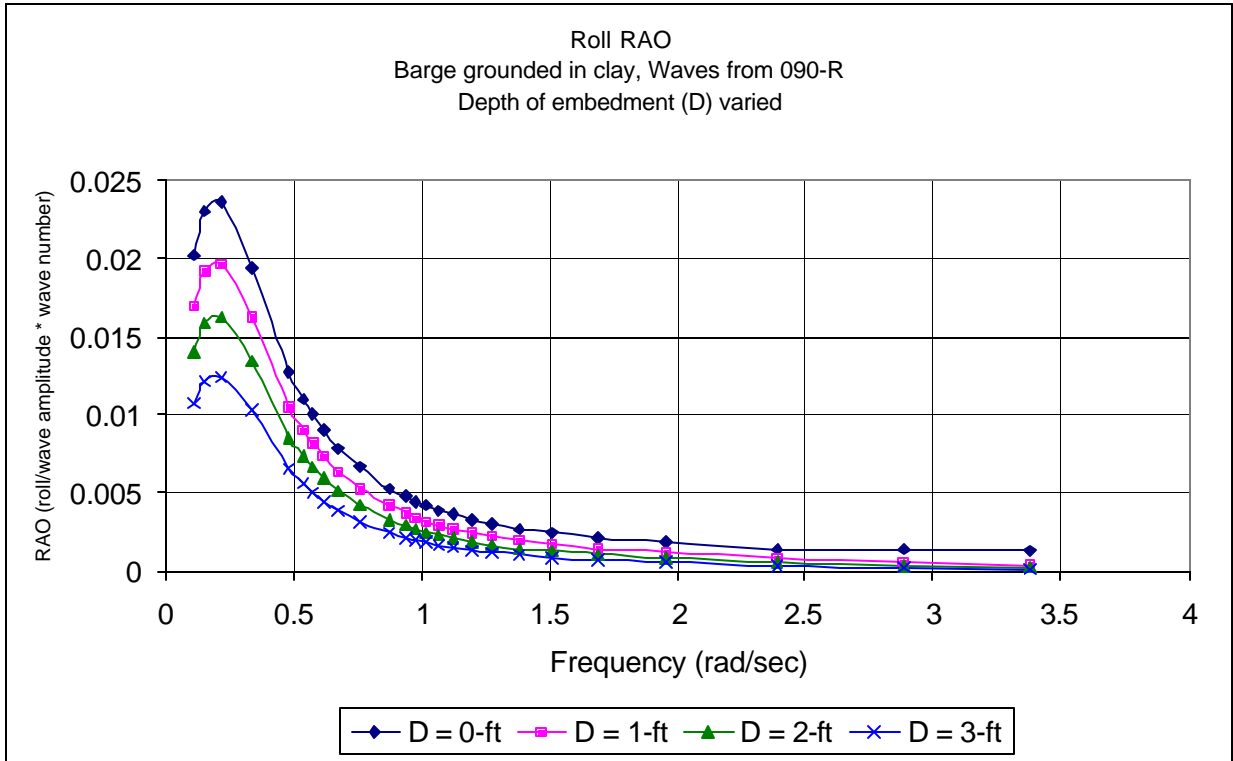


Figure 36 - Roll RAO for barge grounded in clay, depth of embedment varied

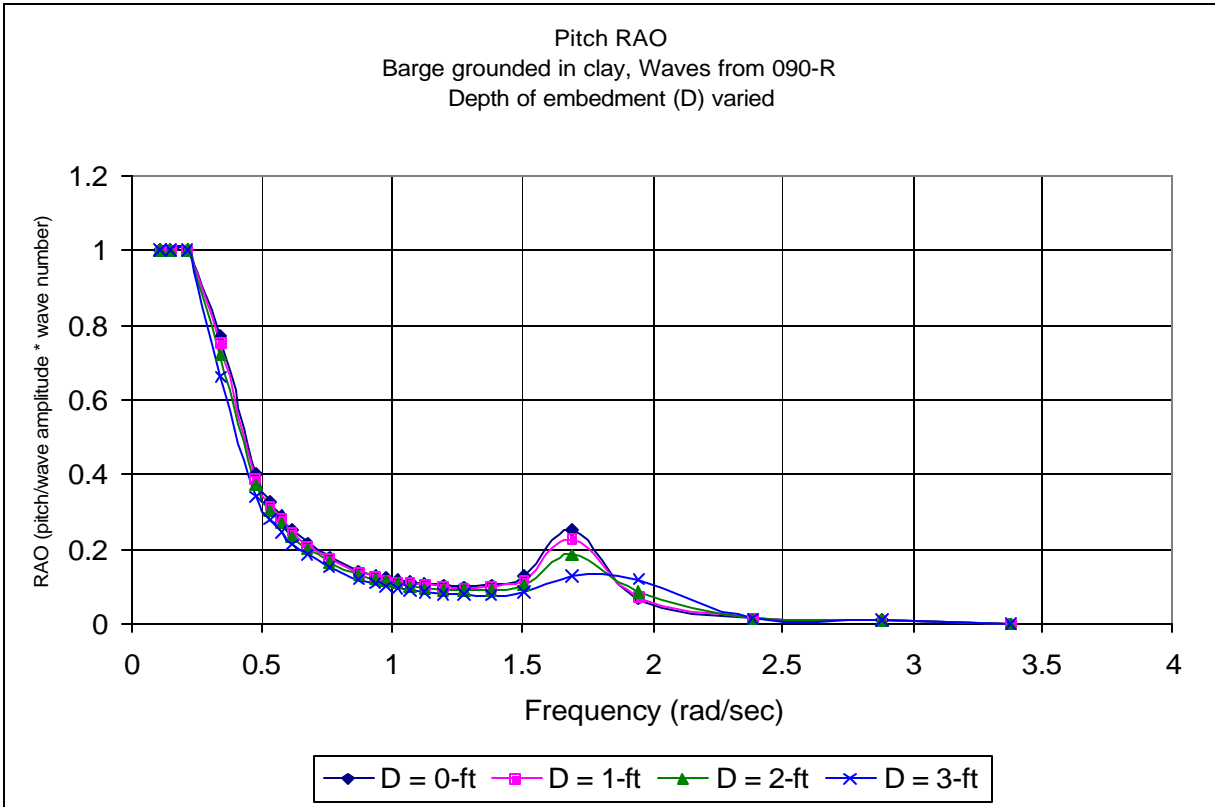


Figure 37 - Pitch RAO for barge grounded in clay, depth of embedment varied

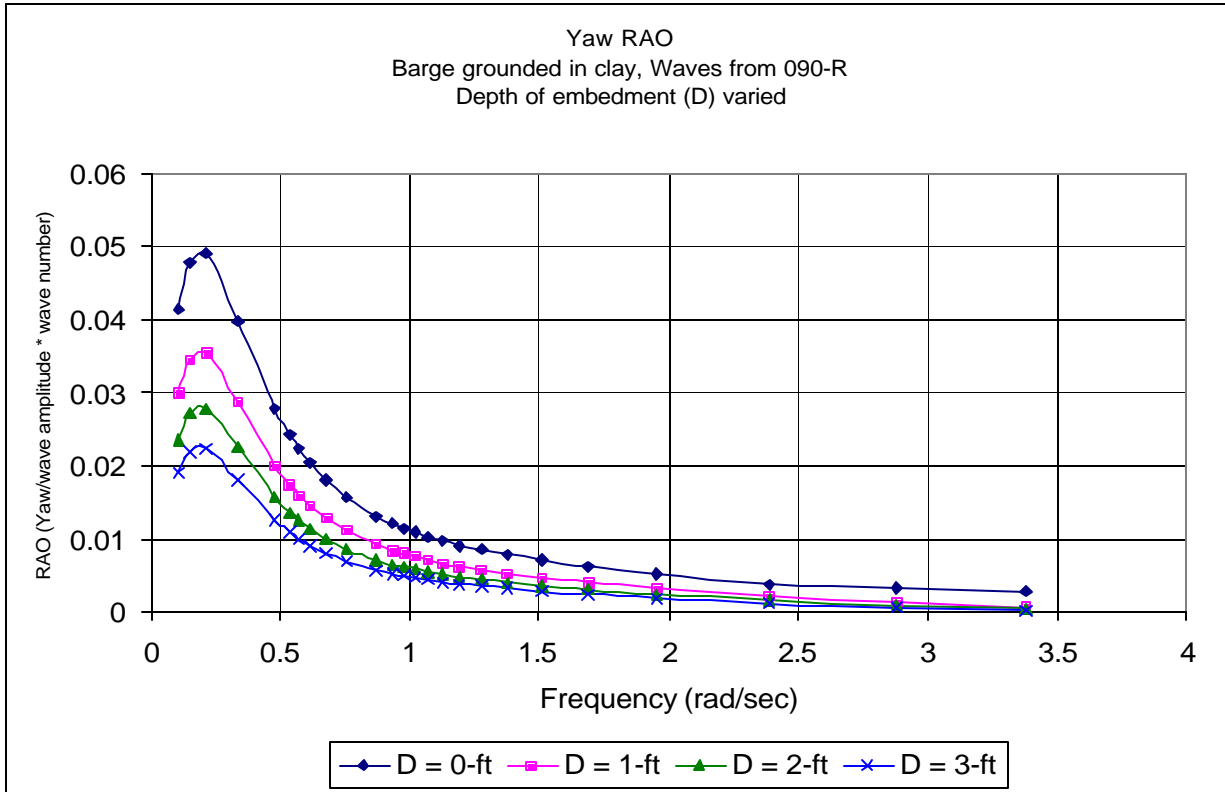


Figure 38 - Yaw RAO for barge grounded in clay, depth of embedment varied

6.1.1.2 Wave Direction Varied

Figure 39 to Figure 44 are the motion RAOs for the barge grounded in clay with the wave direction varied. The depth of embedment for these cases is one foot, and remains constant as the wave direction is varied.

Figure 39 and Figure 40 indicate that the response of the grounded barge in the surge and sway degrees of freedom increases as the wave direction nears the angle which is directly in line with the axis of motion. Hence, the surge response of the grounded barge is greatest when the waves are from 180°R (following seas), and the sway response is greatest when the waves are from 090°R (beam seas).

Figure 41 to Figure 44 indicate that the heave, roll, pitch, and yaw responses of the grounded barge increase as the wave direction varies from 180°R to 090°R. As before, the heave response is greatest in beam seas because the wave force in the vertical direction acts simultaneously along the complete length of the hull when the waves are from 090°R.

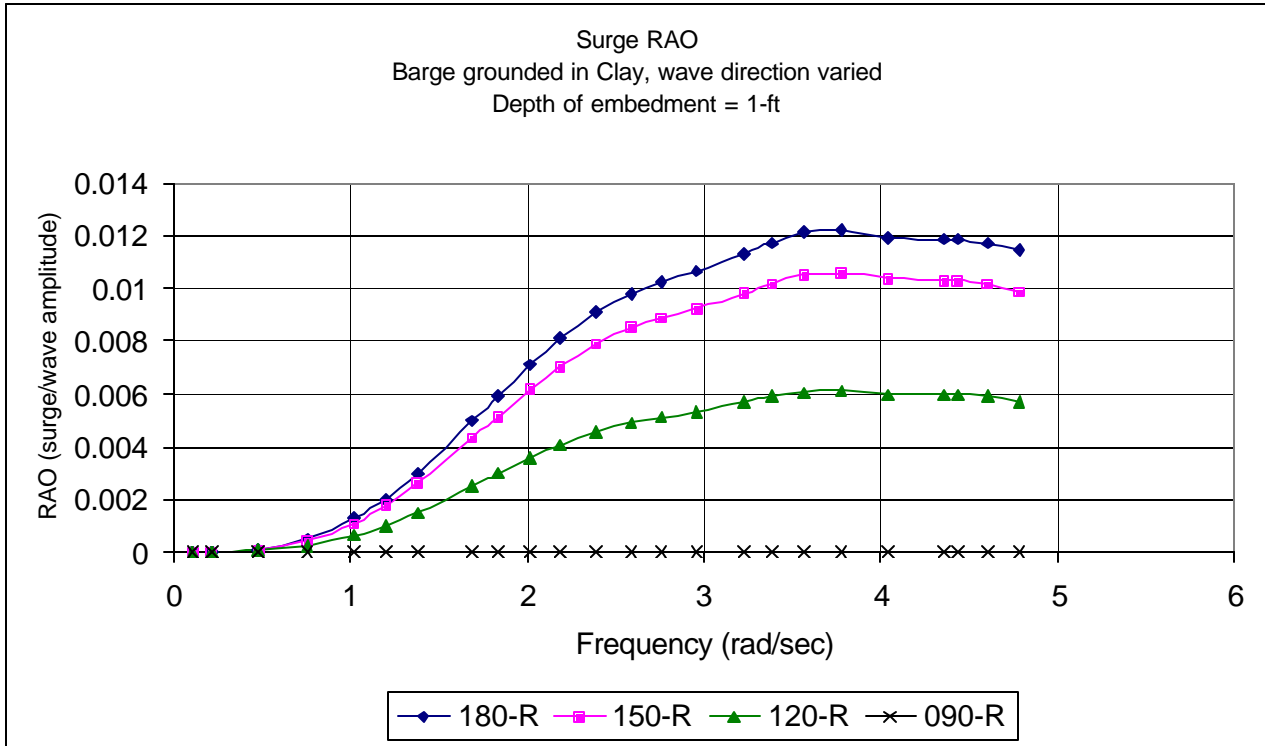


Figure 39 - Surge RAO for barge grounded in clay, wave direction varied

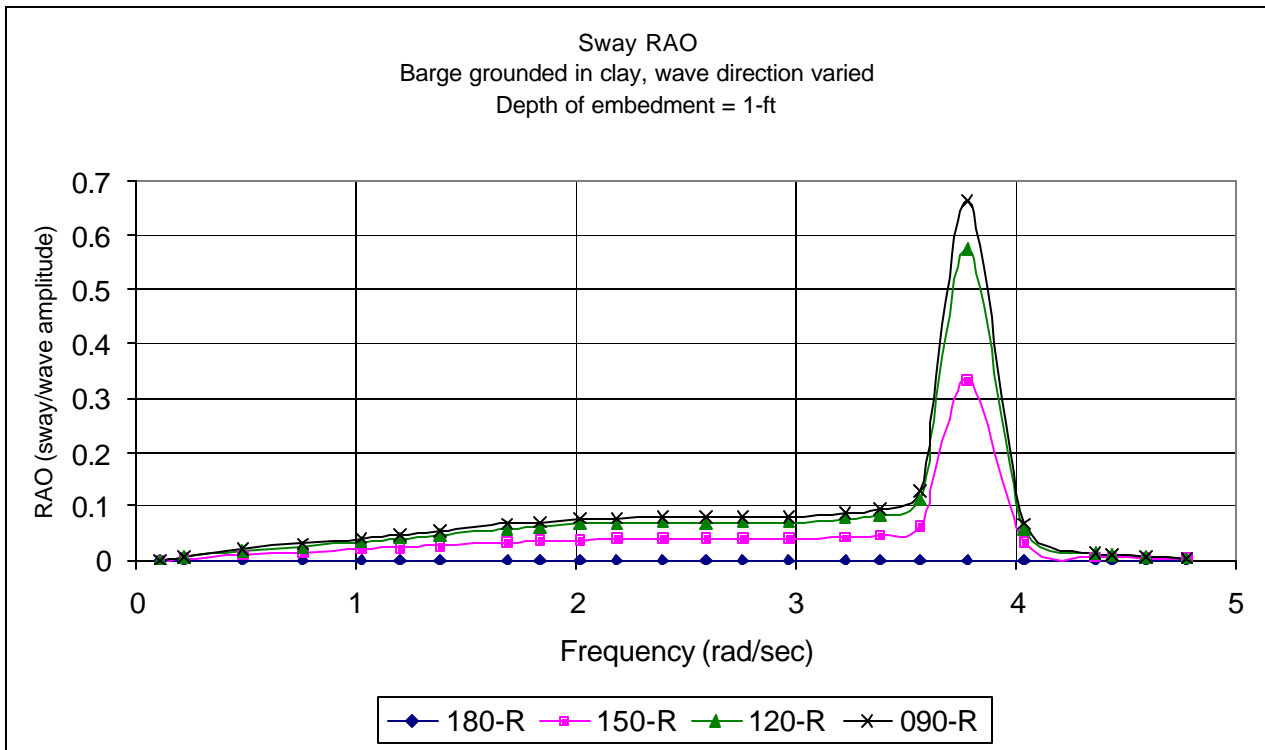


Figure 40 - Sway RAO for barge grounded in clay, wave direction varied

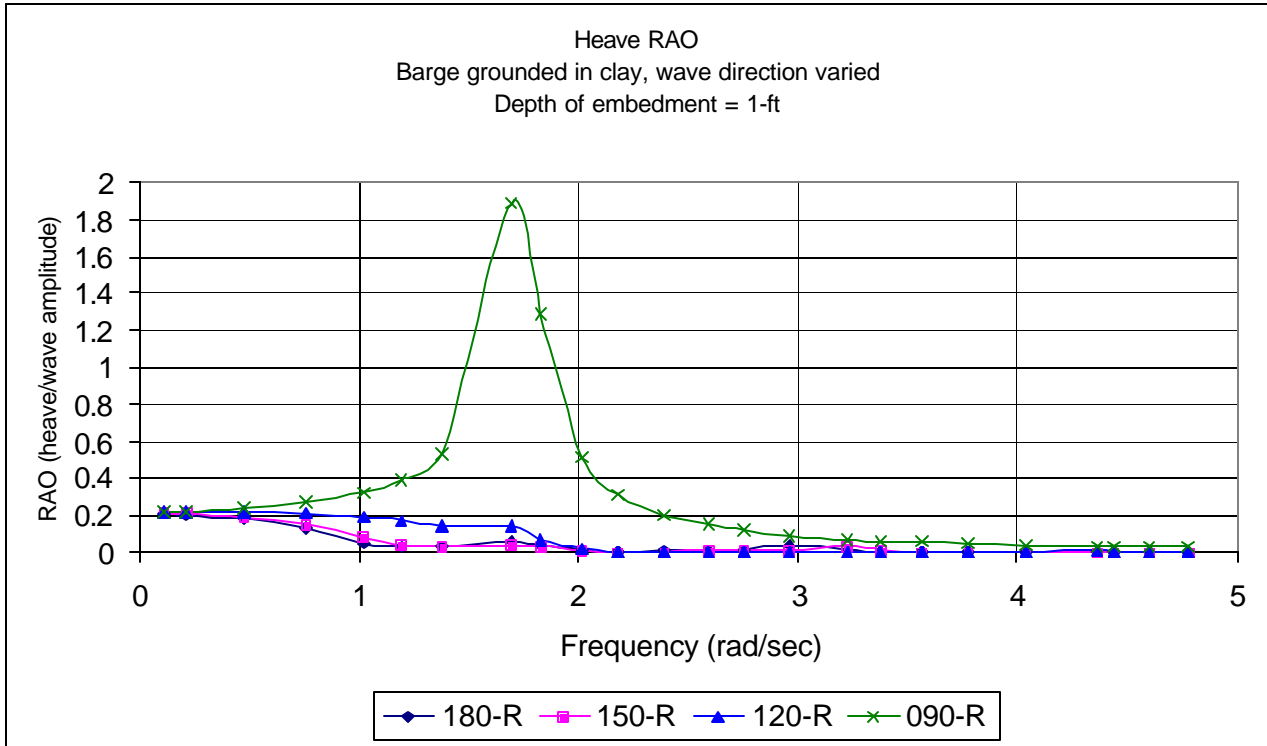


Figure 41 - Heave RAO for barge grounded in clay, wave direction varied

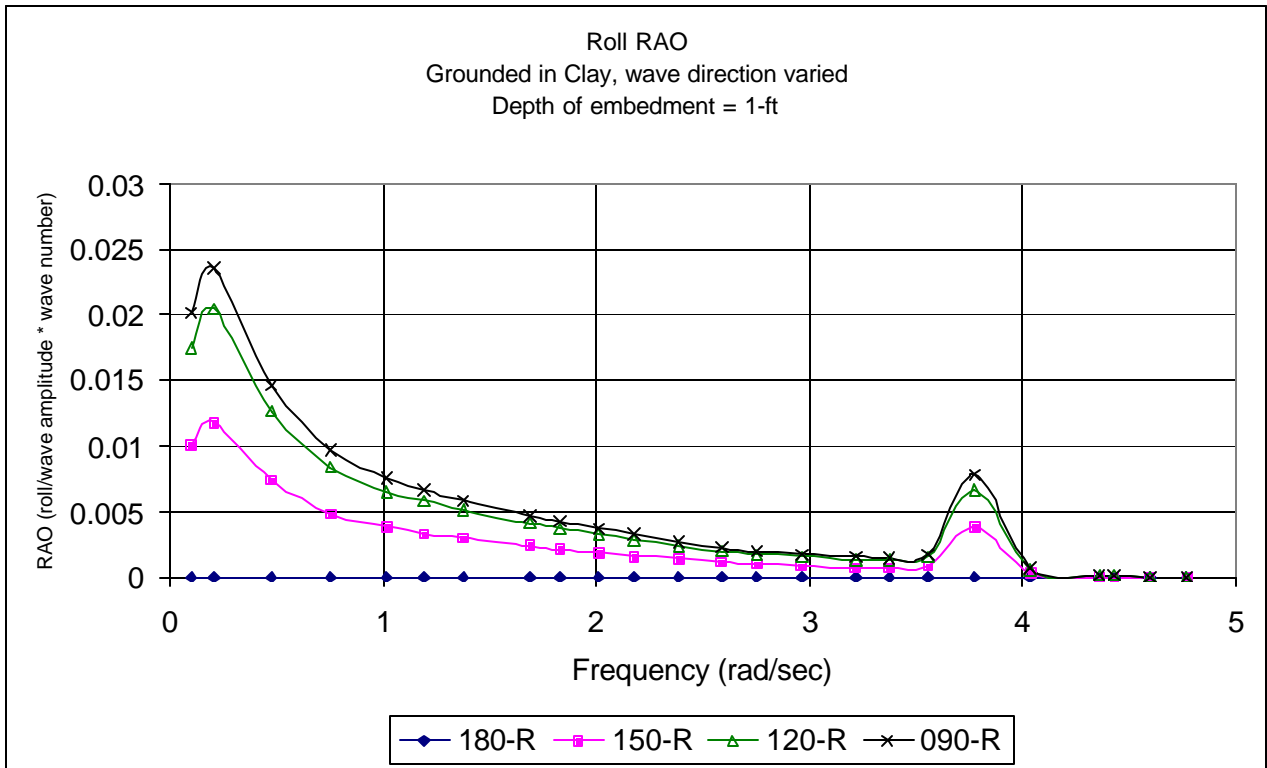


Figure 42 - Roll RAO for barge grounded in clay, wave direction varied

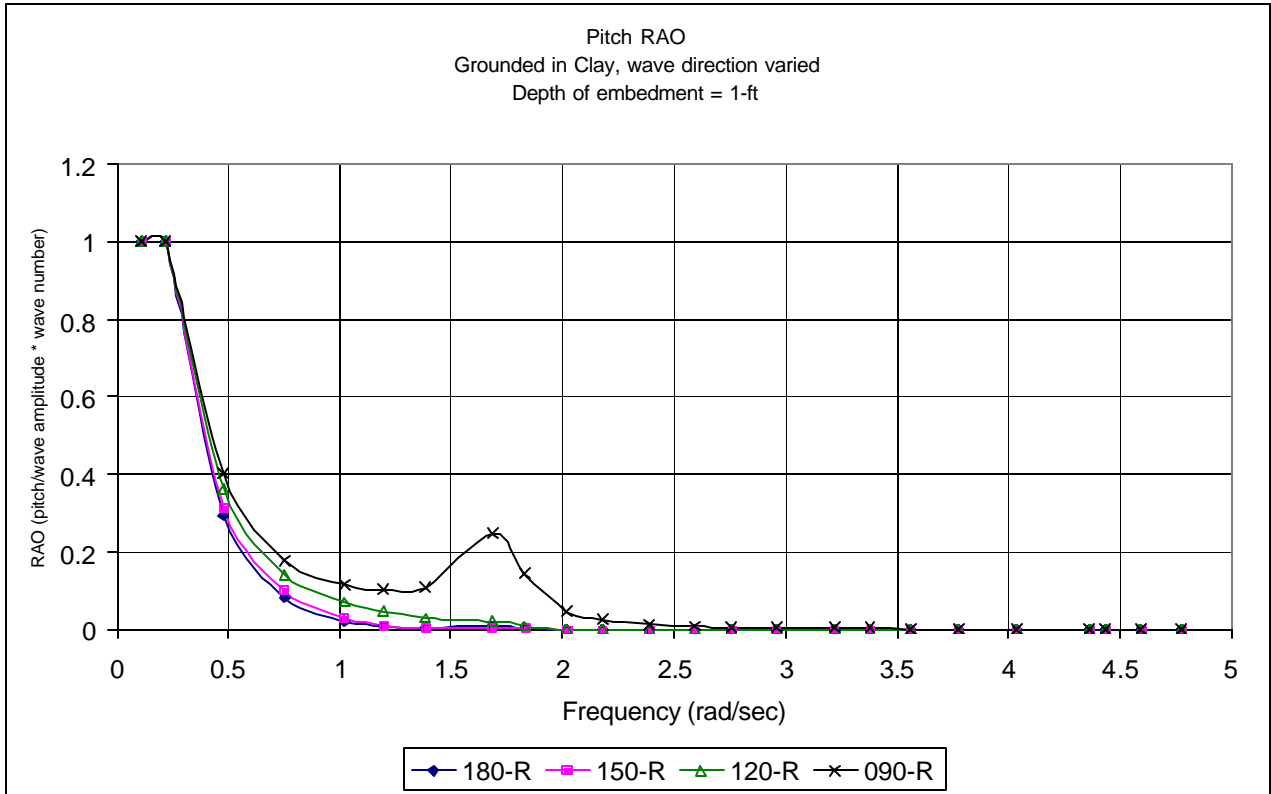


Figure 43 - Pitch RAO for barge grounded in clay, wave direction varied

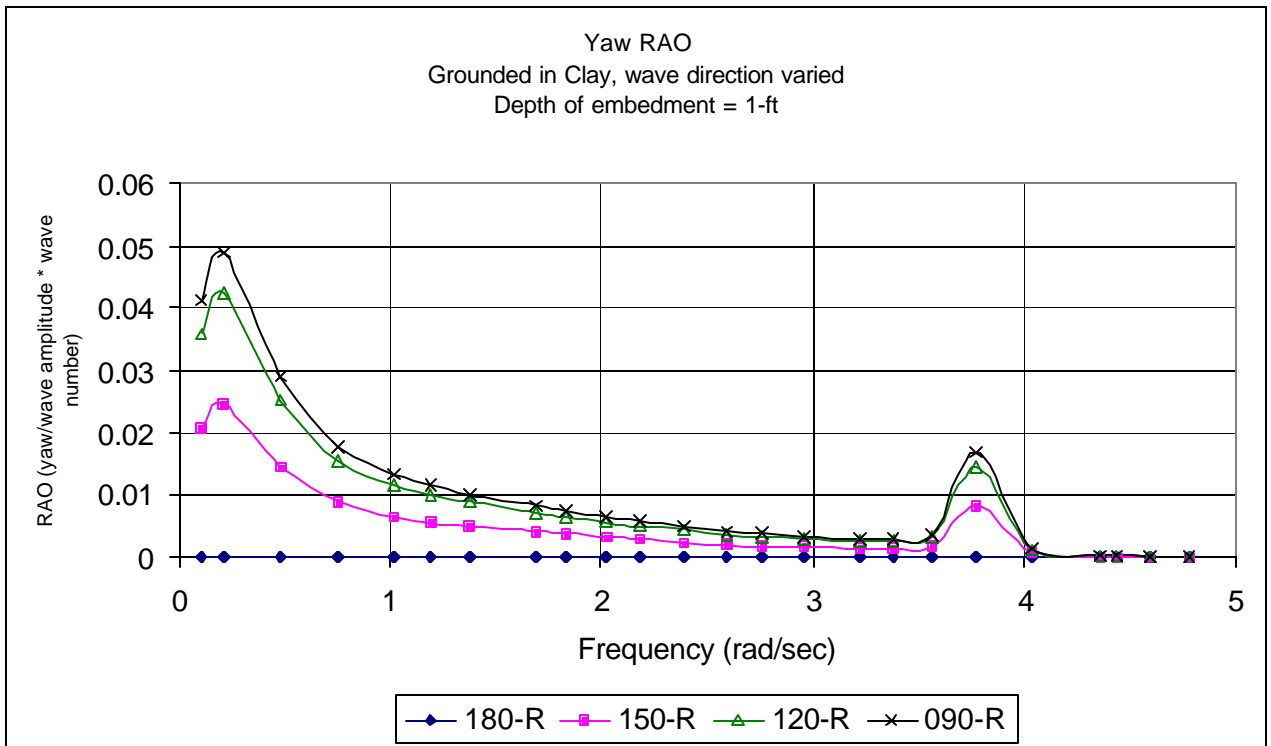


Figure 44 - Yaw RAO for barge grounded in clay, wave direction varied

6.1.1.3 Soil-Type Varied

Figure 45 to Figure 53 compare the grounding effect of each soil-type: clay, sand, soft rock and hard rock. The soil parameters which define each soil type are listed in Table 2. A depth of embedment of one foot is held constant for these calculations. In Figure 45 to Figure 47, the waves are coming from 180°R, and the barge only moves in the horizontal plane (surge, heave, pitch). In Figure 48 to Figure 53, the waves are coming from 090°R, and the barge moves in all degrees of freedom except surge.

The soil which allows the most movement in all degrees of freedom is clay (mud). The soil which provides the most restraint is hard rock. From the softest to hardest soil-type, the soils are ranked as follows: clay, sand, soft rock, hard rock. Although the different soil-types vary in stiffness, comparison of the response of the free-floating and grounded barge shows that the barge is relatively motionless in the surge, sway, roll and yaw degrees of freedom. Since the soil model considers that the grounded barge section is surrounded by soil on the four sides and on the bottom, the fact that there is little motion in these degrees of freedom is expected.

Figure 46 and Figure 50 show the response in the heave degree of freedom. As noted previously, there are resonant frequencies for clay, and the peaks in the response curve are more pronounced in beam seas. These plots also show that there is a resonant frequency for sand. Although there are multiple peaks or resonant frequencies in Figure 46 for clay-type soil, Figure 50 shows that the second peak in the response curve at ~3 radians/second is relatively small when compared to the response at 1.7 radians/second.

Figure 48 and Figure 49 show the response of the grounded barge in the sway degree of freedom. Figure 49 shows only the sway response for the clay-type soil. The range of frequencies was extended in Figure 49 to show the resonant frequency for clay.

6.1.1.4 Ground Reaction Varied

In the static analysis of a stranded ship, the loads and moments on the ship are based solely on the ground reaction. To determine the effect of ground reaction on the stranded ship in waves, the RAOs for three separate grounding cases are calculated in SSMLP. In each case, the barge is grounded as in Figure 21, and the ground reaction is varied as in Figure 22.

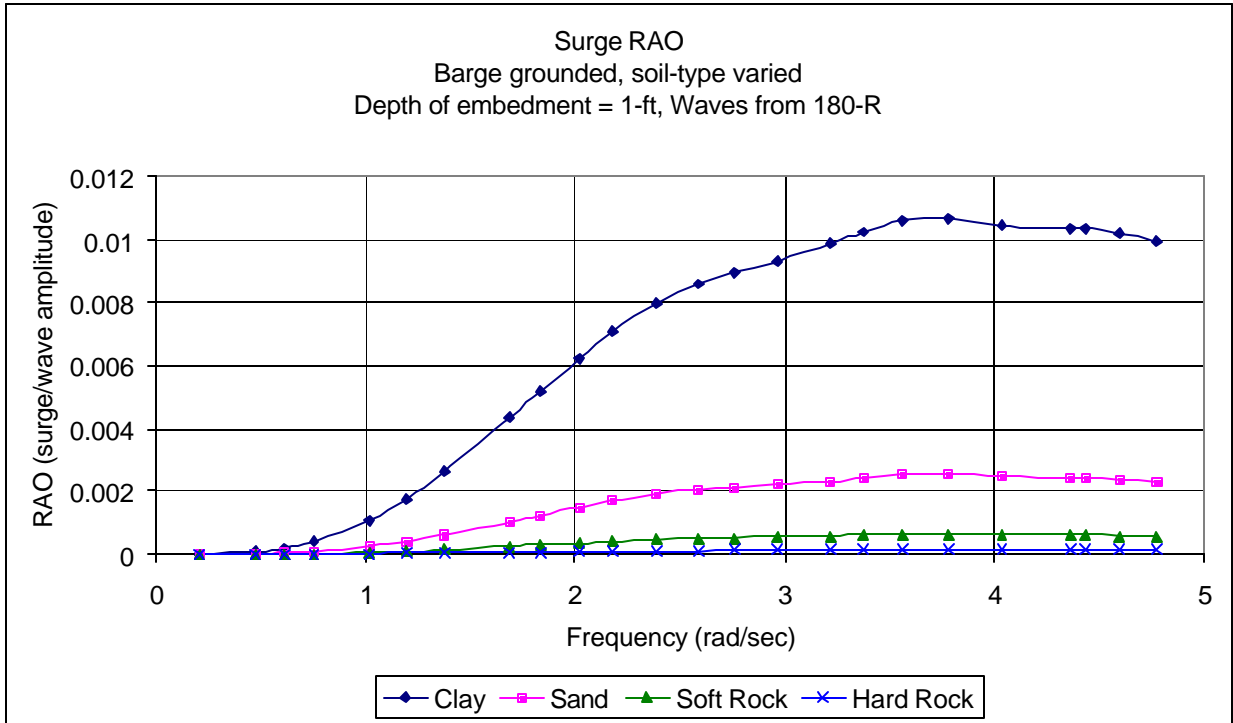


Figure 45 - Surge RAO for grounded barge, soil-type varied

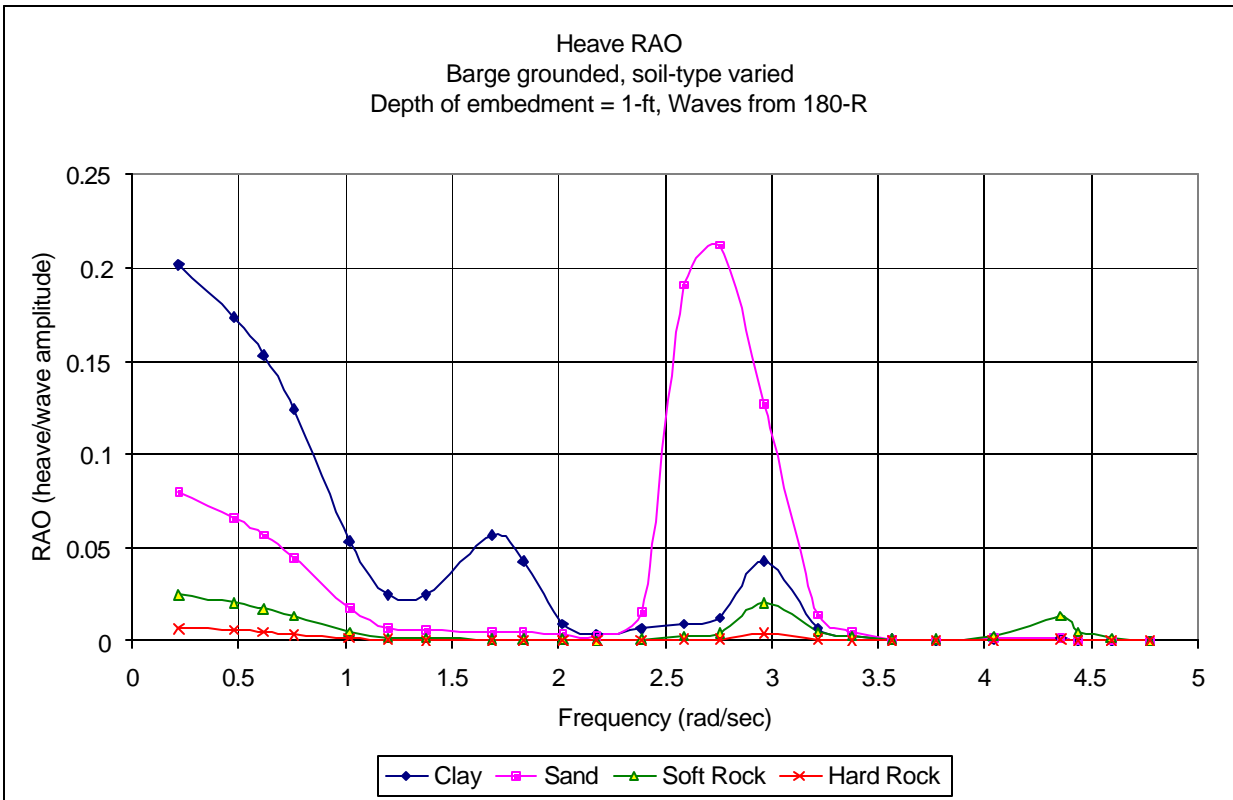


Figure 46 - Heave RAO for grounded barge, soil-type varied

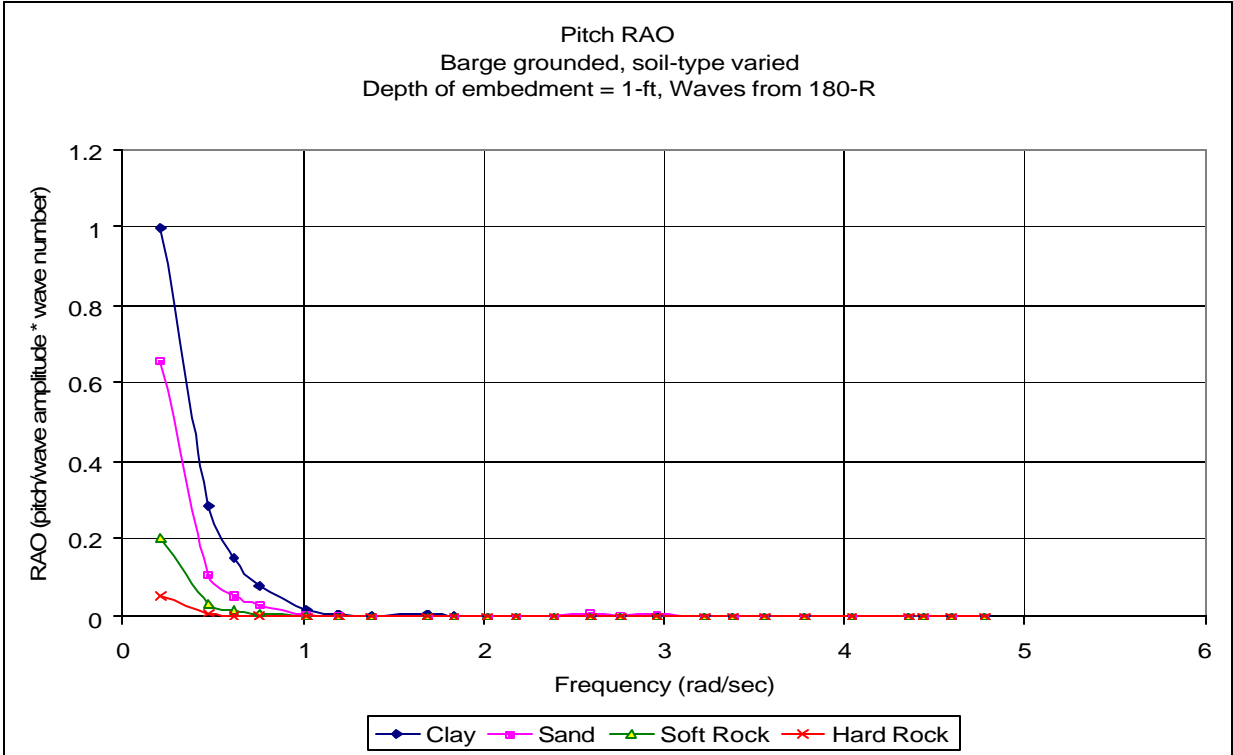


Figure 47 - Pitch RAO for grounded barge, soil-type varied

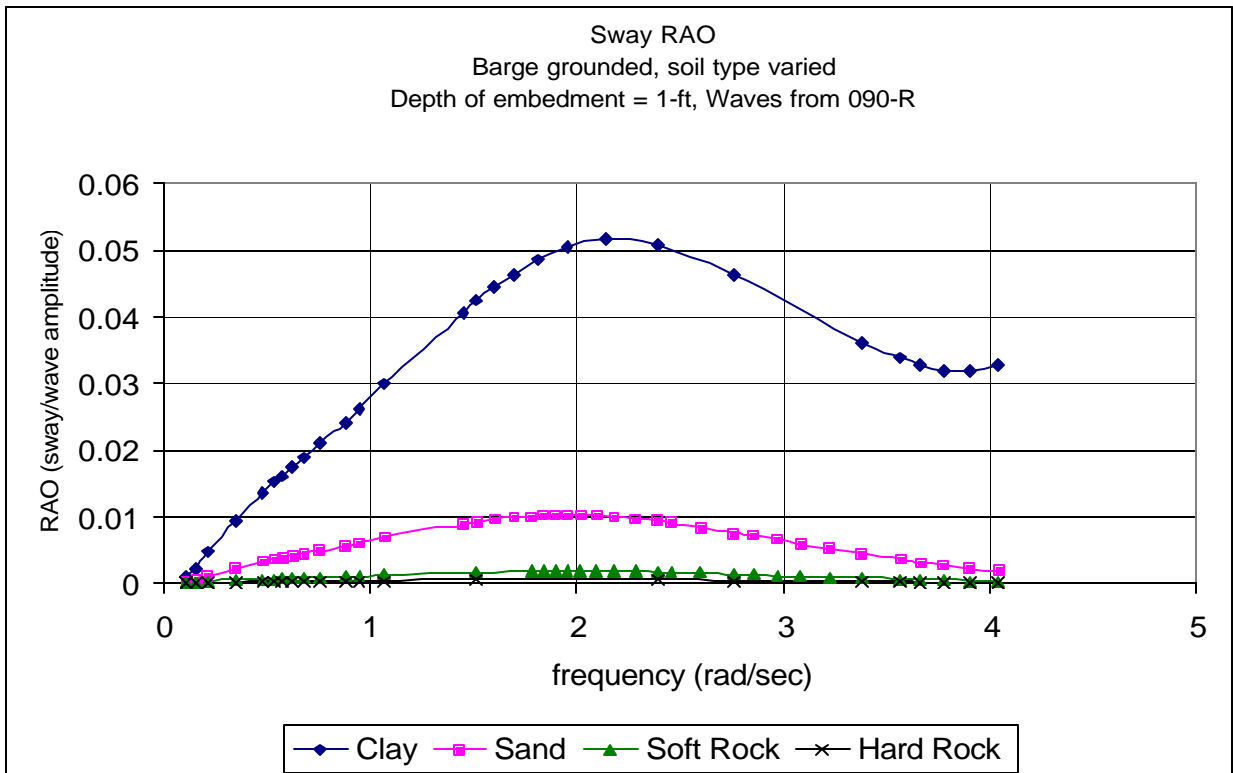


Figure 48 - Sway RAO for grounded barge, soil-type varied

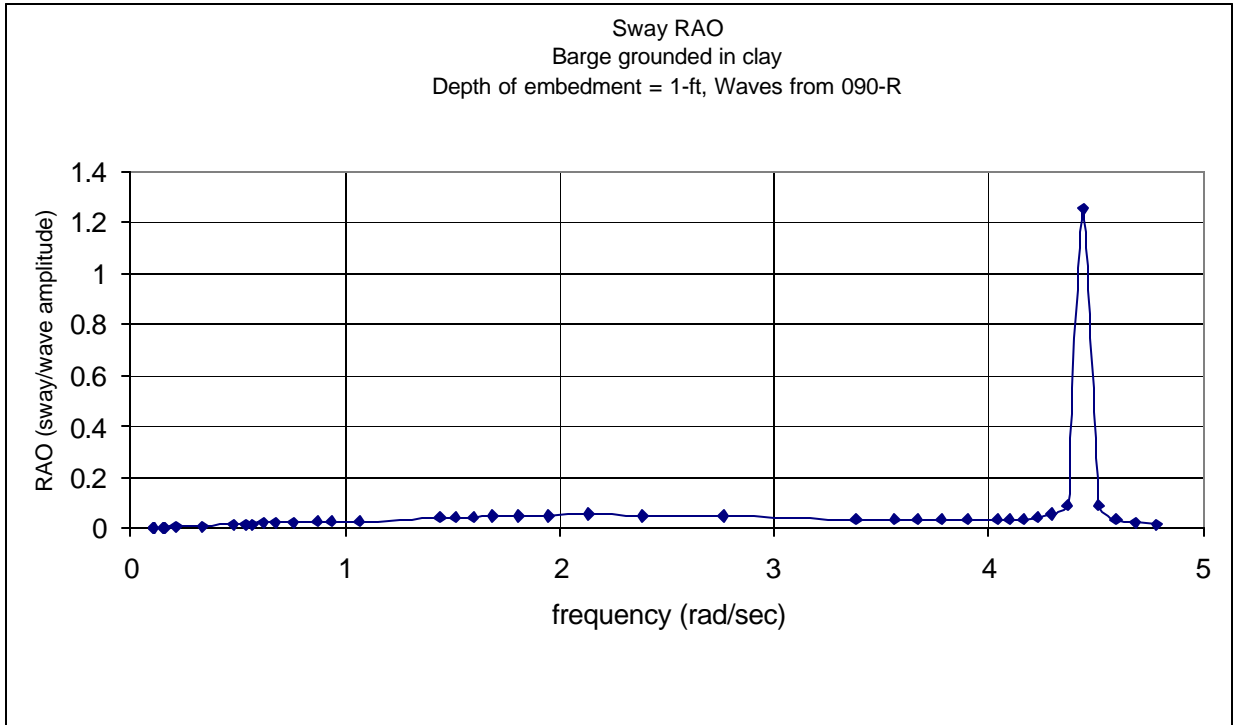


Figure 49 - Sway RAO for grounded barge, clay soil type

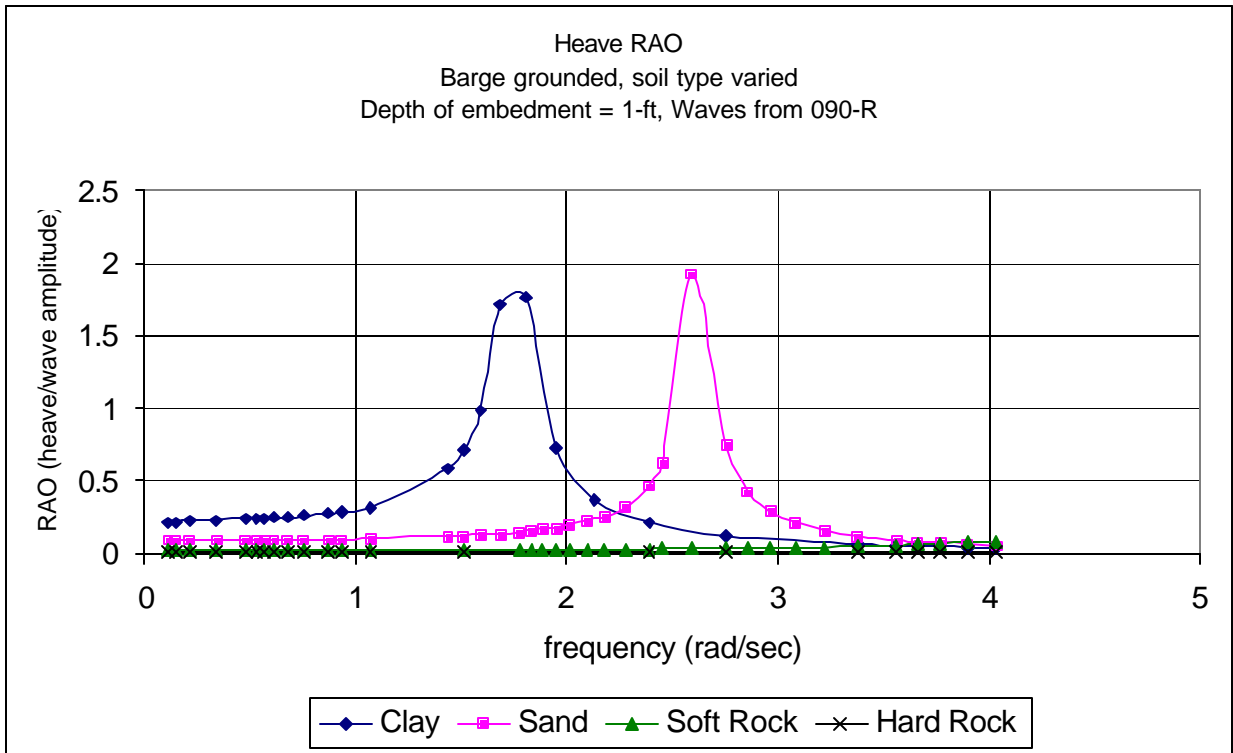


Figure 50 - Heave RAO for grounded barge, soil-type varied

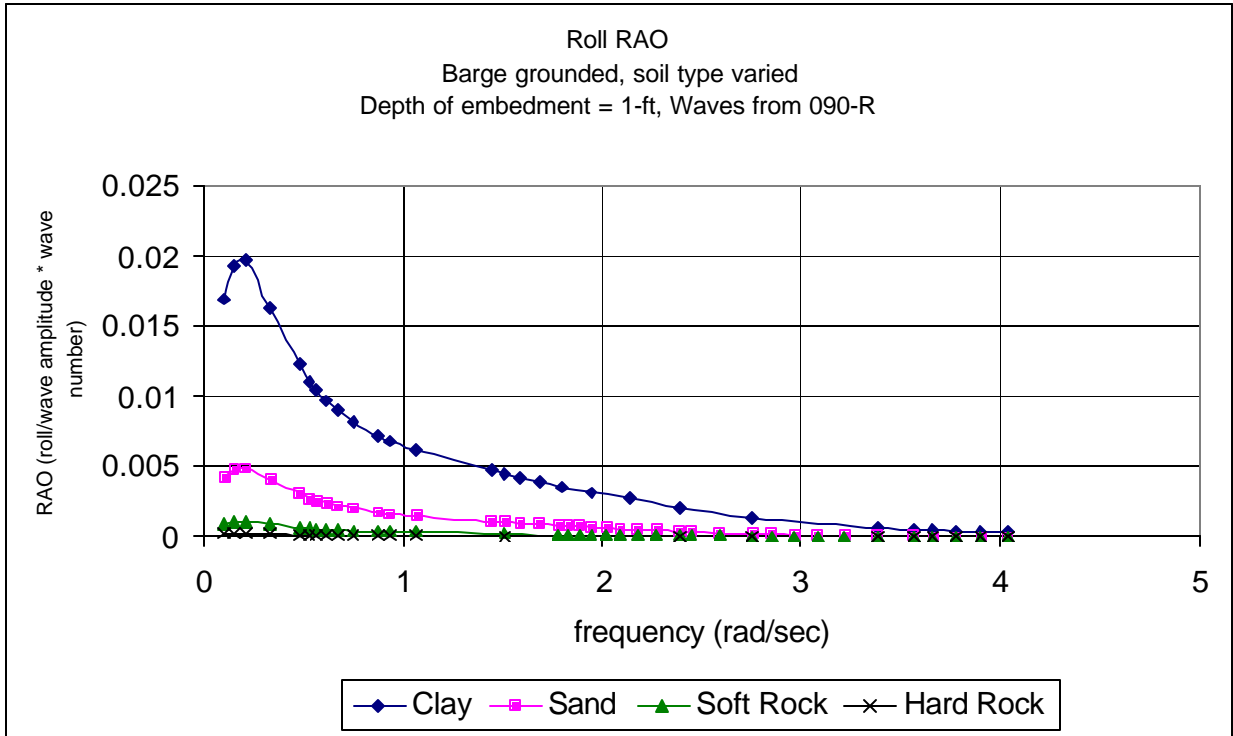


Figure 51 - Roll RAO for grounded barge, soil-type varied

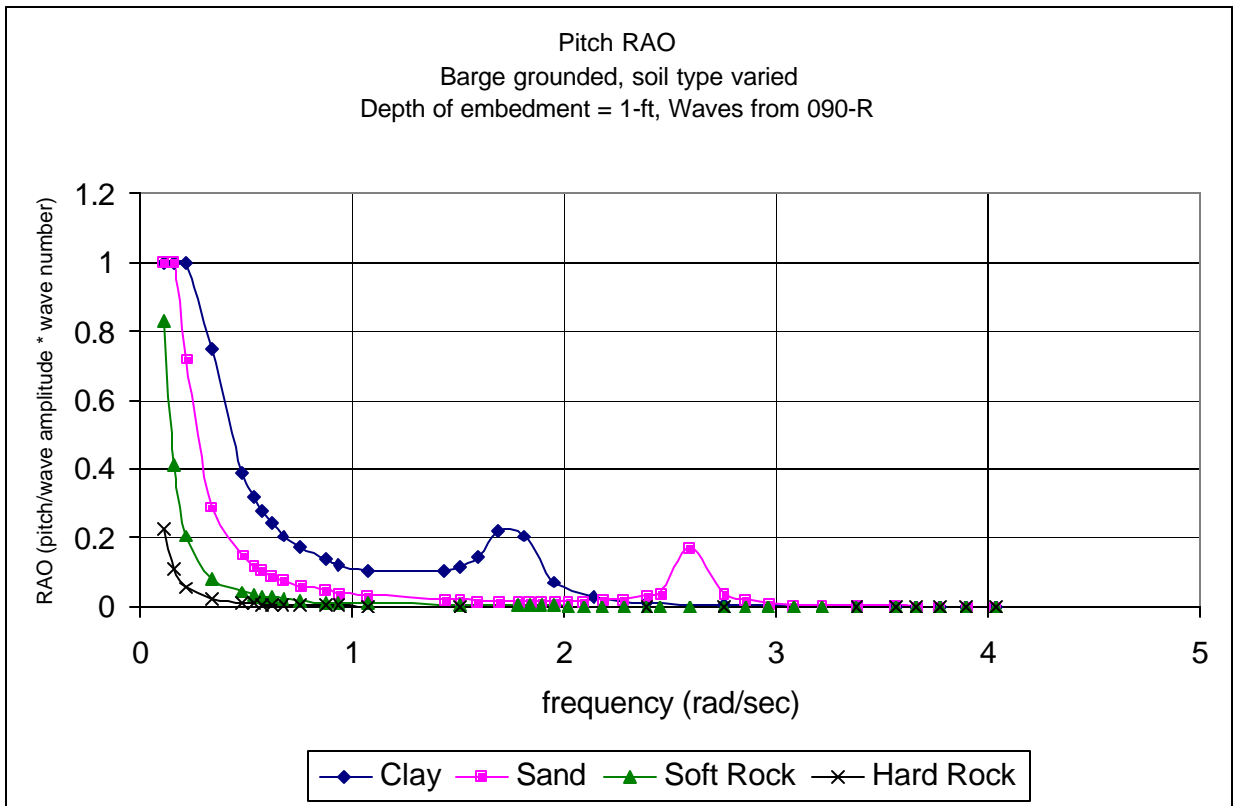


Figure 52 - Pitch RAO for grounded barge, soil-type varied

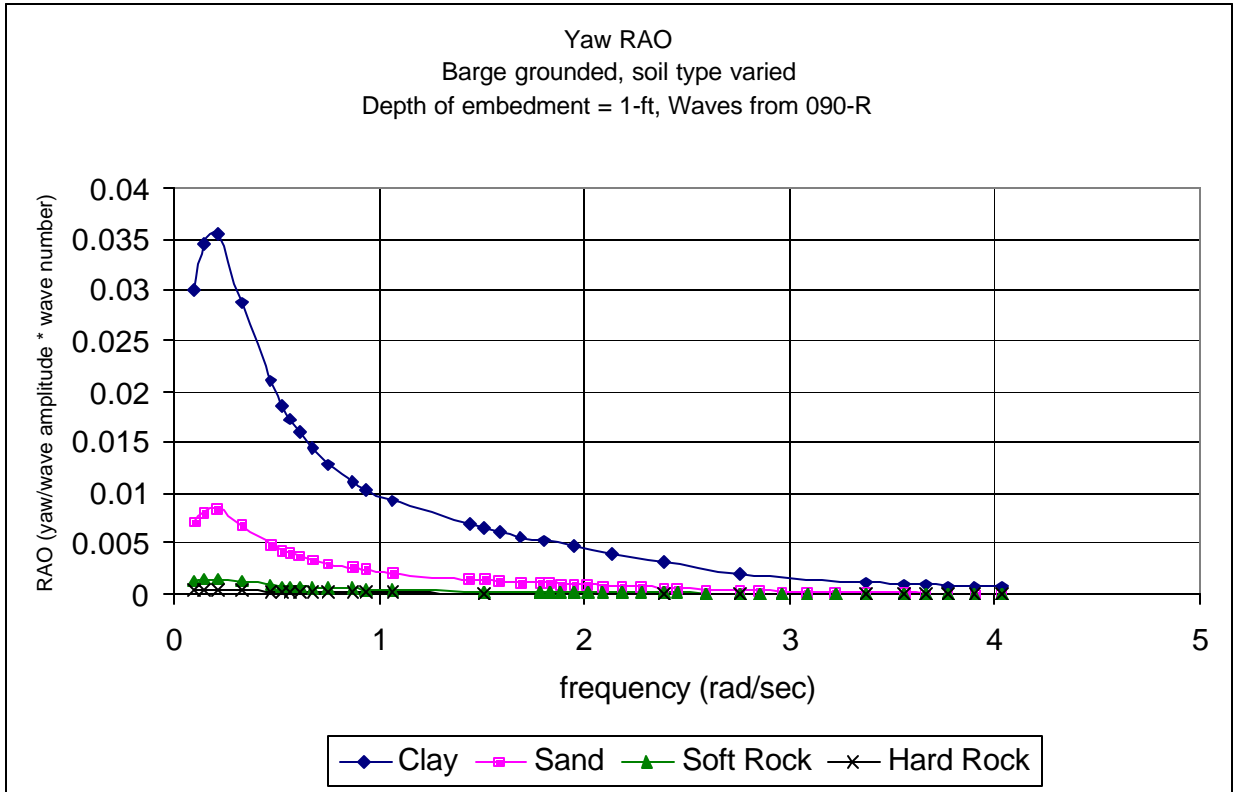


Figure 53 - Yaw RAO for grounded barge, soil-type varied

Figure 54 to Figure 61 compare the effect of ground reaction on motion of the stranded barge. The RAOs for sway, heave, roll, pitch and yaw are calculated. Each line on the RAO plot compares the response in clay while varying the ground reaction. The ground reaction is noted in the legend by the amount of long tons (LT) aground. The free-floating RAO is plotted on some figures for comparison. The depth of embedment of one foot and a wave direction of 090°R remained constant for each case.

Comparing the RAO plots for each ground reaction shows that the ground reaction has only a small effect on the response of the stranded barge in waves. In the sway, heave, and pitch degrees of freedom, the response increased slightly with the increase in ground reaction. This phenomenon results from the change in the underwater hull as the ground reaction changes. When the ground reaction increases, the vertical displacement at the grounding point also increases. As a result, the underwater hullform changes along the length of the hull which in turn creates forces which vary along the length of the hull. In the case of the grounded barge, the more the forces vary along the length of the hull, the greater the response.

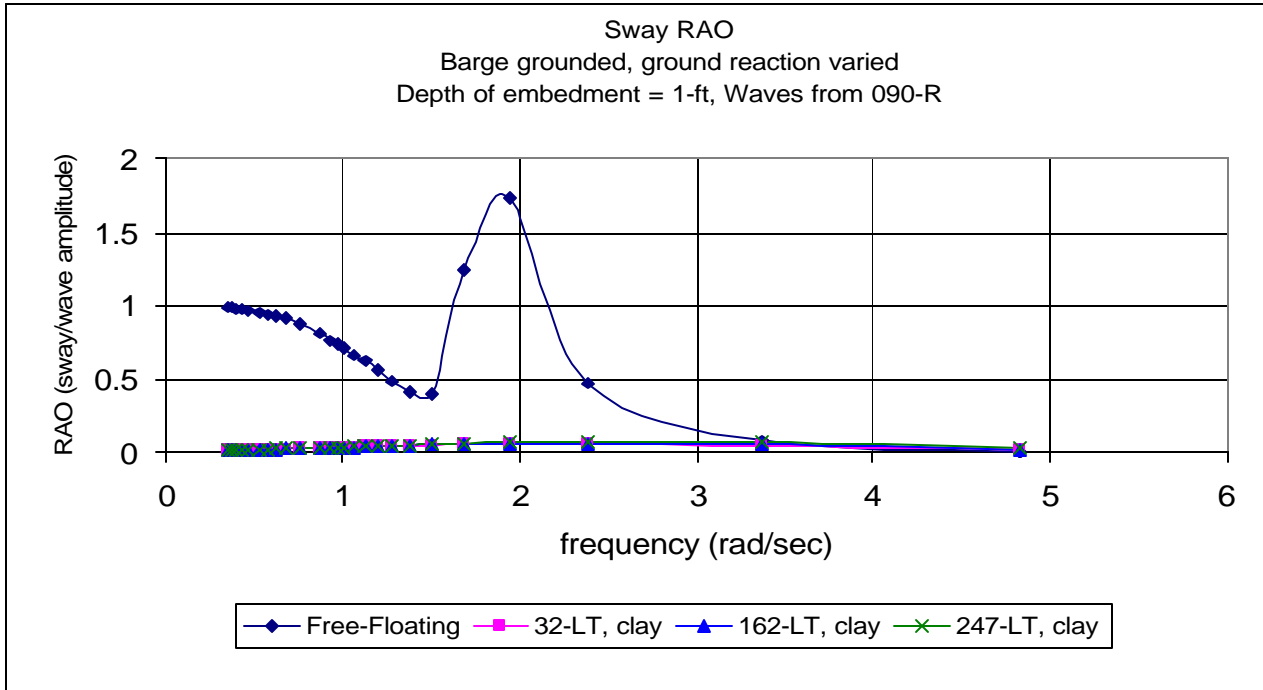


Figure 54 - Sway RAO for barge grounded in clay, ground reaction varied

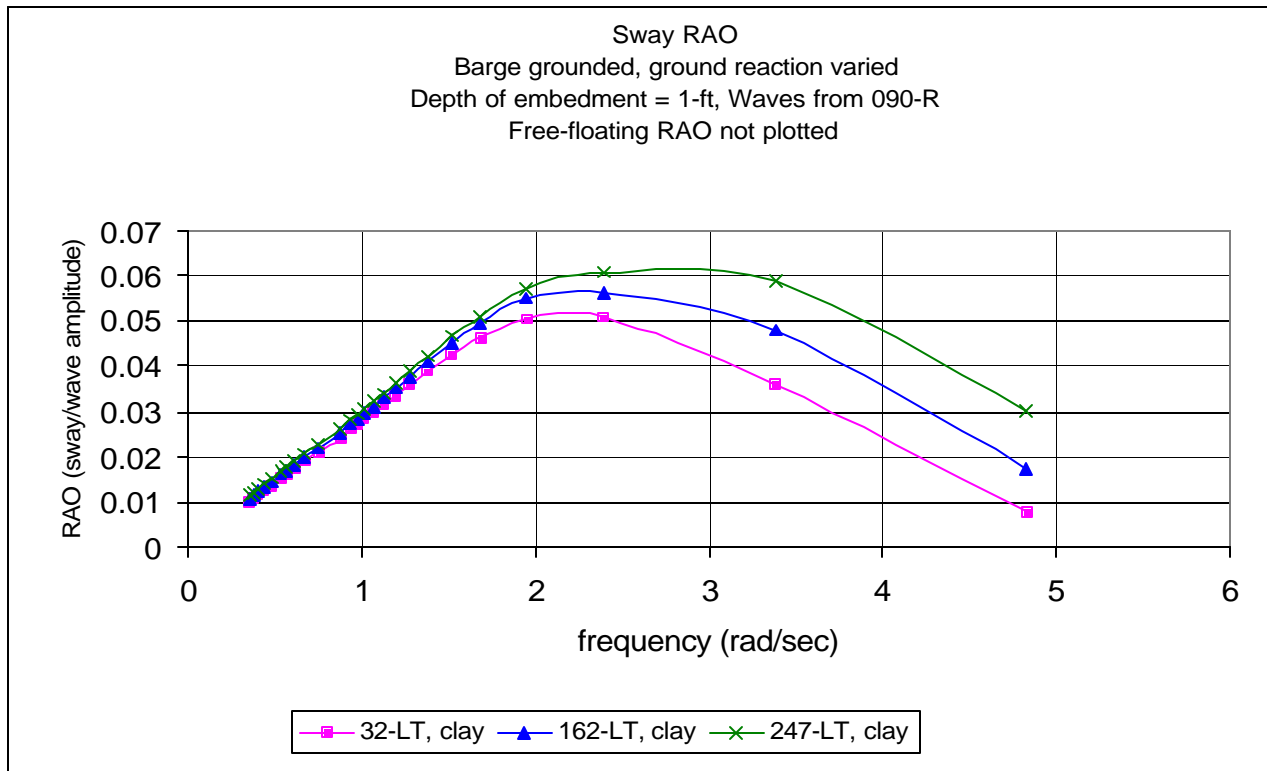


Figure 55 - Sway RAO for barge grounded in clay, ground reaction varied

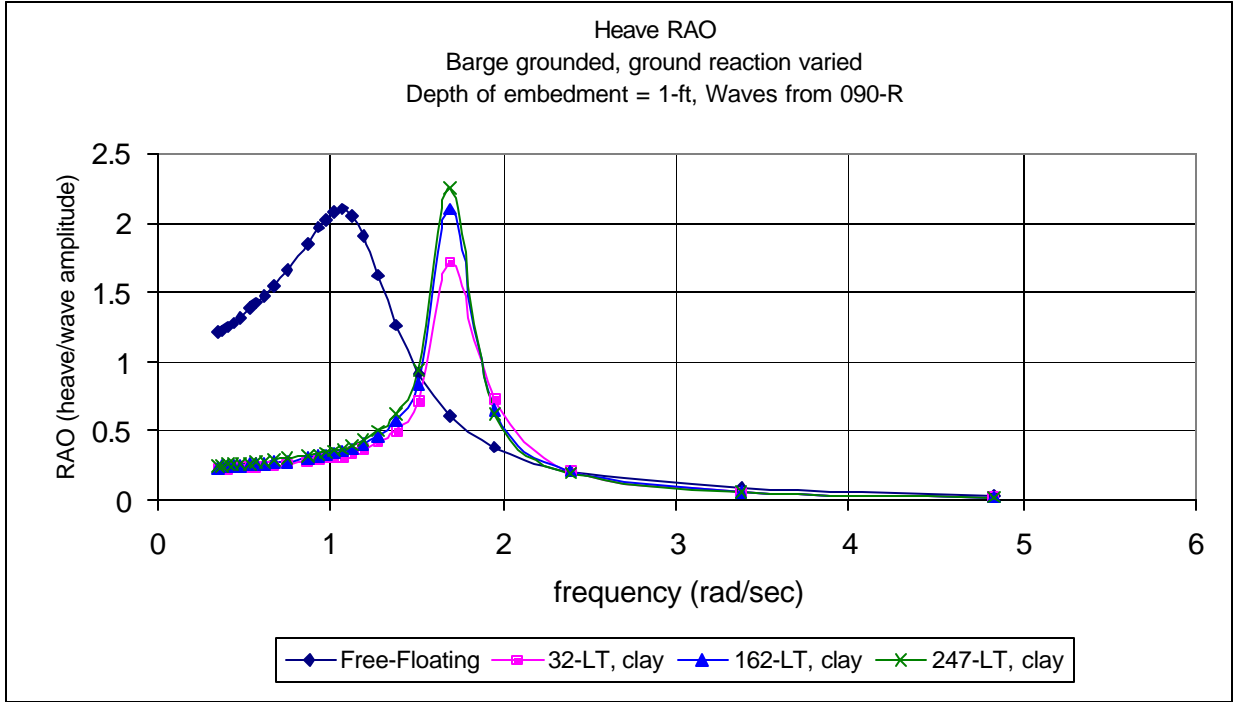


Figure 56 - Heave RAO for barge grounded in clay, ground reaction varied

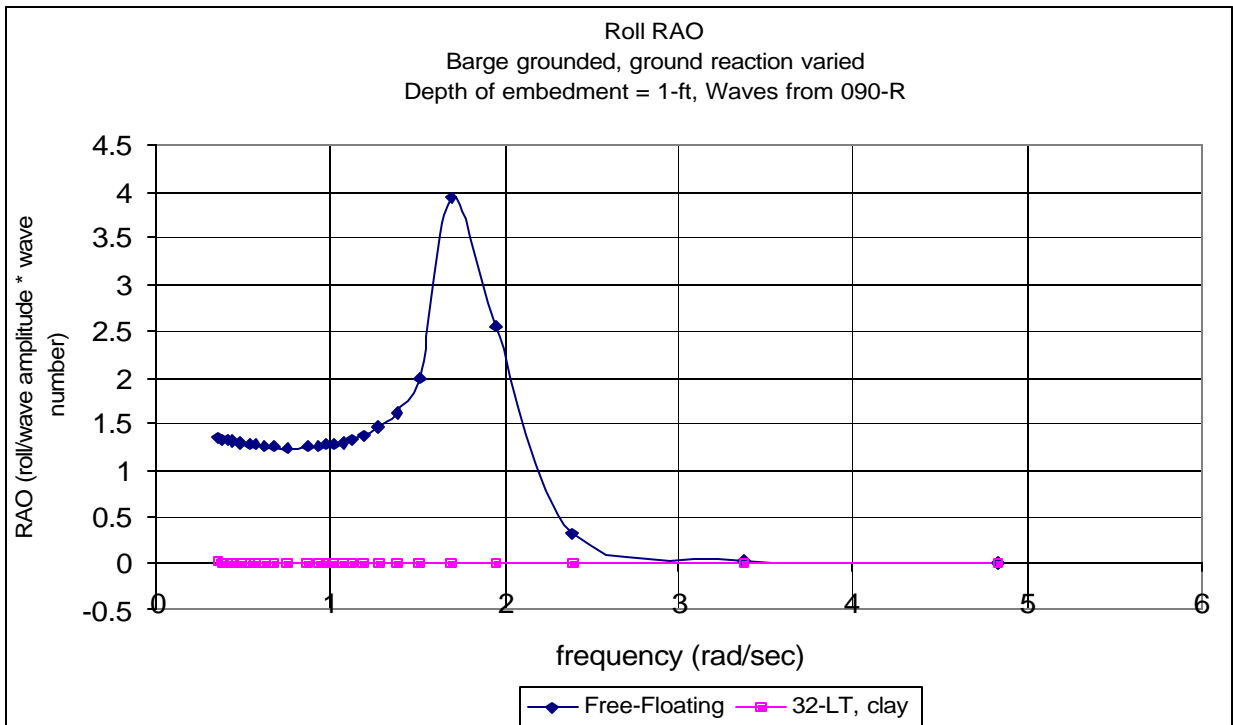


Figure 57 - Roll RAO for barge grounded in clay, ground reaction varied

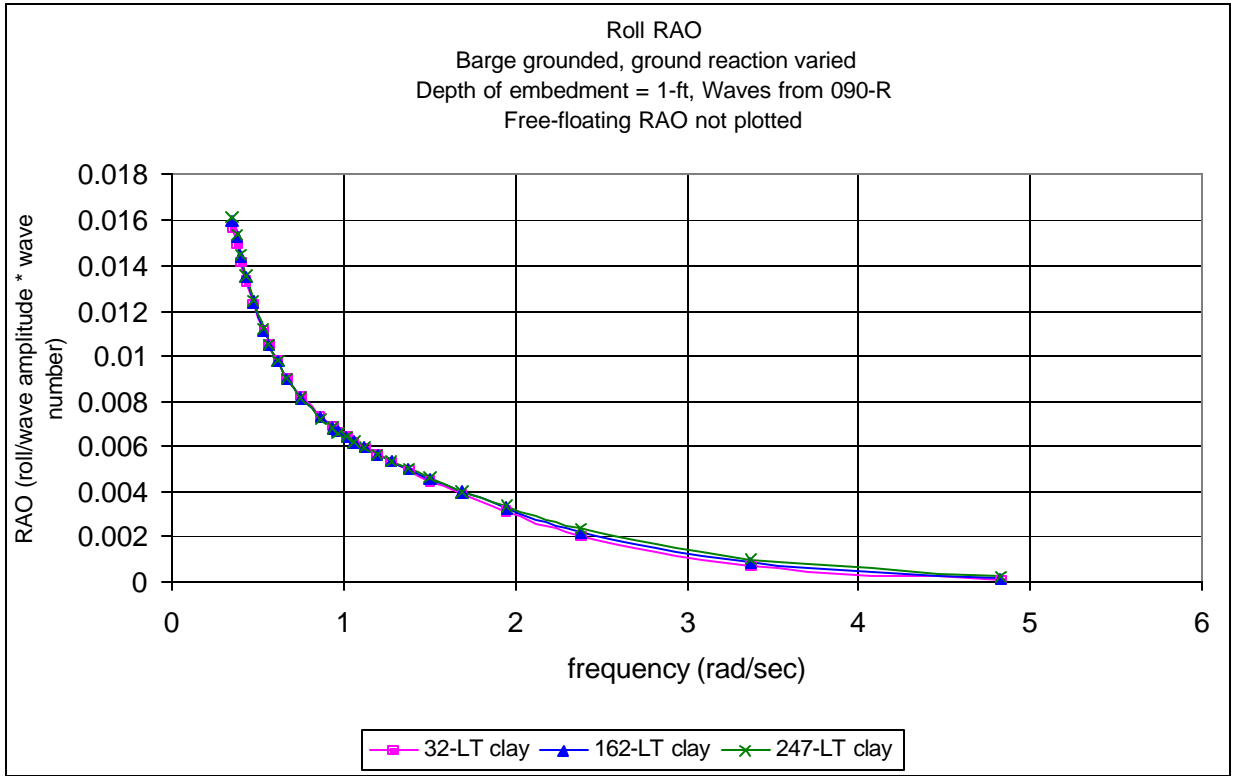


Figure 58 - Roll RAO for barge grounded in clay, ground reaction varied

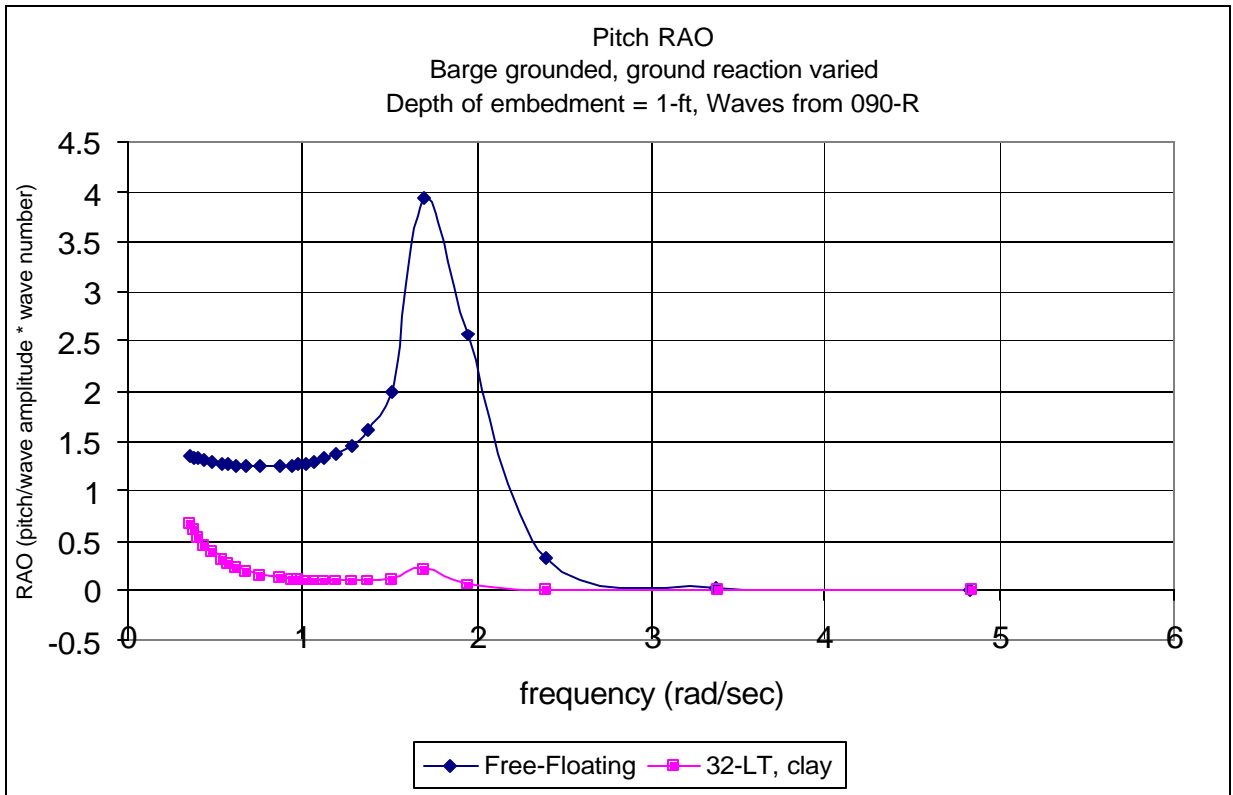


Figure 59 - Pitch RAO for barge grounded in clay, ground reaction varied

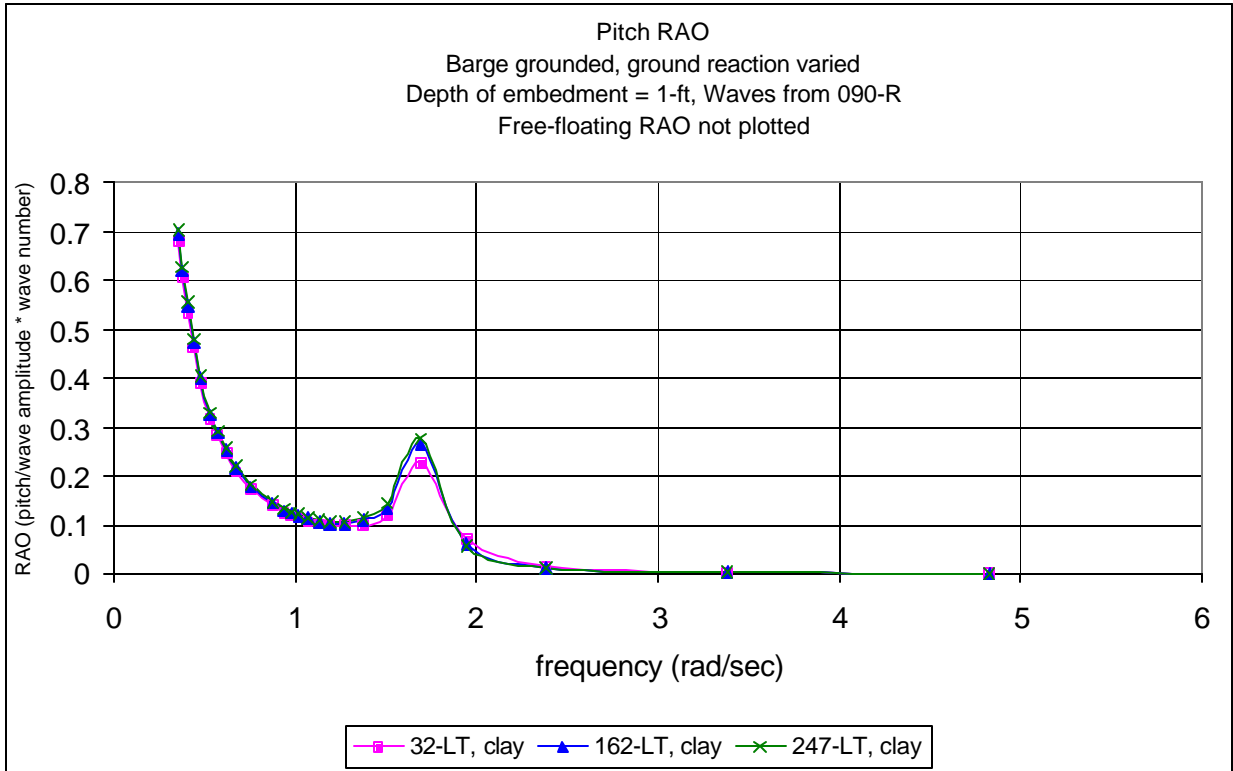


Figure 60 - Pitch RAO for barge grounded in clay, ground reaction varied

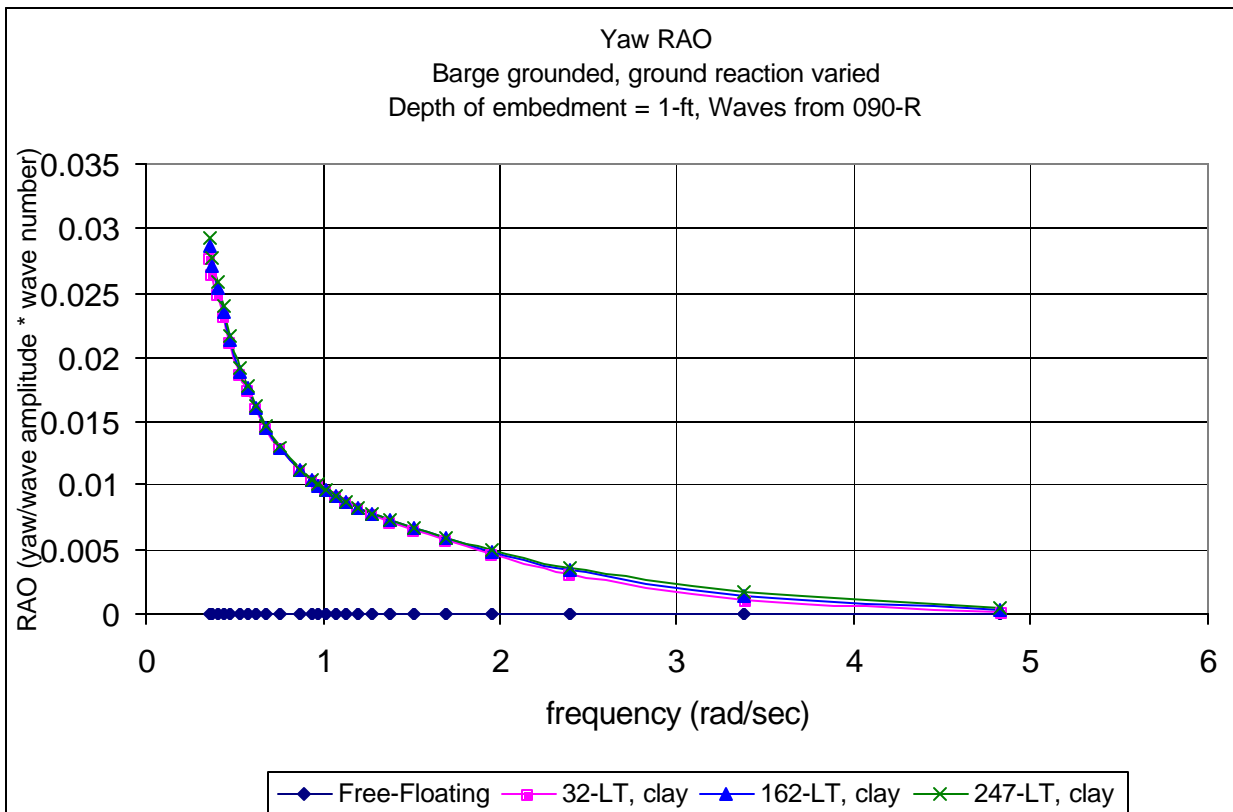


Figure 61 - Yaw RAO for barge grounded in clay, ground reaction varied

6.1.1.5 Roll Response Varying Grounding Dimensions

Since roll response in beam seas is an important factor to consider in salvage operations, this section looks at the behavior of the roll response when the grounding dimensions are varied. Specifically, the length of embedment and width of embedment are varied to examine their effect on roll. In the previous sections, the roll responses were calculated for a stranded barge with an embedded bow. The length of embedment was 10 feet, and the complete width of the barge (59 ft) was in contact with the bottom.

Figure 62 shows the change in roll response as the length of embedment is decreased and the width of the embedded section remains constant (59 feet). Figure 63 shows the change in the roll response as the beam of the embedded section is decreased and the length of the embedded section remains constant (10 feet). As expected, changing the length of embedment does not affect the roll response significantly. However, decreasing the beam of the embedded section produces a larger roll response. In Figure 64, the length and beam of the grounded section are varied simultaneously. As the grounding dimensions decrease, the roll response increases. Figure 64 also shows that there is resonant frequency in roll at 2.4 radians/second for the stranded case where L and B equal one foot. This resonant frequency shifts to the right as the ground reaction increases the stiffness of the system.

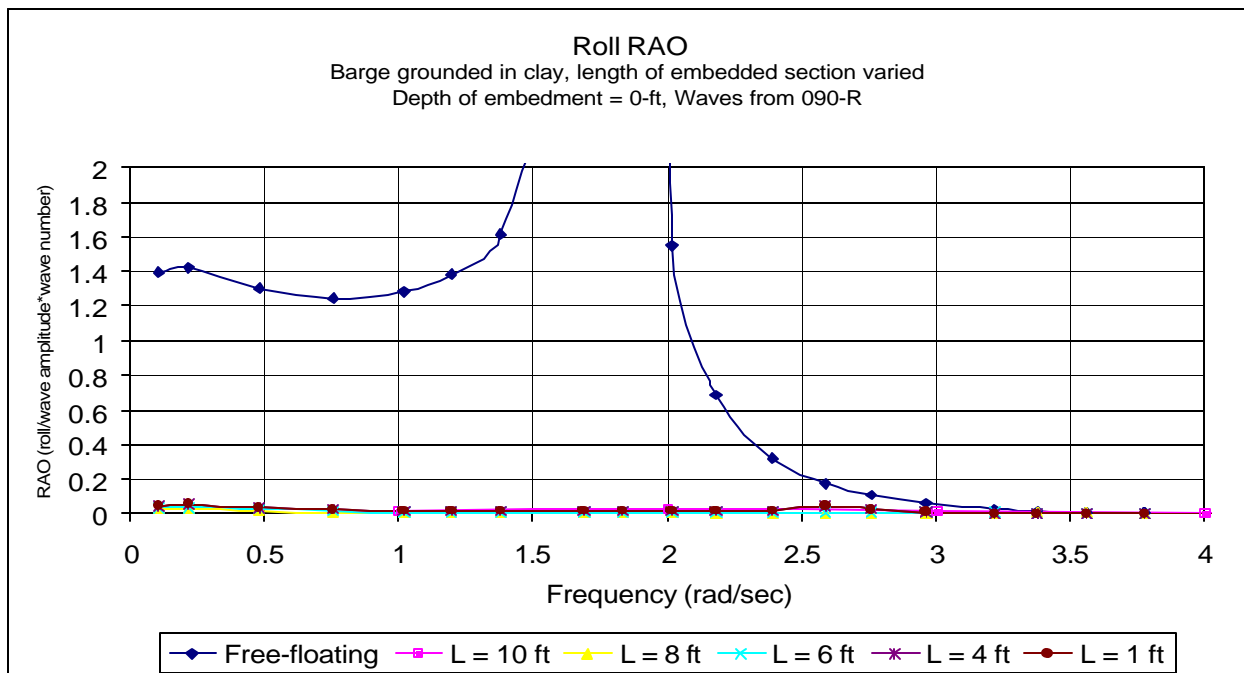


Figure 62 - Roll RAO for barge grounded in clay, length of embedment varied

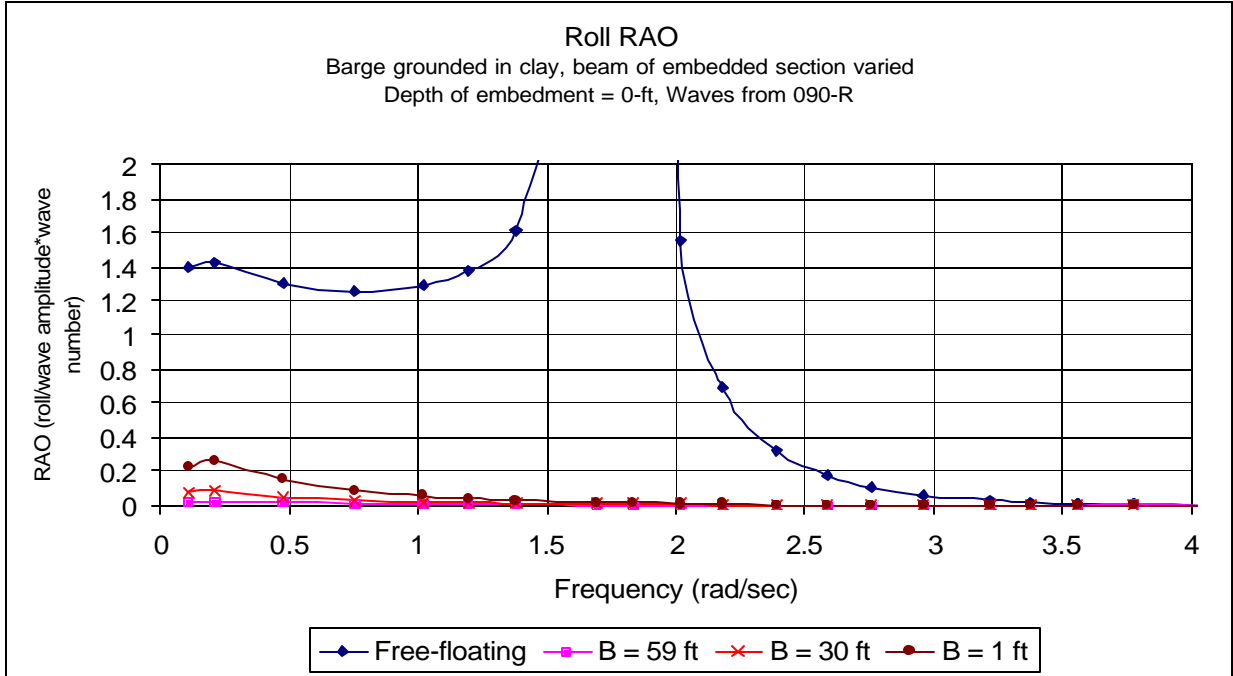


Figure 63 - Roll RAO for barge grounded in clay, beam of embedded section varied

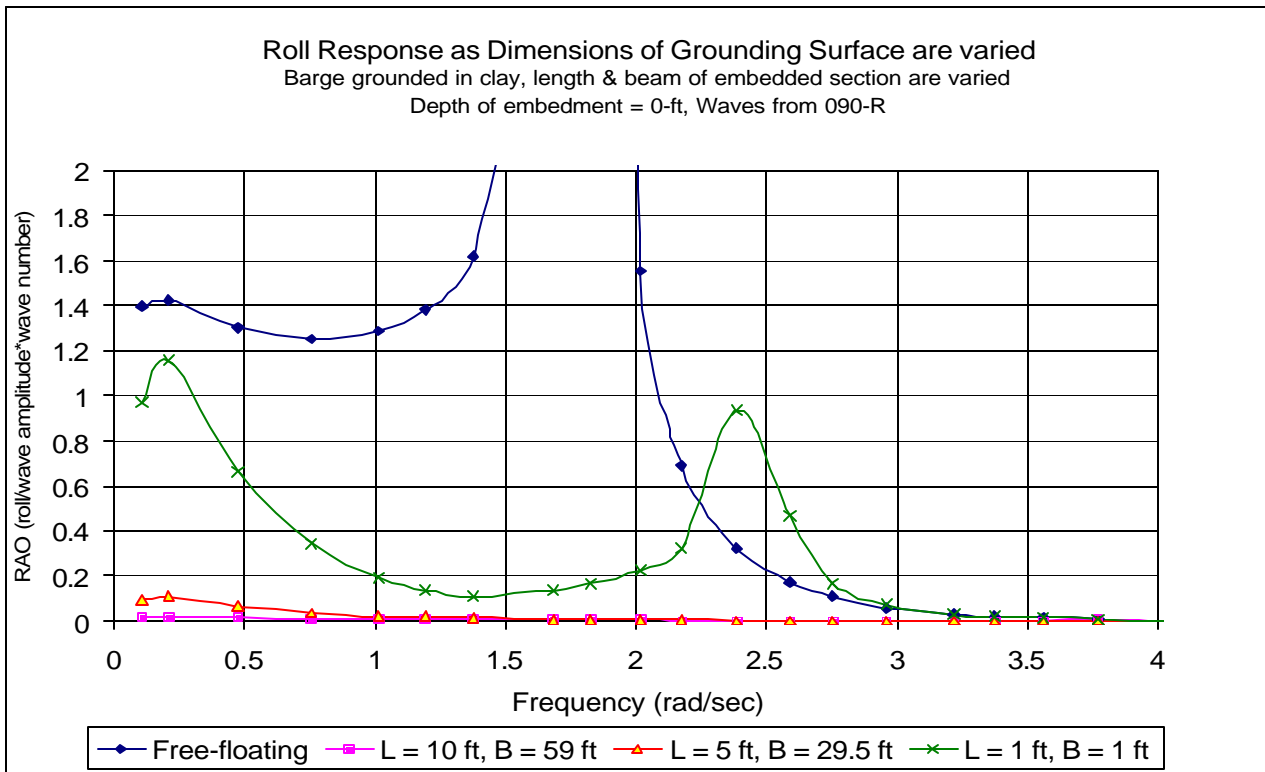


Figure 64 - Roll RAO for barge grounded in clay, length of embedment and beam of embedded section varied simultaneously

6.1.2 Bending Moment Response

6.1.2.1 Static, Grounding-Induced Bending Moment

Paik and Pedersen (1997) develop a “grounding-induced” bending moment formula which relates static bending moment in a grounded ship to vertical displacement at the grounding point. This is a static analysis, and their formula determines the grounding-induced load based on the change in buoyancy.

Results from SSMLP are compared with the “grounding-induced” bending moment values obtained by Paik and Pedersen. The “calm” or “still” water bending moment calculated in SSMLP compares well with the results of the “grounding induced” bending moment formula. Figure 65 and Figure 66 compare the results using the two methods. The bending moment curve generated by SSMLP differs slightly from the Paik and Pedersen curve for the following reasons: 1) the Paik formula assumes a point load and SSMLP assumes that the same load is distributed over the first 10-ft of the barge, and 2) SSMLP does not compute a continuous bending moment curve, but calculates bending moment values for discrete sections of the hull.

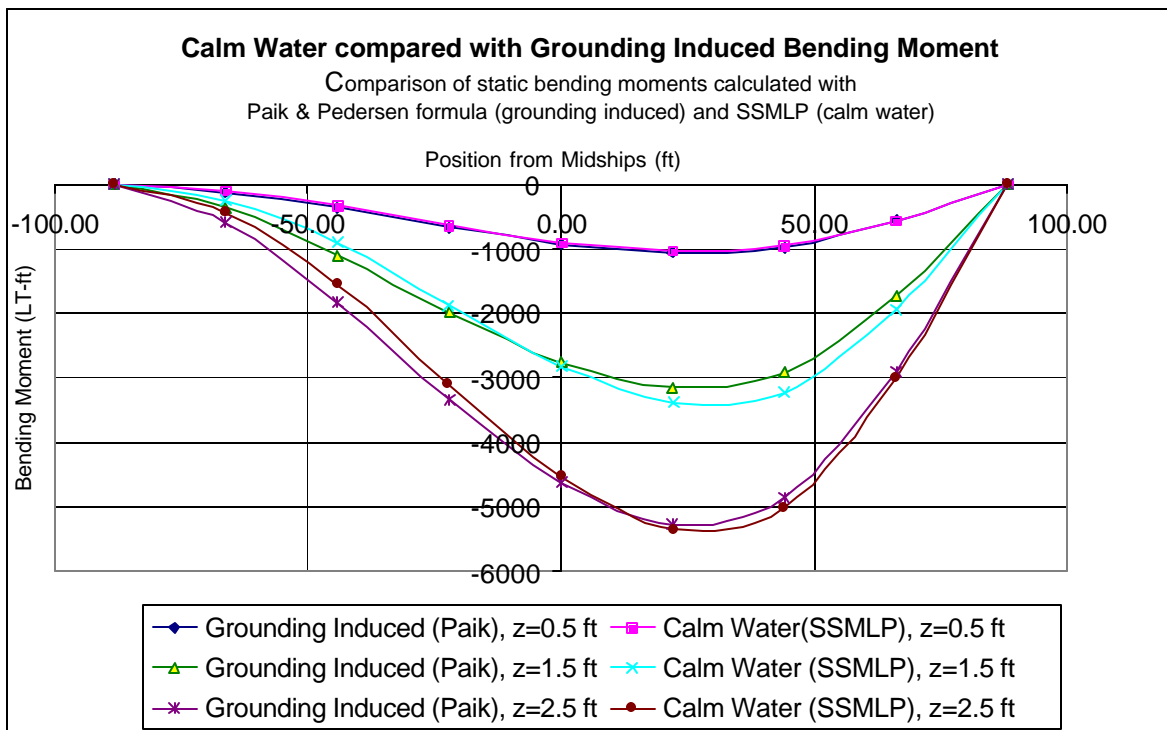


Figure 65 - Bending Moment as vertical displacement (z) or ground reaction is varied

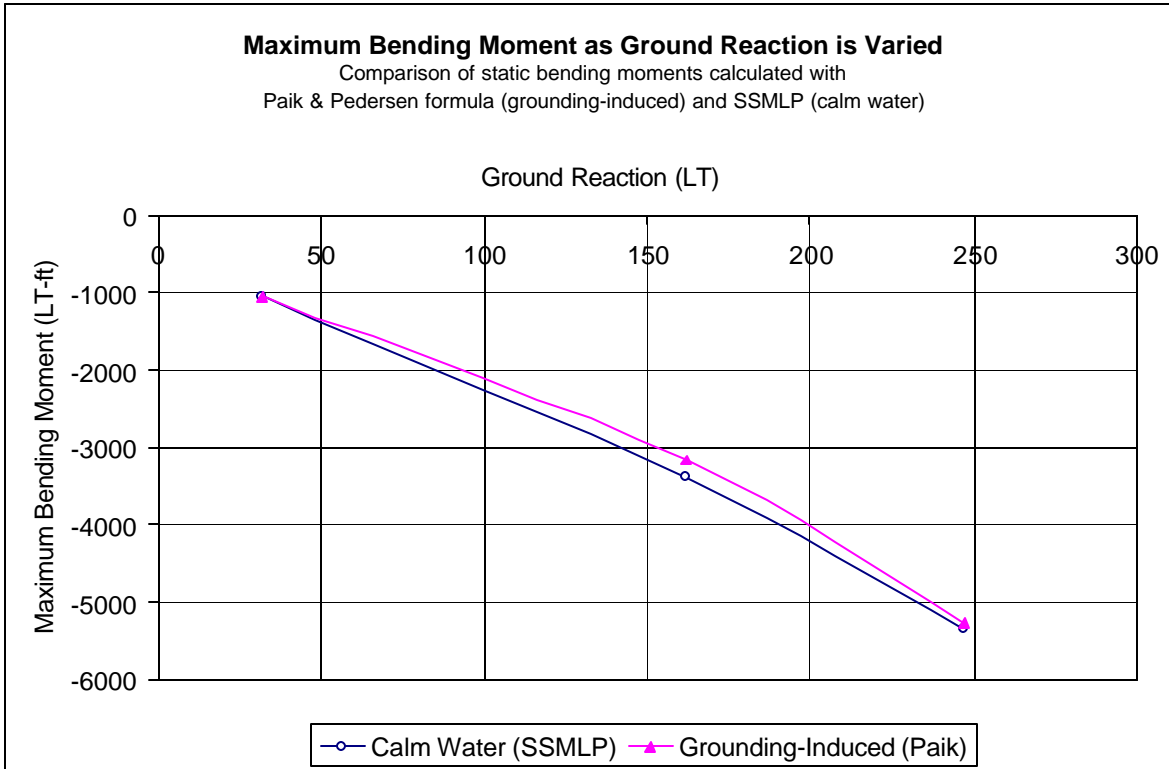


Figure 66 - Maximum longitudinal bending moment as ground reaction is varied

6.1.2.2 Bending Moment Response in Regular Waves

This section describes the analysis of dynamic bending moments for the stranded barge in regular waves. Bending moments are calculated for the free-floating condition and for a ground reaction of 32-LT. Analysis scenarios are illustrated in Figure 67.

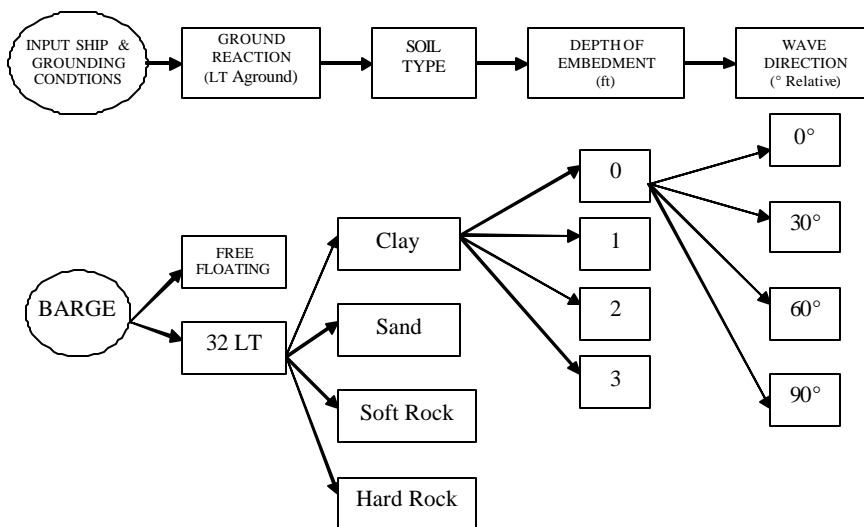


Figure 67 - Barge Case Flow Chart (Bending Moment)

Bending Moment plots for the grounded barge are generated in SSMLP. The barge is grounded as in Figure 21. SSMLP calculates motions and loads due to regular waves with a wave height of one foot. Longitudinal bending moment calculations are generated for a range of wave frequencies. Waves from 180°R degrees relative produce a longitudinal bending moment in the vertical plane. Waves from 090°R produce a longitudinal bending moment in the vertical and horizontal planes, as illustrated in Figure 68. Figure 69 to Figure 72 show the maximum longitudinal bending moments produced by one foot, regular waves over the range of specified frequencies.

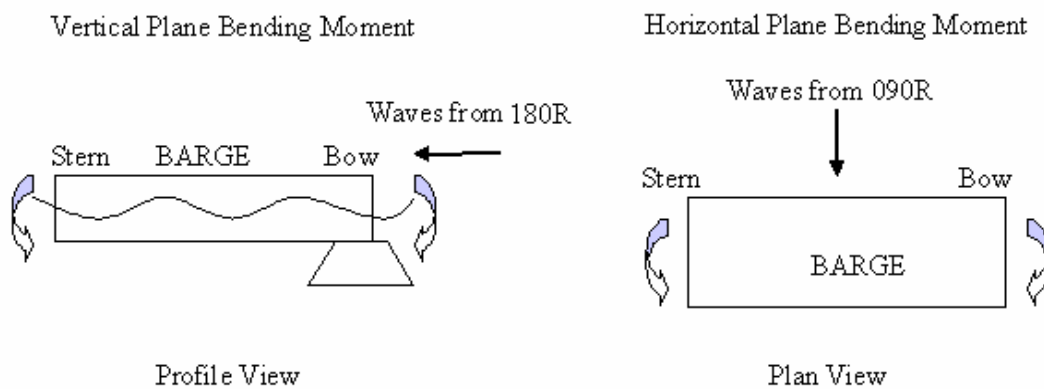


Figure 68 - Diagram of vertical and horizontal bending moments

Figure 69 shows the vertical plane bending moment sustained by the grounded barge in regular waves with a wave height of one foot. Longitudinal bending moments are plotted for waves from 090°R and 180°R; the longitudinal bending moment for calm-water is also plotted for comparison. While both beam seas (090°R) and following seas (180°R) produce vertical plane bending moments, the vertical plane bending moment associated with beam seas is larger. This is expected because the vertical plane wave force is much greater in beam seas. Figure 69 also shows that the maximum bending moment occurs in the vicinity of the center of the ground reaction.

Figure 70 shows the horizontal plane bending moment sustained by the grounded barge in regular waves coming from 090°R. Without a ground reaction and wave force, there is no horizontal bending moment. As such, there are no other plots on Figure 70 for comparison. As in Figure 69, the maximum bending moment value occurs near the center of the ground reaction. Comparing the maximum values on Figure 69 with the maximum values on Figure 70 shows that the vertical plane bending moment is greater, especially in the beam seas case.

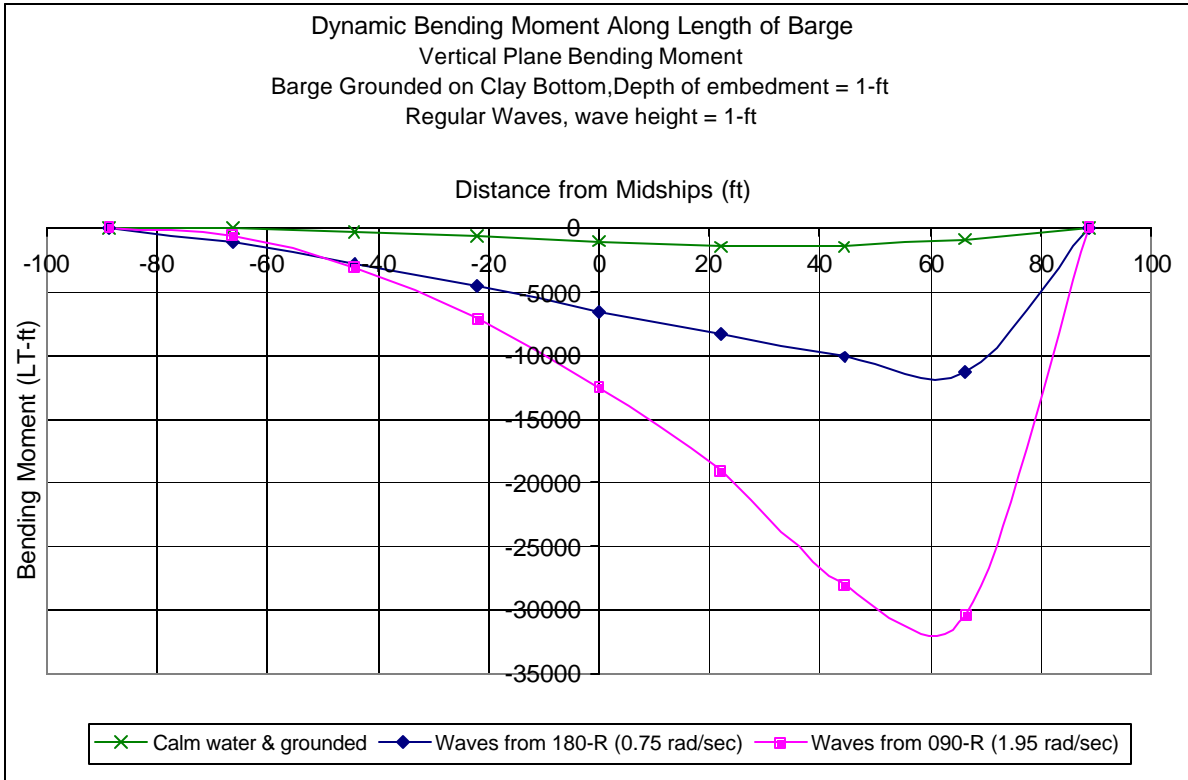


Figure 69 - Longitudinal bending moment, vertical plane, regular waves

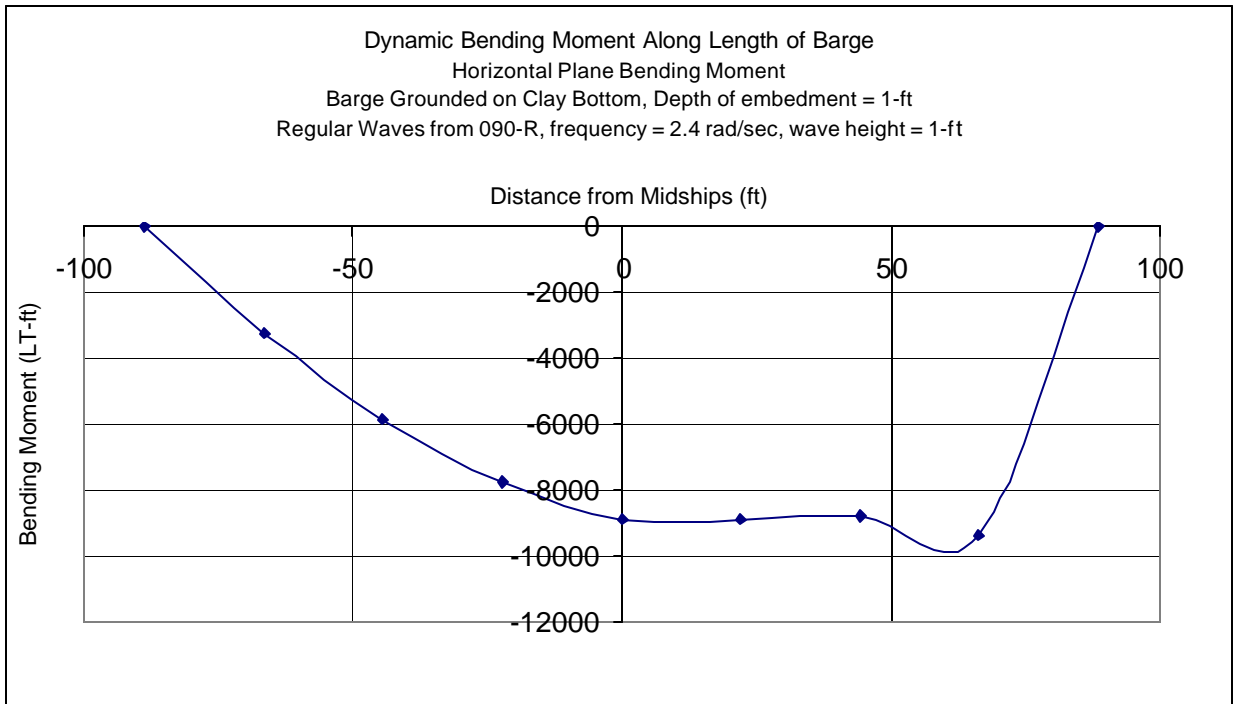


Figure 70 - Longitudinal bending moment, horizontal plane, regular waves

The motions and loads for the stranded barge in beam seas are calculated to simulate “broaching” of the barge. Broaching causes the stranded vessel to rotate and settle in a position where the seas are coming from the beam. However, it may also cause the vessel to become embedded along a greater length of the hull. As such, the scenario used to calculate the bending moments in which the length of embedment is only 10 feet in Figure 70 maybe unrealistic.

Figure 71 shows the vertical plane bending moment along the length of the hull as the length of embedment is increased. The increase in length of embedment decreases the vertical plane bending moment along the length of the hull. This occurs because as the length of embedment increases, the ground reaction supports a longer length of the hull. Since the hull is supported evenly along the grounded and/or embedded length, there is no variation in loading between sections to create bending moment. Figure 71 also shows that the maximum bending moment remains near the center of the ground reaction.

Figure 72 shows that horizontal plane bending moment along the length of the hull as the length of embedment is increased. The horizontal plane bending moment behaves in the same manner as the vertical plane bending moment for the same reasons.

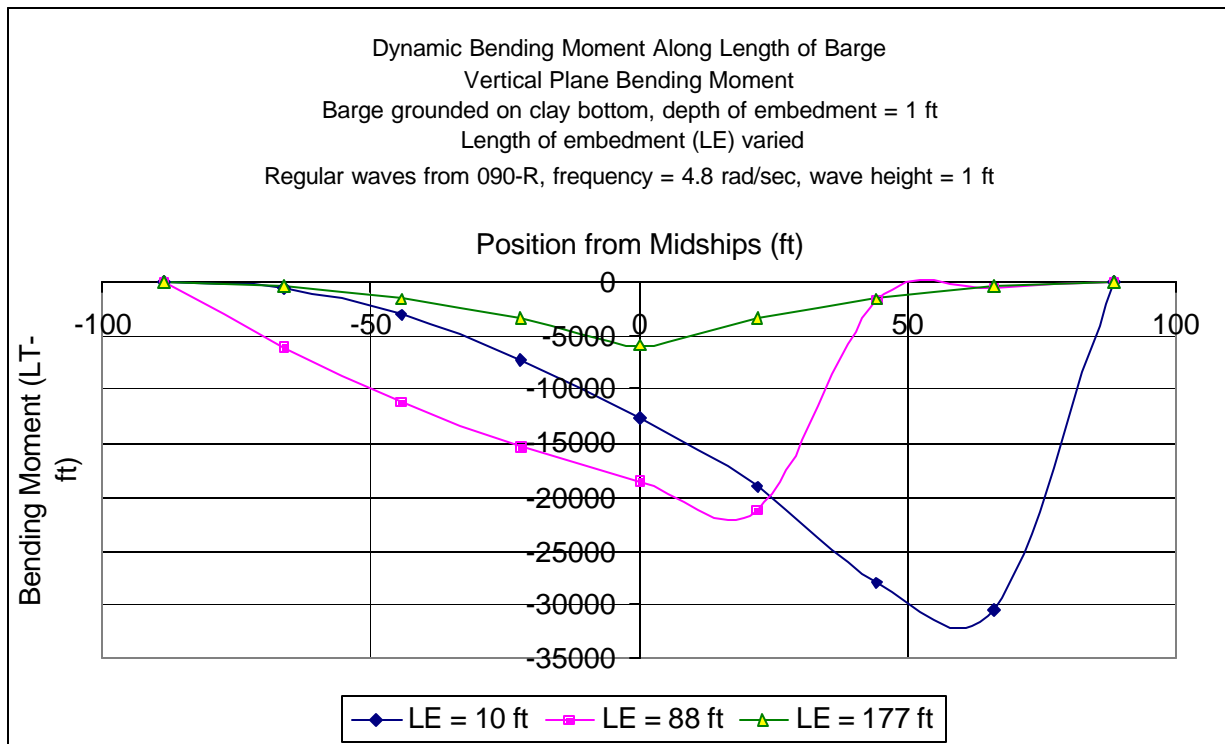


Figure 71 - Longitudinal bending moment, vertical plane, regular waves

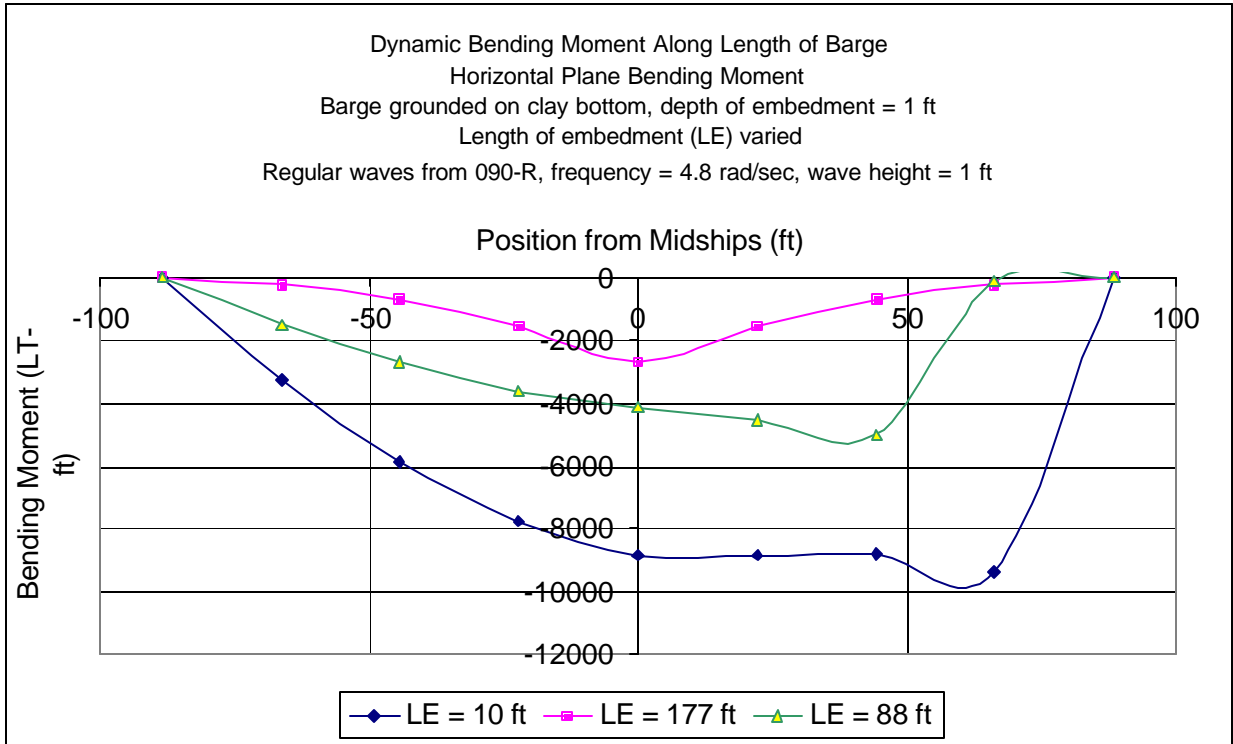


Figure 72 - Longitudinal bending moment, horizontal plane, length of embedment varied

Figure 69 to Figure 72 show that the maximum longitudinal bending moment occurs at or near the center of the ground reaction. The following figures in this section only show the maximum bending moment value found over the length of the hull.

Figure 73 shows the maximum vertical plane bending moment values for the stranded barge as the wave direction is varied. The barge is grounded in clay as shown in Figure 21. The depth of embedment is one foot, and the barge is subject to one foot high, regular waves. As shown in Figure 69, the maximum vertical plane bending moment along the length of the hull increases as the wave direction goes from following to beam seas.

Figure 73 also shows that the horizontal plane bending moments are relatively small in comparison to the vertical plane bending moments for either the beam seas or following seas cases. Furthermore, Figure 71 and Figure 72 have previously shown that the broaching scenario where the length of the hull is in contact with the ground produces vertical and horizontal plane bending moments which are less than the vertical and horizontal plane bending moments calculated for the following seas case. Since the ultimate goal of this analysis is to determine the largest, realistic bending moment value for the stranded condition, the bending moments for the beam seas or broached case are not calculated beyond Figure 74.

Figure 74 shows the maximum vertical plane bending moment values for the stranded barge as the soil type is varied. The barge is grounded per Figure 21, and is subject to one foot high, regular waves coming from 180°R. In comparing the bending moments for each soil type, the bending moment value for clay was the smallest, and the value for hard rock was the largest. This was expected because the RAO plots showed that clay was the least stiff of the four soil types, and hard rock was the stiffest. The stiffer the soil type, the larger the bending moment.

Figure 75 shows the maximum vertical plane bending moment values for the stranded barge as the depth of embedment is varied. The barge is grounded in clay as shown in Figure 21. The barge is subject to one foot high, regular waves coming from 180°R. As expected, the maximum bending moment values increased as the depth of embedment increased. This occurs because the soil or ground reaction stiffness increases when the depth of embedment increases.

Figure 76 shows the maximum vertical plane bending moment values for the stranded barge as the wave height is varied. As the wave height increases, the bending moment increases. This was expected because larger waves produce larger forces on the stranded barge.

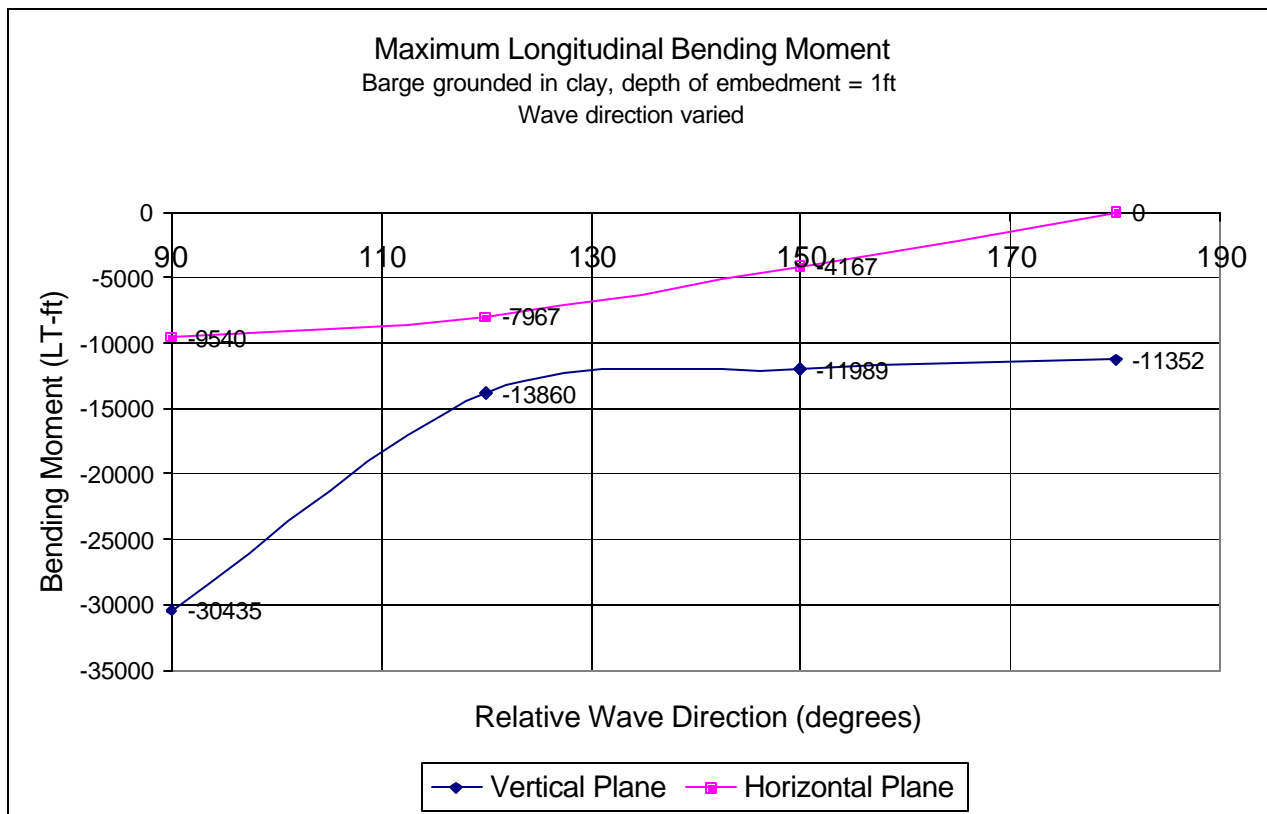


Figure 73 - Maximum longitudinal bending moment, horizontal plane, wave direction varied

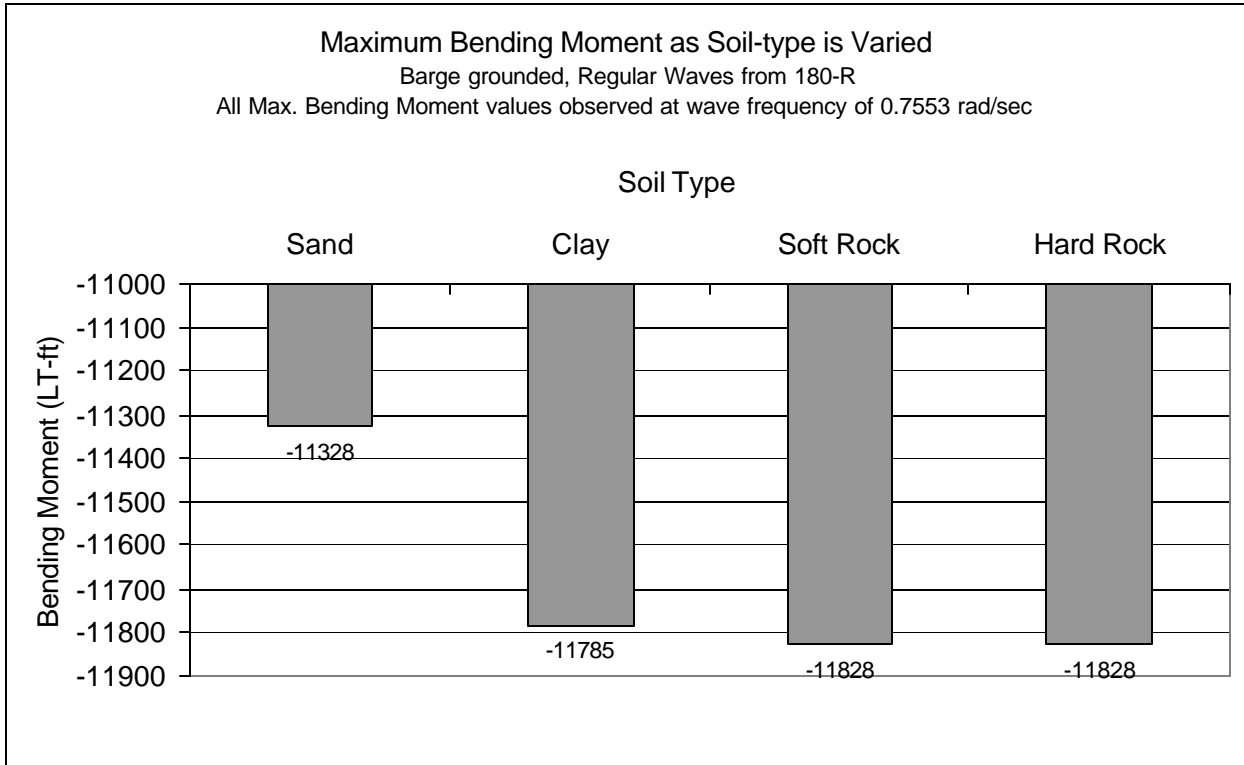


Figure 74 - Maximum longitudinal bending moment, vertical plane, soil type varied

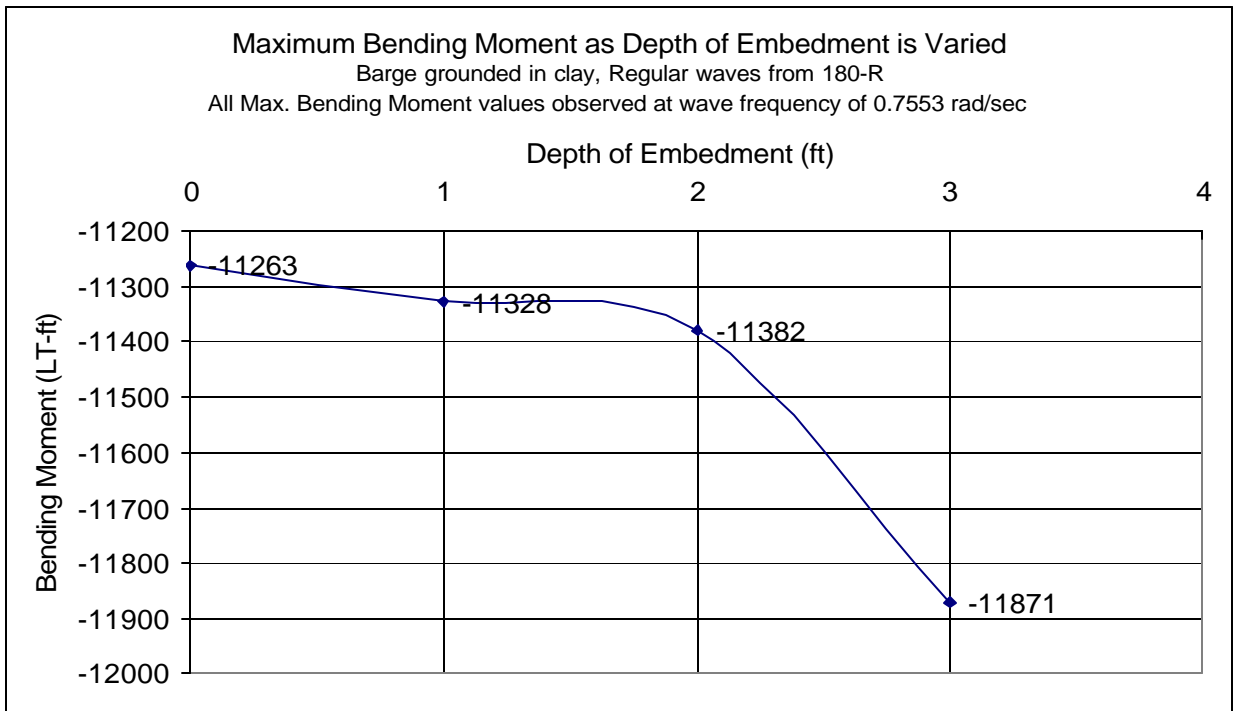


Figure 75 - Maximum longitudinal bending moment, vertical plane, depth of embedment varied

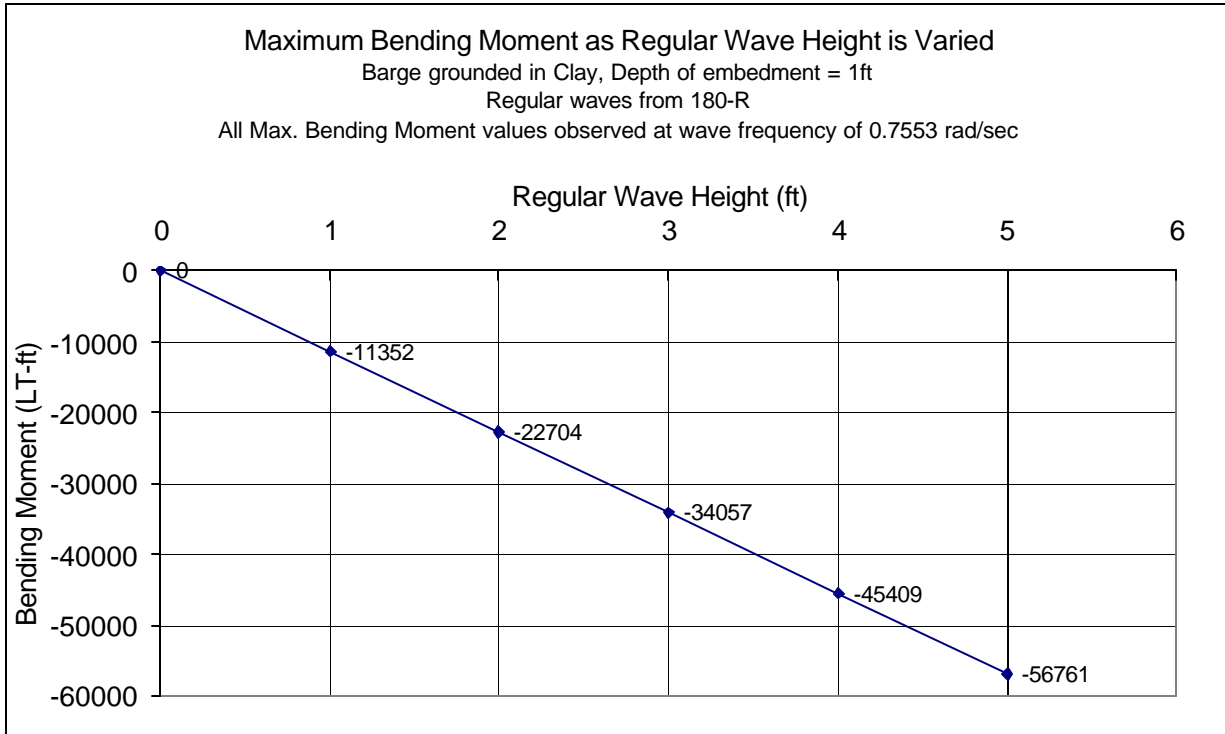


Figure 76 - Maximum longitudinal bending moment, vertical plane, wave height varied

6.1.2.3 Bending Moment Response in Irregular Waves

Although the response of the stranded barge in regular waves provides insight into the loads on the barge, analysis for long-crested irregular waves provides a more realistic response. This topic is discussed in Section 3.7.

Calculations for the grounded barge response in a seaway are performed in SSMLP. RAOs are calculated as described Sections 3.6 and 3.7. The wave energy is defined using a Bretschneider Spectrum for a fully developed sea, Equations (3.27) and (3.28).

Figure 77 shows the Root Mean Square (RMS) and Significant (M-1/3) Bending Moments for a barge stranded in clay. The depth of embedment is one foot. The seaway is irregular and fully-developed. The waves are coming from 180°R. The significant wave height is one foot. In this instance, selection of the significant wave height of one foot is arbitrary. Figure 77 shows that the maximum RMS bending moment does not exceed the calm water bending moment. However, the significant bending moment (M-1/3) exceeds the calm water bending moment by nearly 80% with just a one foot significant wave height.

Paik and Pedersen compare their grounding induced bending moment values with free-floating wave-induced bending moment design values calculated using the IACS/American Bureau of Shipping (ABS 2003) formula (wave-sagging):

$$M_{ws} = k_1 C_1 L^2 B (C_b + 0.7) \times 10^{-3} \quad (6.1)$$

where:

$$k_1 = 1.026$$

$$C_1 = 10.75 - \left[\frac{300 - L}{100} \right]^{1.5}$$

$C_b = 1.0$, block coefficient

L , Length of vessel

In the case of the free-floating barge, $M_{ws} = 22216$ LT-ft.

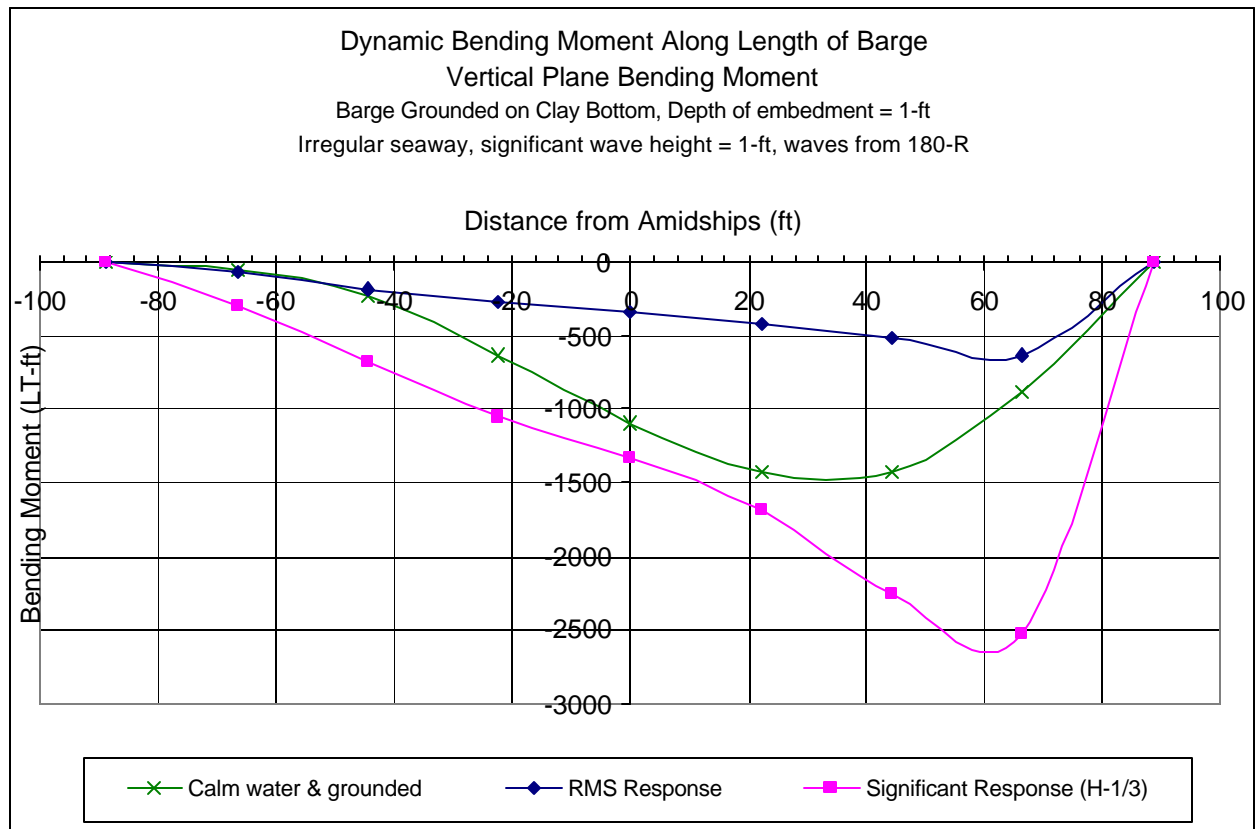


Figure 77 - Longitudinal bending moment, vertical plane, irregular seaway

Figure 78 shows the significant bending moment response of the stranded barge in an irregular seaway as the significant wave height is varied. The barge is stranded in clay with a

depth of embedment of one foot. The waves are coming from 180°R. At a significant wave height of four to five feet, the significant bending moment response exceeds the IACS/ABS wave-induced bending moment.

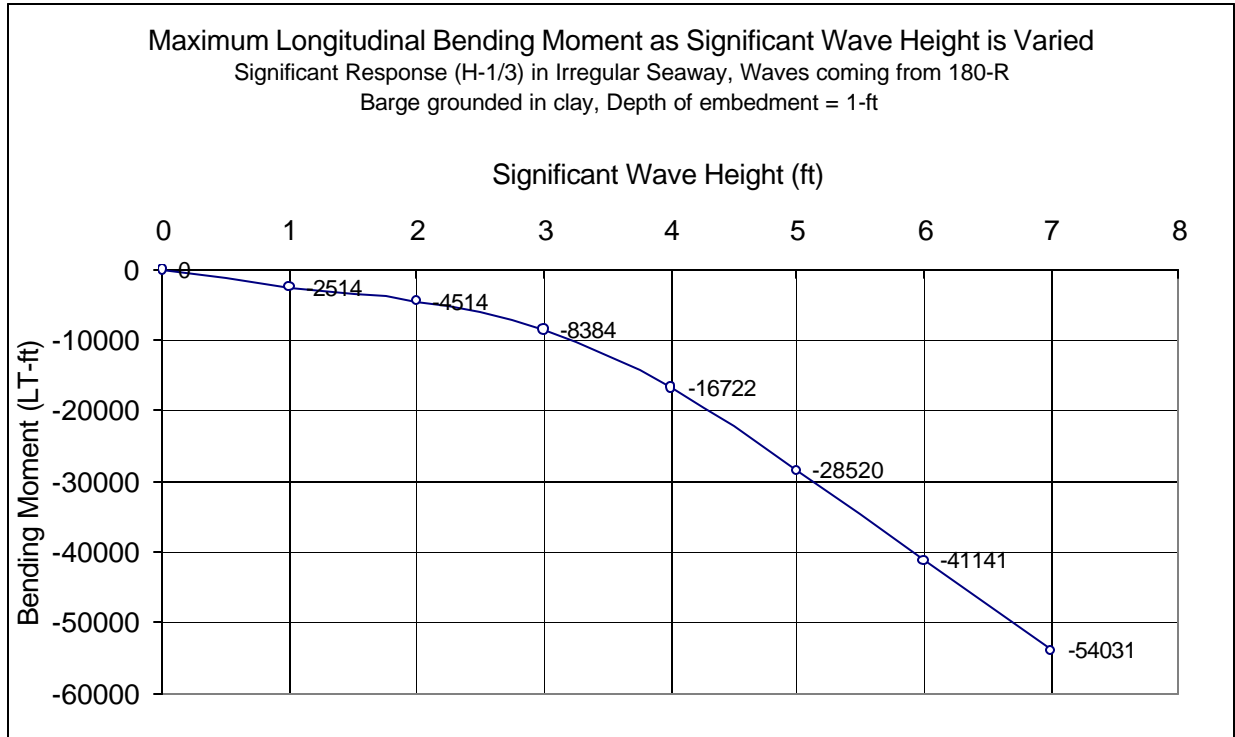


Figure 78 - Maximum longitudinal bending moment, vertical plane, irregular seaway

6.1.2.4 Summary of Bending Moments

Table 4 summarizes the various bending moments calculated for the grounded barge scenario. The design bending moment (M_{ABS}) for the sagging condition is based on the IACS/ABS formula (ABS 2003):

$$M_{ABS} = M_{\text{free-floating, still water}} + M_{\text{wave-induced}} = -22216 \text{ LT-ft} \quad (6.2)$$

with a free-floating, still water bending moment of zero.

Paik and Pedersen calculate the static bending moment for the grounded condition as:

$$M_{Paik} = M_{\text{free-floating, still water}} + M_{\text{static, grounding-induced}} = -1432 \text{ LT-ft} \quad (6.3)$$

with a free-floating, still water bending moment of zero, and a ground reaction of 32 LT due to a 0.5 foot vertical displacement of the grounding point.

Applying the static ground reaction and dynamic soil model, SSMLP calculates the design bending moment in the following manner:

$$M_{SSMLP} = M_{\text{free-floating, still water}} + M_{\text{static, Grounding-induced}} + M_{\text{Grounding-induced, dynamic}} \quad (6.4)$$

with a free-floating, still water bending moment of zero, and a static ground reaction of 32-LT.

SSMLP generates several bending moment values. While the regular wave values provide some insight into the loads on the grounded vessel, the response in irregular seas provides a more realistic, statistically-based design bending moment value. The significant bending moment represents the mean value of the highest third of all bending moments sustained by the grounded barge in an irregular seaway.

The significant bending moment response for the stranded barge in an irregular seaway with waves coming from 180°R and a significant wave height of 5 feet is -28520 LT-ft:

$$M_{SSMLP} = M_{\text{free-floating, still water}} + M_{\text{Grounding induced, static}} + M_{\text{Grounding induced, dynamic}} = -28520 \text{ LT-ft}$$

This equation assumes that $M_{\text{free-floating, still water}}$ is zero.

Table 4 - Calculated Bending Moments

Method	Scenario	Max. Bending Moment (LT-ft) Vertical Plane
ABS rules “still-water”	Still water; free-floating; no waves	Design value based on particular loading scenario; assumed to be zero in this summary
ABS rules “wave-induced”	Free-floating in waves	-22216
Paik & Pedersen “grounding-induced”	Still water; aground with vertical displacement of 0.5-ft	-1432
SSMLP	Vessel aground with regular waves from 180°R; ground reaction = 32 LT	-22704 Wave frequency = 0.75 rad/sec; regular wave height = 2 ft
SSMLP	Vessel aground in irregular sea with waves from 180°R; ground reaction = 32 LT	M(1/3) = -28520 Significant wave height = 5 ft

6.2 Series 60 Tanker

A Series 60 tanker similar to the ship modeled in Paik and Pedersen (1997) is chosen for a second case study. Only vertical plane bending moments are considered as in Paik and Pedersen. To be consistent with their units, all calculations in SSMLP are converted to SI-units.

The Series 60 tanker model was created using the method described by Loukakis (1970). Given the principal characteristics of the vessel found in the Paik and Pedersen, SSMLP generates a Series 60 hull form similar to their hull form.

Table 5 - Series 60 Tanker grounding scenario

Principal dimensions of Series 60 Tanker	
Length between perpendiculars	190.5 m
Breadth	29.26 m
Depth	15.24 m
Design draft	10.36 m
Displacement	49230 ton
Deadweight	38400 ton
Block coefficient	0.83
Waterplane coefficient	0.81
Waterplane area	4521.0 m ²
Description of Grounding Scenario:	
Bow grounded	
Length of embedment	19.05 m
Breadth of embedded section	29.26 m
Center of ground reaction (from bow)	9.525 m
Bottom (soil-type)	Clay
(1) Ground reaction	11449 kN
1-m vertical displacement at grounding point.	
(2) Ground reaction	22867 kN
2-m vertical displacement at grounding point	
Depth of embedment	0 m - 3 m
Wave direction (following and beam seas)	180°R, 090°R

6.2.1 Static, Grounding-Induced Bending Moment

The static, grounding induced bending moment was calculated using Paik and Pedersen. The grounding scenario described in Table 5 is modified slightly for use with this formula; calculated for a point load which is applied at the center of the ground reaction. The grounding induced bending moments are calculated for a range of vertical displacements.

Required design wave-induced bending moment values are also calculated for the tanker using the IACS/ABS formula. For this scenario, the still water bending moments are -1016.85 MN-m (sag), and 1125.24 MN-m (hog). The ABS wave-induced bending moments are -1716.40 MN-m and 1612.45 MN-m. The total ABS design bending moments are:

$$-1016.85 \text{ MN-m} + -1716.40 \text{ MN-m} = \mathbf{-2733.25 \text{ MN-m (sag)}}$$

$$1125.24 \text{ MN-m} + 1612.45 \text{ MN-m} = \mathbf{2737.69 \text{ MN-m (hog)}}$$

Figure 79 shows the grounding-induced bending moment values for the grounded tanker. When the vertical displacement at the grounding point is 5-meters, the total bending moment value (-2767 MN-m) exceeds the ABS design bending moment value (-2733 MN-m). At a vertical displacement of 8-meters, the grounding-induced bending moment alone (-2799 MN-m) exceeds the ABS design bending moment value (-2733 MN-m).

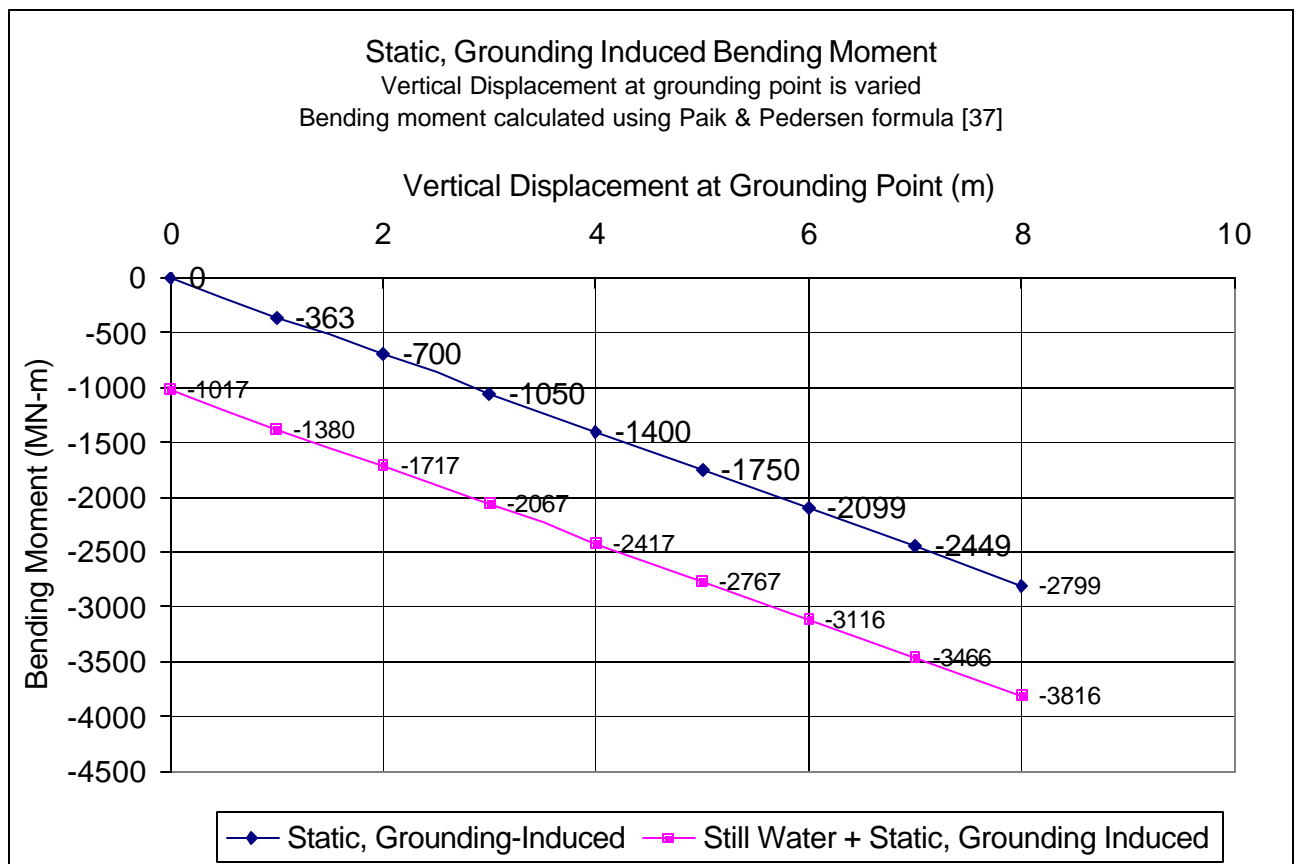


Figure 79 - Static, grounding induced bending moment for Series 60 tanker

6.2.2 Bending Moment in Regular Waves

Bending moments for the stranded tanker in regular waves are calculated in SSMLP. The tanker is aground in clay in regular 1-meter waves. The following parameters are varied: ground reaction, wave frequency, wave direction, and the depth of embedment. The two ground reaction cases that are examined correspond with vertical displacement values of 1-meter and 2-meters. A vertical displacement of 1-meter at the ground point corresponds with a ground reaction of 11449 kN. A vertical displacement of 2-meters at the ground point corresponds with a ground reaction of 22867 kN. Maximum bending moments occur at a wave frequency of 0.1896 radians/second.

Figure 80 shows the regular wave bending moments for the grounded tanker with a wave height of one meter. The overall design bending moment in SSMLP is calculated by adding the still water bending moment (-1017 MN-m) to the SSMLP bending moments from Figure 79. Comparing the ABS design bending moment value (-2733 MN-m) with the SSMLP bending moment values in Figure 79, shows that the SSMLP bending moment value for a depth of embedment of 2-meters and following seas (-2856 MN-m) with 1 meter wave height exceeds the ABS design value.

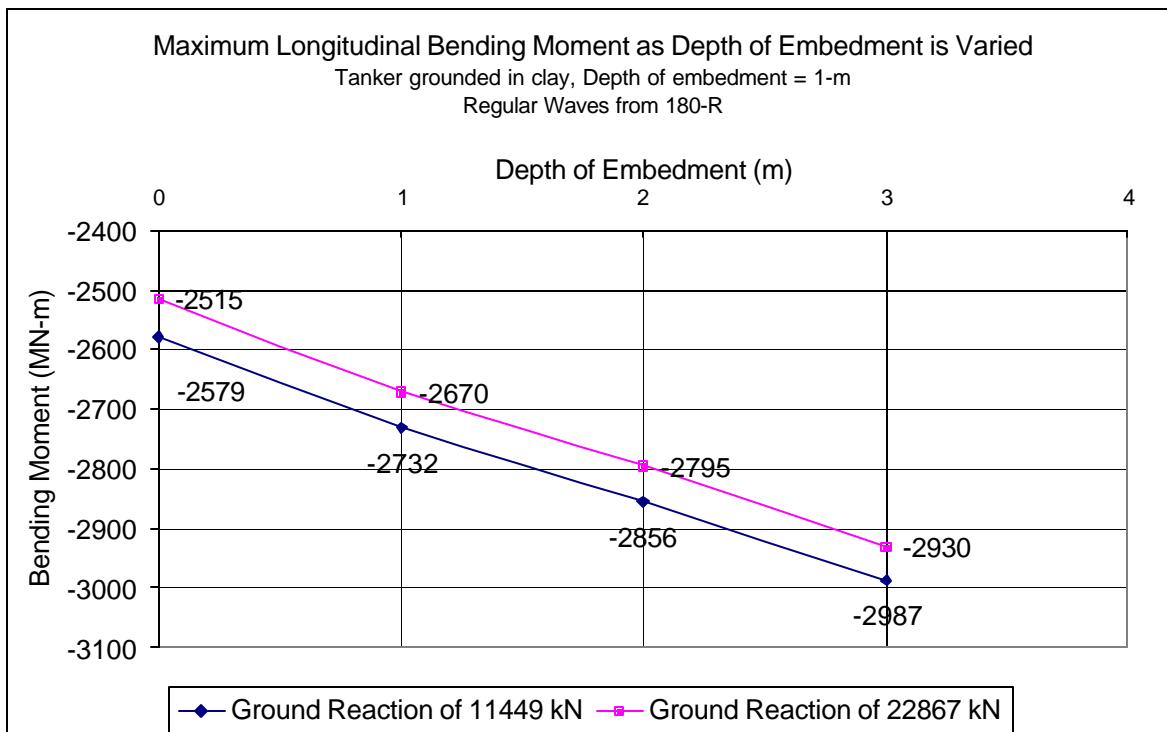


Figure 80 - SSMLP bending moment for tanker grounded in clay, regular waves, depth of embedment varied, wave height = 1 meter

6.2.3 Bending Moment in Irregular Seaway

The bending moments for the stranded tanker in an irregular sea are calculated in SSMLP. The following parameters are varied: ground reaction, and the depth of embedment.

Figure 81 shows the significant bending moment values for the stranded tanker as the depth of embedment increases. In following seas with a wave height of one meter, increasing the depth of embedment does not produce a significant bending moment which is greater than the ABS wave-induced bending moment (-1716 MN-m). Figure 82 shows the significant bending moment for the stranded tanker as the significant wave height is increased. When the significant wave height is 4 meters, the significant bending moment response exceeds the ABS wave-induced bending moment, demonstrating that wave-induced bending moments can be significant and exceed undamaged design limits in moderate sea states

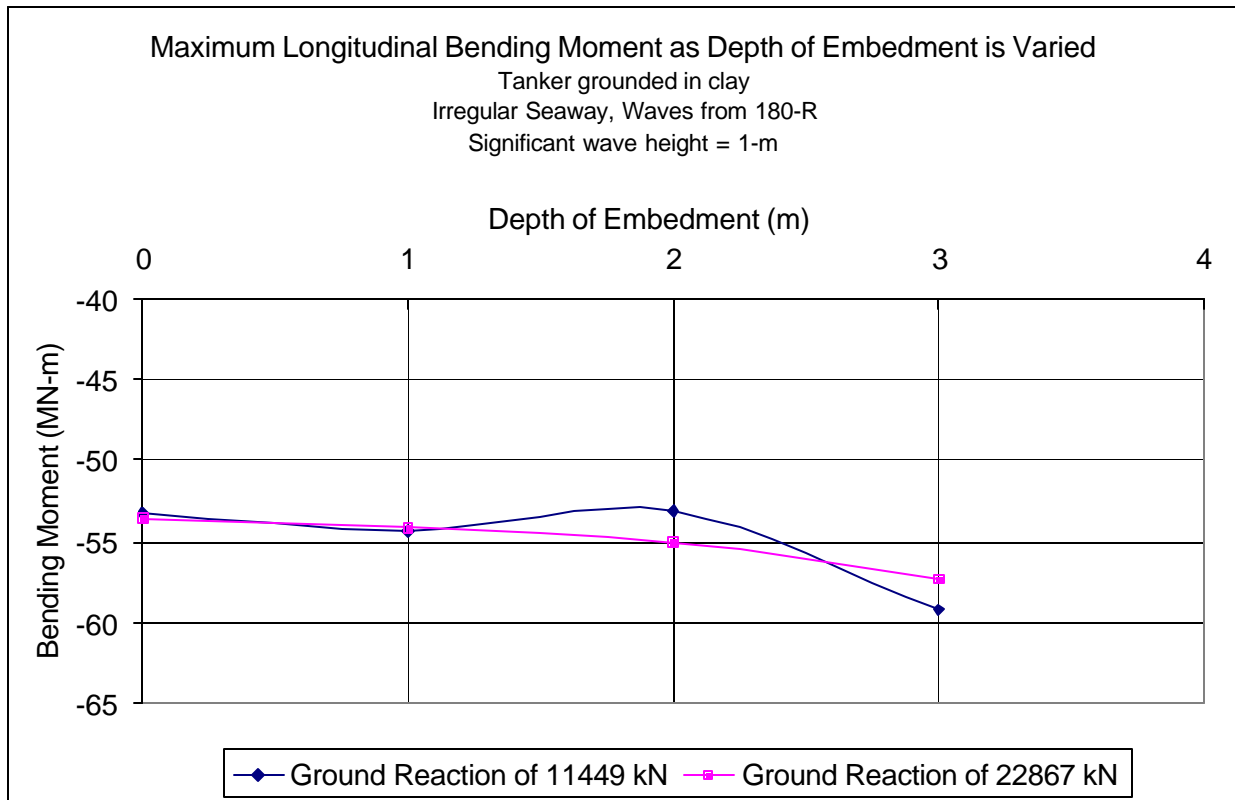


Figure 81 - SSMLP bending moment for tanker grounded in clay, irregular seaway, depth of embedment varied

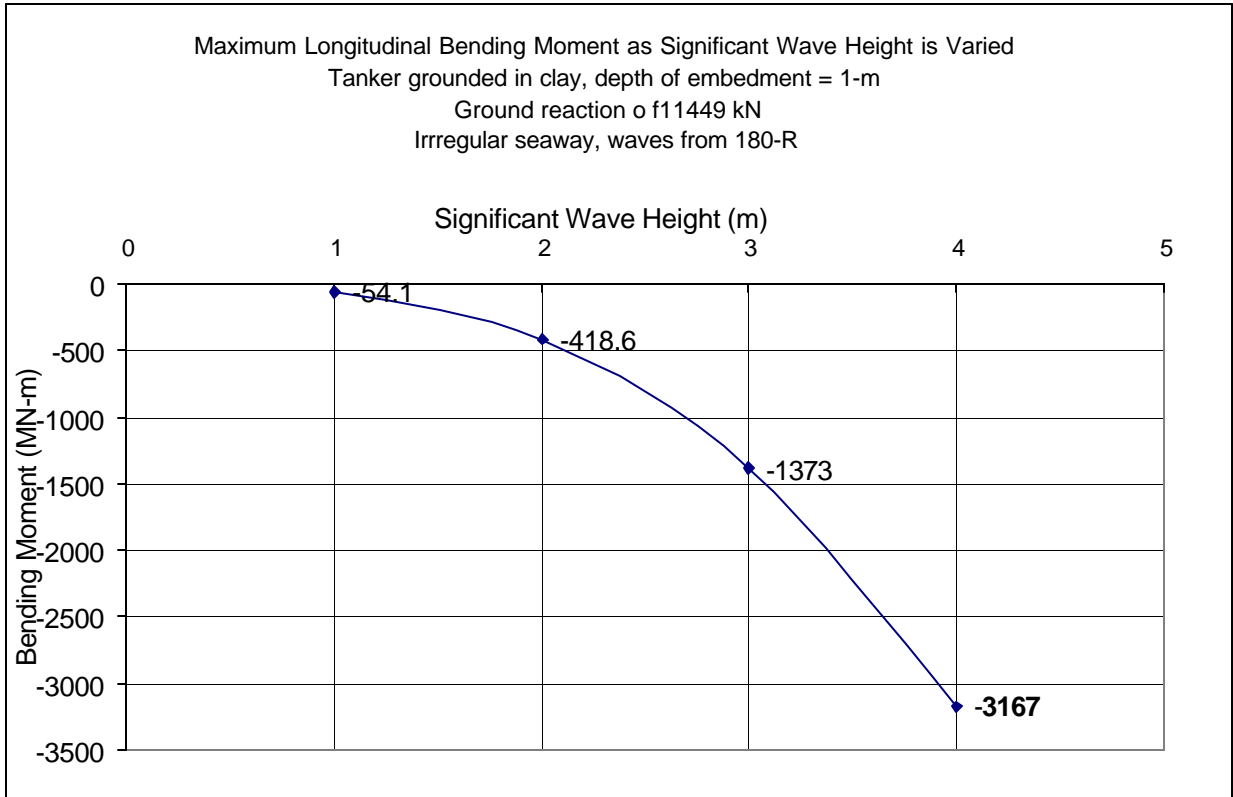


Figure 82 - SSMLP bending moment for tanker grounded in clay, irregular seaway, significant wave height varied

6.3 Conclusions

This report describes a simple preliminary model for predicting the dynamic effect of waves on stranded ship motion and loads. A theoretical analysis of the motions and loads in six-degrees of freedom of a grounded ship in waves is developed with an appropriate soil reaction model to estimate dynamic ground reaction forces. The steady-state grounded motion of the stranded ship in waves around the quasi-equilibrium position is treated as a steady-state linear dynamic problem. Comparisons are made to static grounding results and to current IACS/ABS design rules.

A grounded ship in waves can produce significantly higher loads and bending moments than predicted by static analysis. In moderate sea states, the bending moment induced on a stranded ship can exceed the wave-induced bending moment calculated using the IACS/ABS rules for longitudinal strength, and the Paik and Pedersen grounding-induced bending moment. **It is**

concluded that the dynamic bending moment on a grounded ship in waves can be significant and must be considered in grounded ship loads and residual strength analyses.

6.4 Future Work

Future work should address the following:

- Model testing and model assessment
- Shallow water effects including Green Function motion coefficients, wave form, phase and group velocities and the effect of flow in the small gap between bottom and hull
- Other non-linear effects including breaking incident waves and body geometry (ships frequently heeled, not wall sided)
- More appropriate near-shore wave definition and spectra
- Non-linear soil effects
- Grounded hull stabilization and the effect of beach gear
- Application of model to actual grounding case study with data such as New Carissa or LST 93 Valdivia

The most immediate need is for model testing to assess the preliminary computational results, determine if preliminary conclusions are correct, and determine if model improvements are required or warranted. This is the scope of the proposed Phase 2 in this project.

References

- ABC (2002), ABC News Online, "Attempts to Refloat Ship on Barrier Reef Suspended", <http://www.abc.net.au/news/2000/11/item200011021304311.htm>
- ABS (2003), *ABS Rules for Building and Classing Steel Vessels*, Part 3, Chapter 2, Section 1, Wave Loads.
- Abascal, R. (1984), *Estudio de Problemas Dinámicos en Interacción Suelo-Estructura por el Método de los Elementos de Contorno*, Doctoral Thesis, Escuela Técnica Superior de Ingenieros Industriales de la Universidad de Sevilla.
- ATSB (2002), Investigation Reports on Groundings, from ATSB Marine Safety website: <http://www.atsb.gov.au/marine/incident/index.cfm>, 15 July 2002.
- Bartholomew, C.A., (1990), *Mud, Muscle, and Miracles - Marine Salvage in the United States Navy*. Washington D.C.: Naval Historical Center and Naval Sea Systems Command.
- Bartholomew, C.A., Marsh, B., Hooper, R. (1992), *U.S. Navy Salvage Engineer's Handbook, Volume 1*, Washington D.C., Naval Sea Systems Command.
- Bretschneider, C.L. (1967), "Maximum Sea State for the North Atlantic Hurricane Belt", *Ocean Industry*.
- Brown, A.J., Tikka, K., Daidola, J.C., Lutzen, M., Choe, I.H. (2000), "Structural Design and Response in Collision and Grounding", *SNAME Transactions*, 108, pp 447-473.
- Cahill, R.A. (1991), *Disasters at Sea -Titanic to Exxon Valdez*, Texas and New York: Nautical Books and U.S. Merchant Marine Library Association.
- D'Appolonia Consulting Engineers (1979), *Seismic Input and Soil-Structure Interaction*. Pittsburgh, PA.
- Demanche, J. F. (1968), "Added Mass and Damping Coefficient for Cylinders with a Bulb-like Cross Section Oscillating in a Free Surface", M.Sc. Thesis, M.I.T., Department of Naval Architecture and Marine Engineering.
- Dominguez, J. (1978), *Dynamic Stiffness of Rectangular Foundations*, Report No. R78-20, MIT, Cambridge, Massachusetts.
- Gazetas, G. (1983), "Analysis of Machine Foundation Vibrations: State of the Art", *International Journal of Soil Dynamics and Earthquake Engineering*, Vol. 2, No.1, pp. 2-42.
- Grim, O. and Kirsch, M. (1966), "Program zur Berechnung der Hydrodynamischen Kräfte, der Bewegungen und des Biegemomentes für ein Schiff in Langlaufden Wellen".
- Hudson, P.J. (2001), *Wave-Induced Migration of Grounded Ships*, Doctoral Dissertation, Johns Hopkins University.
- Journee, J.M. (2001), *Theoretical Manual of Seaway*, Report No1216a, Delft University of Technology, Netherlands.
- Kausel, E. (1974), "Forced Vibrations of Circular Foundations on Layered Media", Report No. R74-11, MIT Dept. of Civil Engineering, Cambridge, Massachusetts.

- Lloyd, ARJM (1998), *Seakeeping: Ship Behavior in Rough Weather*, Published by ARJM Lloyd, Hampshire, United Kingdom.
- Loukakis, T.A. (1970), *Computer Aided Prediction of Seakeeping Performance in Ship Design*, Report No. 70-3, Massachusetts Institute of Technology, August 1970.
- McCormick, M.E. and Hudson, P.J. (2001), "An Analysis of the Motions of Grounded Ships," *International Journal of Offshore and Polar Engineering*, Vol. II (2), pp 99-105.
- McCormick, M.E. (1999), *On the Motions of Grounded Ships*, Johns Hopkins University Technical Report produced under NSWC Carderock Contract N00167-99-M-0226, Baltimore, Maryland.
- NAVSEA OOC (2002), U.S. Navy Supervisor of Salvage Case Files, Washington D.C.: Naval Sea Systems Command.
- Newman, J.N. (1977), *Marine Hydrodynamics*, Massachusetts Institute of Technology Press, Cambridge, Massachusetts.
- Paik, J.K. (2003), "Innovative Structural Design of Tankers against Ship Collisions and Grounding: A Recent State-Of-The-Art Review", *Marine Technology*, 40:1, 1-9.
- Paik, J.K. and Pedersen, P.T. (1997), "Simple Assessment of Post-Grounding Loads and Strength of Ships", *International Journal of Offshore and Polar Engineering*, 7:2, pp 141-145.
- Pais, A. and Kausel, E. (1985), *Stochastic Response of Foundations*, Research Report R85-6 sponsored by the National Science Foundation Grant CEE-8211021 and LNEC and INVOTAN in Lisbon, Portugal. Massachusetts: Massachusetts Institute of Technology.
- Rawson, C., Crake, K. and Brown, A.J. (1998), "Assessing the Environmental Performance of Tankers in Accidental Grounding and Collision", *SNAME Transactions* **106**, 41-58.
- Reissner, E. (1936), "Stationäre, axialsymmetrische durch eine schüttelnde Masse erregte Schwingungen eines homogenen elastischen Halbraumes", *Ingenier-Archiv*, Vol. 7, pp. 381-396.
- Salvesen, N., Tuck, E.O., Faltinsen, O.M. (1970), "Ship Motions and Sea Loads", *SNAME Transactions*, Vol. 78.
- Schauer, T. (2002), "NEW CARISSA Complete Hull Failure in a Stranded Bulk", Case Study 1, Ship Structure Committee website: http://www.shipstructure.org/case_studies.shtml
- Sirkar, J., Ameer, P., Brown, A.J., Goss, P., Michel, K., Willis, W. (1997), "A Framework for Assessing the Environmental Performance of Tankers in Accidental Grounding and Collision", *SNAME Transactions* **105**, 253-295.
- SNAME (1989), *Principles of Naval Architecture*, Vol. 3, Society of Naval Architects and Marine Engineers, Jersey City, NJ.
- Stettler, J. (1997), "LST 93 VILDIVIA Grounding", Ship Structure Committee Case Study VI, <http://www.shipstructure.org/chile.shtml>.
- Ursell, F. (1949), "On the Heaving Motion of a Circular Cylinder on the Surface of a Fluid," *Quarterly Journal of Applied Mathematics*, Vol. 2.

- Veletsos, A.S. and Wei, Y.T. (1971), "Lateral and Rocking Vibration of Footings", *Journal of the Soil Mechanics and Foundations Division, ASCE*, Vol. 97, No. SM9, pp. 1227-1248.
- Whitman, R.V., and Richart, F.E., Jr. (1967), "Design Procedures for Dynamically Loaded Foundations," *Journal of the Soil Mechanics and Foundations Division, ASCE* 93 (SM6), 169-193.
- Wolf, J.P. (1985), *Dynamic Soil-Structure Interaction*. New Jersey: Prentice-Hall, Inc., 1985.
- Wolf, J.P. (1994), *Foundation Vibration Analysis Using Simple Physical Models*, New Jersey: PTR Prentice Hall.
- Wolf, J.P. and Weber, B. (1986), "Approximate Dynamic Stiffness of Embedded Foundation Based on Independent Thin Layers With Separation of Soil", *Proceedings of the 8th European Conference on Earthquake Engineering*, pp 5.6/33-5.6/40.
- Wong, H. L. and Luco, J. E. (1978), Tables of Impedance Functions and Input Motions for Rectangular Foundations, Report No. CE78-15, University of Southern California.

SHIP STRUCTURE COMMITTEE PARTNERS AND LIAISON MEMBERS

PARTNERS

The Society of Naval Architects and Marine Engineers

Mr. Joe Cuneo
President,
Society of Naval Architects and Marine Engineers

Dr. John Daidola
Chairman,
SNAME Technical & Research Steering
Committee

The Gulf Coast Region Maritime Technology Center

Dr. John Crisp
Executive Director,
Gulf Coast Maritime Technology Center

Dr. Bill Vorus
Site Director,
Gulf Coast Maritime Technology Center

LIAISON MEMBERS

American Iron and Steel Institute
American Society for Testing & Materials
American Society of Naval Engineers
American Welding Society
Bethlehem Steel Corporation
Canada Center for Minerals & Energy Technology
Colorado School of Mines
Edison Welding Institute
International Maritime Organization
International Ship and Offshore Structure Congress
INTERTANKO
Massachusetts Institute of Technology
Memorial University of Newfoundland
National Cargo Bureau
Office of Naval Research
Oil Companies International Maritime Forum
Tanker Structure Cooperative Forum
Technical University of Nova Scotia
United States Coast Guard Academy
United States Merchant Marine Academy
United States Naval Academy
University of British Columbia
University of California Berkeley
University of Houston - Composites Eng & Appl.
University of Maryland
University of Michigan
University of Waterloo
Virginia Polytechnic and State Institute
Webb Institute
Welding Research Council
Worcester Polytechnic Institute
World Maritime Consulting, INC

Mr. Alexander Wilson
Captain Charles Piersall (Ret.)
Captain Dennis K. Kruse (USN Ret.)
Mr. Richard Frank
Dr. Harold Reemsnyder
Dr. William R. Tyson
Dr. Stephen Liu
Mr. Dave Edmonds
Mr. Tom Allen
Dr. Alaa Mansour
Mr. Dragos Rauta
Mr. Dave Burke / Captain Chip McCord
Dr. M. R. Haddara
Captain Jim McNamara
Dr. Yapa Rajapaksie
Mr. Phillip Murphy
Mr. Rong Huang
Dr. C. Hsiung
Commander Kurt Colella
Dr. C. B. Kim
Dr. Ramswar Bhattacharyya
Dr. S. Calisal
Dr. Robert Bea
Dr. Jerry Williams
Dr. Bilal Ayyub
Dr. Michael Bernitsas
Dr. J. Roorda
Dr. Alan Brown
Dr. Kirsi Tikka
Dr. Martin Prager
Dr. Nick Dembsey
VADM Gene Henn, USCG Ret.

RECENT SHIP STRUCTURE COMMITTEE PUBLICATIONS

Ship Structure Committee Publications on the Web - All reports from SSC 392 and forward are available to be downloaded from the Ship Structure Committee Web Site at URL:

<http://www.shipstructure.org>

SSC 391 and below are available on the SSC CD-ROM Library. Visit the National Technical Information Service (NTIS) Web Site for ordering information at URL:

<http://www.ntis.gov/fpc/cpn7833.htm>

SSC Report Number	Report Bibliography
SSC 433	<u>Interactive Buckling Testing of Stiffened Steel Plate Panels</u> Q. Chen, R.S. Hanson, G.Y. Grondin 2004
SSC 432	<u>Adaptation of Commercial Structural Criteria to Military Needs</u> R.Vara, C.M. Potter, R.A. Sielski, J.P. Sikora, L.R. Hill, J.C. Adamchak, D.P. Kihl, J. Hebert, R.I. Basu, L. Ferreiro, J. Watts, P.D. Herrington 2003
SSC 431	<u>Retention of Weld Metal Properties and Prevention of Hydrogen Cracking</u> R.J. Wong 2003
SSC 430	<u>Fracture Toughness of a Ship Structure</u> A.Dinovitser, N. Pussegoda, 2003
SSC 429	<u>Rapid Stress Intensity Factor Solution Estimation for Ship Structures Applications</u> L. Blair Carroll, S. Tiku, A.S. Dinovitser 2003
SSC 428	<u>In-Service Non-Destructive Evaluation of Fatigue and Fracture Properties for Ship Structure</u> S. Tiku 2003
SSC 427	<u>Life Expectancy Assessment of Ship Structures</u> A. Dinovitser 2003
SSC 426	<u>Post Yield Stability of Framing</u> J. DesRochers, C. Pothier, E. Crocker 2003
SSC 425	<u>Fatigue Strength and Adequacy of Weld Repairs</u> R.J. Dexter, R.J. Fitzpatrick, D.L. St. Peters 2003
SSC 424	<u>Evaluation of Accidental Oil Spills from Bunker Tanks (Phase I)</u> T. McAllister, C. Rekart, K. Michel 2003
SSC 423	<u>Green Water Loading on Ship Deck Structures</u> M. Meinhold, D. Liut, K. Weems, T. Treacle, Woe-Min Lin 2003
SSC 422	<u>Modeling Structural Damage in Ship Collisions</u> Dr. A.J. Brown 2003